BULLETIN OF RUSSIAN STATE MEDICAL UNIVERSITY

BIOMEDICAL JOURNAL OF PIROGOV RUSSIAN NATIONAL RESEARCH MEDICAL UNIVERSITY

SUBMISSION http://vestnikrgmu.ru/login?lang=en
CORRESPONDENCE editor@vestnikrgmu.ru
COLLABORATION manager@vestnikrgmu.ru
ADDRESS ul. Ostrovityanova, d. 1, Moscow, Russia, 117997

Indexed in Scopus. CiteScore 2022: 0.5

Indexed in WoS. JCR 2021: 0.5

Five-year h-index is 8

SCImago Journal & Country Rank 2020: 0.14

Listed in HAC 31.01.2020 (№ 507)

Open access to archive

Issue DOI: 10.24075/brsmu.2023-05
The mass media registration certificate № 012769 issued on July 29, 1994
Founder and publisher is Pirogov Russian National Research Medical University (Moscow, Russia)

Approved for print 31.10.2023
Circulation: 100 copies. Printed by Print.Formula
www.print-formula.ru

ВЕСТНИК РОССИЙСКОГО ГОСУДАРСТВЕННОГО МЕДИЦИНСКОГО УНИВЕРСИТЕТА

НАУЧНЫЙ МЕДИЦИНСКИЙ ЖУРНАЛ РНИМУ ИМ. Н. И. ПИРОГОВА

ПОДАЧА РУКОПИСЕЙ http://vestnikrgmu.ru/login
ПЕРЕПИСКА С РЕДАКЦИЕЙ editor@vestnikrgmu.ru
СОТРУДНИЧЕСТВО manager@vestnikrgmu.ru
АДРЕС РЕДАКЦИИ ул. Островитянова, д. 1, г. Москва, 117997

Журнал включен в Scopus. CiteScore 2022: 0,5

Журнал включен в WoS. JCR 2021: 0,5

Индекс Хирша (h^5) журнала по оценке Google Scholar: 8

SCImago Journal & Country Rank 2020: 0,14

Журнал включен в Перечень 31.01.2020 (№ 507)

Здесь находится открытый архив журнала

DOI выпуска: 10.24075/vrgmu.2023-05
Свидетельство о регистрации средства массовой информации № 012769 от 29 июля 1994 г.
Учредитель и издатель — Российский национальный исследовательский медицинский университет имени Н. И. Пирогова (Москва, Россия)

Подписано в печать 31.10.2023
Тираж 100 экз. Отпечатано в типографии Print.Formula
www.print-formula.ru

BULLETIN OF RSMU **5, 2023**
ВЕСТНИК РГМУ

Contents
Содержание

ATOH1 FACTOR EXPRESSION INDUCES RAPID DIFFERENTIATION OF IPSCS INTO NEURONS

Stepanov AI[1,2], Putlyaeva LV[1,2], Didych DA[2], Galiakberova AA[3,4], Gurskaya NG[1,3] ✉, Lukyanov KA[2]

[1] Skolkovo Institute of Science and Technology, Center for Molecular and Cellular Biology, Moscow, Russia
[2] Shemyakin-Ovchinnikov Institute of Bioorganic Chemistry, Moscow, Russia
[3] Pirogov Russian National Research Medical University, Moscow, Russia
[4] Lomonosov Moscow State University, Moscow, Russia

The study of human induced pluripotent stem cells (iPSCs) and developing the technology for their practical use is one of the most knowledge-intensive areas of modern biomedical research. Despite the potential of using iPSCs in personalized medicine and to build cell-based models for disorders of various etiology, iPSC utilization remains challenging. Thus, the iPSC intercellular heterogeneity and the lack of effective identity determination and assessment methods considerably hamper reproducibility of such studies. The study was aimed to generate an iPSC line carrying the gene encoding the ATOH1 transcription factor controlled by the Tet-One expression induction system, along with TagBFP2 fluorescent protein and the puromycin resistance gene for cell selection. Molecular cloning, lentiviral transduction, cell culturing, immunofluorescence staining, and fluorescence microscopy were used during the study. The created cell model will allow analyzing the state of single cells and, therefore, has great practical potential for both laboratory and medical research.

Keywords: IPSC, ATOH1, lentivirus, neural differentiation

Funding: the study was supported through the grant by RSF (№ 22-14-00141).

Author contribution: Stepanov AI — experimental procedure; Putlyaeva LV — experiment planning, manuscript writing; Didych DA — design and molecular cloning of the leniviral plasmid components, processing of figures; Galiakberova AA — cell culture; Gurskaya NG — concept and design of iPSC study; Lukyanov KA — general management.

✉ **Correspondence should be addressed:** Nadya G. Gurskaya
Ostrovitianova, 1, str. 1, Moscow, 117997, Russia; ngurskaya@mail.ru

Received: 01.08.2023 **Accepted:** 09.09.2023 **Published online:** 22.09.2023

DOI: 10.24075/brsmu.2023.036

ЭКСПРЕССИЯ ФАКТОРА ATOH1 ИНДУЦИРУЕТ БЫСТРУЮ ДИФФЕРЕНЦИРОВКУ ИПСК В НЕЙРОННОМ НАПРАВЛЕНИИ

А. И. Степанов[1,2], Л. В. Путляева[1,2], Д. А. Дидыч[2], А. А. Галиакберова[3,4], Н. Г. Гурская[1,3] ✉, К. А. Лукьянов[2]

[1] Сколковский институт науки и технологии, Центр молекулярной и клеточной биологии, Москва, Россия
[2] Институт биоорганической химии имени М. М. Шемякина и Ю. А. Овчинникова, Москва, Россия
[3] Российский национальный исследовательский медицинский университет имени Н. И. Пирогова, Москва, Россия
[4] Московский государственный университет имени М. В. Ломоносова, Москва, Россия

Изучение индуцированных плюрипотентных стволовых клеток человека (иПСК) и создание технологий их практического использования — одно из самых наукоемких направлений современных биомедицинских исследований. Несмотря на потенциал применения иПСК в персонализированной медицине и в создании клеточных моделей заболеваний различной этиологии, использование иПСК остается крайне сложным. Так, межклеточная гетерогенность иПСК при отсутствии эффективных способов определения идентичности и оценки существенно затрудняет воспроизводимость подобных исследований. Целью работы было создать линию иПСК, несущую ген транскрипционного фактора ATOH1 под контролем системы индукции экспрессии Tet-One, ген флуоресцентного белка TagBFP и ген устойчивости к пуромицину для селекции клеток. В работе использовали методы молекулярного клонирования, лентивирусную трансдукцию, культивирование клеток, иммунофлуоресцентное окрашивание и флуоресцентную микроскопию. Созданная клеточная модель позволит анализировать состояние единичных клеток и, следовательно, имеет большой практический потенциал как для лабораторных, так и для медицинских исследований.

Ключевые слова: иПСК, ATOH1, лентивирус, нейронная дифференцировка

Финансирование: работа была поддержана грантом РНФ № 22-14-00141.

Вклад авторов: А. И. Степанов — проведение эксперимента; Л. В. Путляева — планирование эксперимента, написание статьи; Д. А. Дидыч — дизайн и молекулярное клонирование элементов лентивирусной плазмиды, обработка рисунков; А. А. Галиакберова — культивирование клеток; Н. Г. Гурская — концепция и дизайн работы с ИПСК; К. А. Лукьянов — общее руководство исследованием.

✉ **Для корреспонденции:** Надежда Георгиевна Гурская
ул. Островитянова, д. 1, стр. 1, г. Москва, 117997, Россия; ngurskaya@mail.ru

Статья получена: 01.08.2023 **Статья принята к печати:** 09.09.2023 **Опубликована онлайн:** 22.09.2023

DOI: 10.24075/vrgmu.2023.036

Human induced pluripotent stem cells (iPSCs) were first obtained in 2007 [1]. iPSCs, that are similar to embryonic stem cells, can differentiate into various cell types. Since iPSCs can be obtained from the easily accessible patients' somatic cells (for example, dermal fibroblasts or peripheral blood mononuclear cells), the use of iPSCs solves important methodological and ethical problems, such as the problem of the neuronal cells' accessibility. iPSCs represent an extremely interesting model for fundamental studies of the human cells' differentiation and dedifferentiation, these cells are also of considerable practical relevance for medicine. Human iPSCs can be used to generate cells of various types and potentially for further transplantation in patients [2]. Many problems on the way to this (such as incomplete differentiation of human iPSCs and the development of teratomas) remain to be resolved and require further research. Testing of drugs on human cells, including in order to select the treatment regimen for individual patient (personalized medicine), is an equally important area of using iPSCs [3, 4]. Researchers can use iPSCs of patients generated from somatic cells to obtain isogenic cell lines, in which the

disease patterns are reproduced, through differentiation and use these cell lines for drug screening. Thus, iPSCs of patients after their differentiation into neurons or glial cells are used to study neurodegenerative diseases [5, 6].

Differentiation of iPSCs into neurons can be accomplished by using methods of two groups: 1) chemical induction; 2) genetically mediated induction [7]. In the first case, the mixture of small-molecule inhibitors and peptides suppressing the expression of pro-neuronal growth factors, as well as molecular pathways inducing neuronal induction are used to trigger differentiation. Dual SMAD inhibition is a well-known example [8]. The genetically mediated induction is aimed to introduce cDNAs encoding the gene of the transcription factor specific for the neuronal differentiation program (such as neurogenin-2) or regulatory sequences, such as promoters or enhancers, into the cell [9]. However, both strategies make it possible to ensure iPSC differentiation into neurons in at least two weeks.

In 2021, a groundbreaking report was published, where the authors proposed a new method for directed differentiation of iPSCs into neurons using the ATOH1 transcription factor overexpression [10]. The new approach is superior to earlier applied methods in terms of speed and simplicity, it allows one to ensure differentiation (up to 99%) in the standard medium within just a few days.

The study was aimed to generate an iPSC line carrying the gene encoding the ATOH1 transcription factor controlled by the Tet-One expression induction system and the TagBFP2 fluorescent protein as a selective marker. One of the objectives was to obtain a stable iPSC line allowing one to induce differentiation into neurons by adding doxycycline to the growth medium. This cell line can be used in various studies, including for analysis of the iPSC intercellular heterogeneity, development of the genetically encoded fluorescent sensors, testing of new drugs on human cells, and selection of treatment regimens for individual patients (development of personalized medicine protocols).

METHODS

Molecular cloning

The *ATOH1* transcription factor nucleotide sequence was amplified from the Addgene pTet-O-ATOH1-T2A-PuroR plasmid (Addgene #162342) using the ATOH1 for ATATGAAGACTTGAT CATGTCCCGCCTGCTGCATGCAGAAGAG and ATOH1 rev AT ATGAAGACAAACCTCTAGAACTTGCCTCATCCGAGTCACT GTAATGGGAATG primers. Then *ATOH1* and *TagBFP2* were inserted in the pRRLSIN.cPPT.EF1 lentiviral vectors at the BamH1 and EcoR1 (Thermo Scientific, Waltham, MA; USA) restriction sites. The following primers were used for *TagBFP2* amplification: TagBFP2 for ATATGAAGACGGAGGTGTGAGCG AGCTGATTAAGGAGAACATGC and TagBFP2 rev GCATGAAG ACATTCGATCATCACTTGTGCCCCAGTTTGCTAGGGAGGTC GCAGTATCTGGCC. The ATOH1 and TagBFP2 fusion was by using the T2A GSGEGRGSLLTCGDVEENPGP proteolytically cleaved peptide. The pRRLSIN.cPPT.EF1 lentiviral vector was kindly provided by Dr. D. Trono (Lausanne; Switzerland). Then the ATOH1-t2a-TagBFP2 DNA was transferred to the pLVX-TetOne-Puro vector (Clontech, #631847; USA) at the BamH1 and Age1 restriction sites (Thermo Scientific, Waltham, MA; PanEco; Russia). The T4 DNA ligase (Evrogen; Russia) was used for sticky end ligation.

Cell line cultivation

The HEK293T cells were cultured at 37 °C (5% CO_2) in the DMEM medium (PanEco; Russia) supplemented with 10% fetal bovine serum (BioSera, Nuaille; France), 100 U/mL of penicillin and 100 mg/mL of streptomycin (PanEco; Russia).

The iPS-KYOU iPSC cell line was purchased at the ATCC cell bank (KYOU-DXR0109B, ATCC® ACS-1023™). iPSCs were cultured in the mTeSR medium (StemCell Technologies; USA) at 37 °C (5% CO_2) changed daily to ensure optimal growth and Matrigel (Corning; USA) as a matrix for the surface cover. Accutase (StemCell Technologies; USA) was used to detach cells from the flask surface.

Generating a stable cell line

The TetOne-ATOH1-t2a-TagBFP2 iPSC cell line was generated by lentiviral transduction. A total of 1.5×10^6 HEK293T cells were seeded on a cell culture dish with a diameter of 60 mm 24 h before transfection. In total, 2 μg of the pR8.91 plasmid, 0.6 μg of the pMD.G plasmid, and 6 μg of the TetOne-ATOH1-t2a-TagBFP2 plasmid were used for transfection. The Transfectin reagent (IBCh RAS; Moscow, Russia) in the ratio 2.5 μL of the reagent to 1μg of the plasmid was used for transient transfection of the HEK293T cells. The mixture of DNA and Transfectin was incubated for 20 min at room temperature and then added dropwise. After 4 h the medium was replaced with 2 mL of fresh DMEM. On the next day the medium containing the lentiviruses acquired was filtered (filter with the pore size of 0.45 μm) and concentrated by ultracentrifugation at 100,000 g (Beckman; USA) for 3 h at 4 °C. Precipitate was resuspended in 500 μL of mTeSR (StemCell Technologies; USA) and used for transduction of iPSCs. Lentiviral particles were added to 1×10^5 iPSCs to generate stable cell lines. Then the transduced cells were selected by adding the puromycin antibiotic (Thermo Fisher Scientific, Waltham, MA; USA) to the growth medium to a final concentration of 5 μg/mL.

Immunostaining of fixed cells

Cells were seeded and grown as described above, fixed in 4% formaldehyde solution in PBS for 15 min at room temperature, triple washed with PBS, permeabilized for 20 min in 0.1% Triton X-100 (Helicon; USA) in PBS, and incubated for 1 h with 1% BSA (Sigma; USA) in PBS to ensure blocking. Incubation with primary antibody was performed for 1 h, incubation with secondary antibody was performed for 1 h at room temperature. Cells were washed with PBS and imaged in the imaging medium using the BZ-9000 microscope (Keyence, Osaka; Japan). The rabbit anti-TUBB3 and goat anti-rabbit IgG Alexa Fluor 568 antibodies (ThermoFisher, Waltham, MA; USA) were used at a dilution of 1 : 500 and 1 : 1000, respectively.

Fluorescence microscopy of living cells

When conducting experiments on living cell imaging, cells were grown in confocal dishes with glass bottom (SPL Life Sciences; Korea). The mTESR medium was replaced with the MEM imaging medium (PanEco; Russia) supplemented with 10% fetal bovine serum (BioSera, Cholet; France) and 20 mM HEPES (Corning, NY; USA) immediately before microscopy.

The Keyence Biorevo BZ-9000 fluorescence microscope (Keyence; Japan) was used for in vivo fluorescence microscopy. Cells were imaged at 60× magnification using the CFI Plan Apo λ60xH/NA1.40 lens. Imaging was performed in the blue channel using the DAPI filter cube (excitation wavelength 360/40 nm, emission wavelength 460/50 nm) for detection of the TagBFP2 fluorescence.

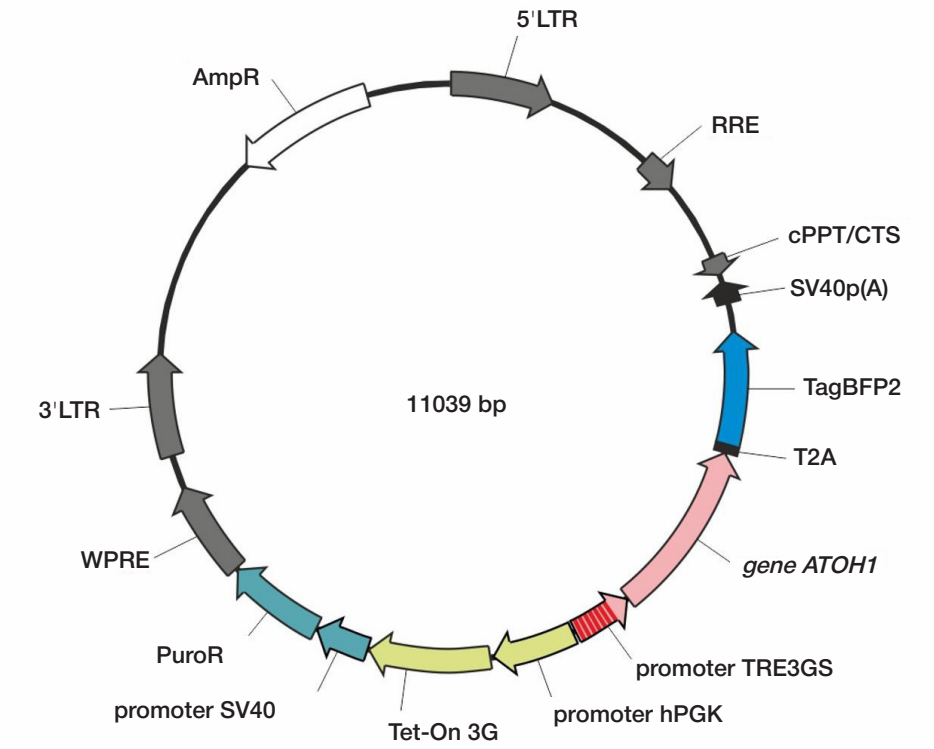

Fig. 1. Scheme of the *TetOne-ATOH1-t2a-TagBFP2* lentiviral plasmid used to generate a stable iPSC line with induced expression of the *ATOH1-T2A-TagBFP2* fusion gene. The *ATOH1-T2A-TagBFP2* gene is controlled by the TRE3GS inducible doxycycline-dependent promoter containing seven repeats of the tetO operator sequence. The plasmid also comprises the *Tet-On 3G* (TRE3GS promoter transactivator) and *PuroR* (puromycin resistance gene) genes controlled by the hPGK (promoter of human gene *PGK1*) and SV40 constitutive promoters, respectively. Standard components of lentiviral plasmids that are essential for correct and effective assembly of functional viral particles in the packaging cells and that ensure high expression of transgenes (5'LTR/3'LTR — long terminal repeats, RRE — Rev viral protein binding site (Rev response element); cPPT/CTS — central polypurine tract/central termination sequence; WPRE — Woodchuck hepatitis virus post–transcriptional regulatory element; SV40p(A) — SV40 transcription terminator with a poly(A) signal; AmpR — ampicillin resistance gene) are highlighted in gray

RESULTS

When constructing the most effective model of inducing iPSC differentiation into neurons, we used the approach reported by the group of G. Church in 2021 [10]. In this study a large-scale screening of three human iPSC lines was performed; it was found that the ATOH1 transcription factor was the most effective driver of the neuronal differentiation induction. In contrast to other pathways of iPSC differentiation into neurons, the ATOH1-induced differentiation requires no specific media or extra factors. Furthermore, this process takes little time (4 days). To create the most biologically relevant model of the ATOH1-induced neuronal differentiation, we decided to construct a stable iPSC line carrying the *ATOH1* gene controlled by under the control of the TRE3Gs inducible promoter. For that we made a lentiviral plasmid with induced ATOH1 expression (Fig. 1). This plasmid comprised three independent expression cassettes:

TRE3G promoter-ATOH1-t2a-TagBFP2 — the *ATOH1* gene controlled by the tetracycline promoter and fused with the expression marker, the fluorescent protein TagBFP2, through the T2A peptide. Induction of *ATOH1-t2a-TagBFP2* expression was achieved by adding doxycycline to the growth medium.

hPGK promoter-TetOn3G — *TetOn3G*, the gene encoding the TetOn tetracycline promoter activator, was controlled by the hPGK promoter;

SV40 promoter-PuroR — ensured puromycin expression that was essential for selection of iPSCs carrying a target construct only.

This genetic construct referred to as *TetOne-ATOH1-t2a-TagBFP2* was used to generate lentiviral particles and infect the iPS-KYOU cell line (Fig. 2A). After that the cells were subjected to selection in the puromycin-containing medium, then doxycycline was added for the tetracycline promoter activation. Within 24 h after adding doxycycline we recorded weak fluorescence of the TagBFP2 blue protein, indicating the earliest stage of the ATOH1 factor expression. On day two the signal was strong and well-detectable for the fluorescence microscope, the neuron-like cell morphology changes were reported (Fig. 2B; *above*).

Differentiation efficiency was assessed by immunofluorescence staining aimed at detecting the neuronal stem cell marker (class III β-tubulin, TUBB3) expression (Fig. 3A). We showed that the cell culture obtained after differentiation was heterogeneous in terms of TUBB3 expression: some cells showing TagBFP2 fluorescence did not express TUBB3 and had no morphological features specific for neurons (Fig. 3B).

The findings suggest that the TetOne-ATOH1-t2a-TagBFP2 human iPSC line shows stable ATOH1 transcription factor expression controlled by the TetOne expression induction system. The use of this cell line in laboratory studies can provide unique information about the chromatin state changes during iPSC differentiation into neurons. This biological model can potentially be used to address diverse biological and biomedical challenges.

DISCUSSION

The generated TetOne-ATOH1-t2a-TagBFP2 cell line showed successful inducible expression activation within 1–2 days after the start of the experiment. However, the expression of blue protein reflecting the ATOH1 protein levels in the cell was heterogeneous (Fig. 2B, *below*; Fig. 3B). Perhaps, this phenomenon was due to heterogeneity of original iPSC line and no clonal selection among transduced cells in this experiment. We also assume that methylation of the tetracycline promoter

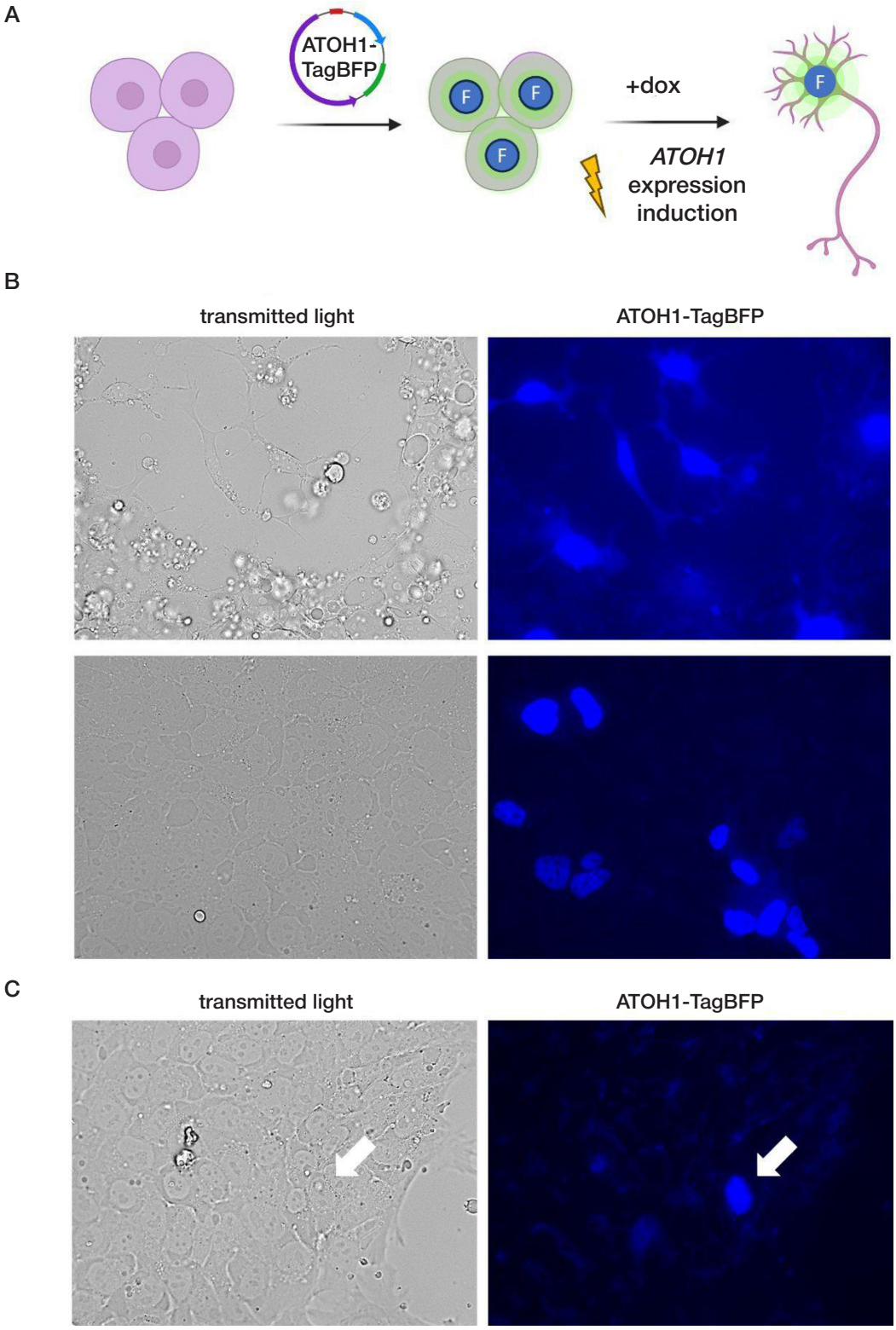

Fig. 2. Expression of the *TetOne-ATOH1-t2a-TagBFP2* construct in iPSCs. **A**. Scheme to generate a stable iPSC line carrying the *ATOH1* gene controlled by the TRE3G inducible promoter. F — TagBFP fluorescent protein. **B**. Cells 24 h after induction of expression by doxycycline. **C**. After freezing and thawing the majority of cells become incapable of doxycycline-dependent expression (the only cell in the field of view showing a bright TagBFP2 expression signal after adding doxycycline is marked with *arrow*)

and/or hPGK promoter can occur in iPSCs over time, resulting in the decrease in the tetracycline promoter activator protein levels. The ATOH1-t2a-TagBFP2 downregulation represents a cumulative effect of these processes. Indeed, we have found out that the number of cells showing the TagBFP2 expression has reduced after thawing a new aliquot of TetOne-ATOH1-t2a-TagBFP2 cells and repeating the experiment (Fig. 1C).

CONCLUSIONS

The use of the new method of directed iPSC differentiation into neurons makes it possible to quickly (in 4 days) generate the populations enriched with cells that differentiate into neurons. The cell line generated showing *ATOH1* expression controlled by the TRE3Gs inducible promoter is suitable for experiments

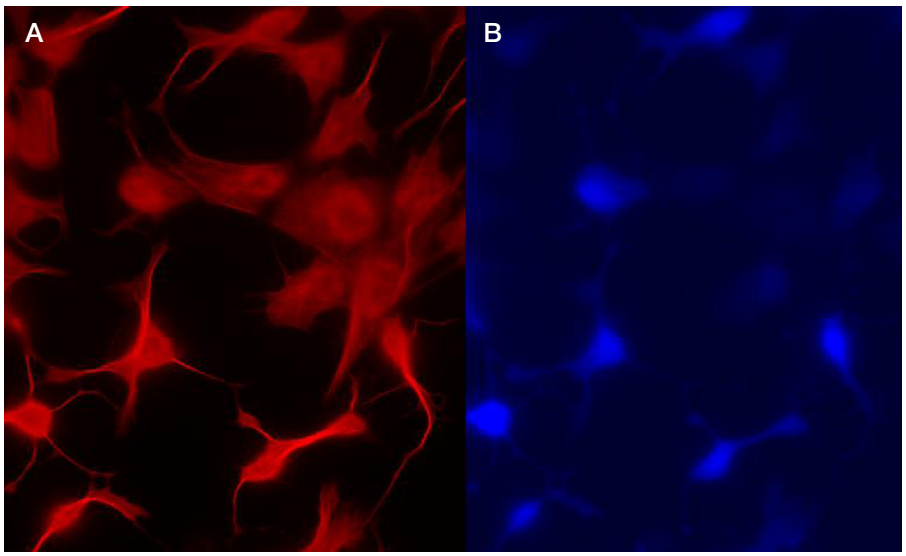

Fig. 3. Immunofluorescence analysis of simultaneous class III β-tubulin (TUBB3) and TagBFP2 expression in the cells on day 4 of differentiation after induction with *TetOne-ATOH1-t2a-TagBFP2*. **A**. *Red signal* — rabbit anti-TUBB3 (Affinity) antibody was used along with the goat anti-rabbit IgG Alexa Fluor 568 (ThermoFisher) secondary antibody. **B**. Blue signal — TagBFP2 fluorescence

requiring rapid iPSC differentiation, however, the experiment has to be carried out continuously (with no freezing/thawing cycles), which represents a limitation of this method when used to acquire experimental data.

References

1. Takahashi K, Tanabe K, Ohnuki M, Narita M, Ichisaka T, Tomoda K, et al. Induction of pluripotent stem cells from adult human fibroblasts by defined factors. Cell. 2007; 131: 861–72.
2. Chang C-Y, Ting H-C, Su H-L, Jeng J-R. Combining Induced Pluripotent Stem Cells and Genome Editing Technologies for Clinical Applications. Cell Transplant. 2018; 27: 379–92.
3. Kleiman RJ, Engle SJ. Human inducible pluripotent stem cells: Realization of initial promise in drug discovery. Cell Stem Cell. 2021; 28: 1507–15.
4. Madrid M, Sumen C, Aivio S, Saklayen N. Autologous Induced Pluripotent Stem Cell-Based Cell Therapies: Promise, Progress, and Challenges. Curr Protoc. 2021; 1: e88.
5. Zhang N, Bailus BJ, Ring KL, Ellerby LM. iPSC-based drug screening for Huntington's disease. Brain Res. 2016; 1638: 42–56.
6. Chang C-Y, Ting H-C, Liu C-A, Su H-L, Chiou T-W, Lin S-Z, et al. Induced Pluripotent Stem Cell (iPSC)-Based Neurodegenerative Disease Models for Phenotype Recapitulation and Drug Screening. Molecules. 2020; 25. DOI: 10.3390/molecules25082000.
7. Telias M. Neural differentiation protocols: how to choose the correct approach. Neural Regeneration Res. 2023; 18: 1273–4.
8. Chambers SM, Fasano CA, Papapetrou EP, Tomishima M, Sadelain M, Studer L. Highly efficient neural conversion of human ES and iPS cells by dual inhibition of SMAD signaling. Nat Biotechnol. 2009; 27: 275–80.
9. Zhang Y, Pak C, Han Y, Ahlenius H, Zhang Z, Chanda S, et al. Rapid single-step induction of functional neurons from human pluripotent stem cells. Neuron. 2013; 78: 785–98.
10. Ng AHM, Khoshakhlagh P, Rojo Arias JE, Pasquini G, Wang K, Swiersy A, et al. A comprehensive library of human transcription factors for cell fate engineering. Nat Biotechnol. 2021; 39: 510–9.

Литература

1. Takahashi K, Tanabe K, Ohnuki M, Narita M, Ichisaka T, Tomoda K, et al. Induction of pluripotent stem cells from adult human fibroblasts by defined factors. Cell. 2007; 131: 861–72.
2. Chang C-Y, Ting H-C, Su H-L, Jeng J-R. Combining Induced Pluripotent Stem Cells and Genome Editing Technologies for Clinical Applications. Cell Transplant. 2018; 27: 379–92.
3. Kleiman RJ, Engle SJ. Human inducible pluripotent stem cells: Realization of initial promise in drug discovery. Cell Stem Cell. 2021; 28: 1507–15.
4. Madrid M, Sumen C, Aivio S, Saklayen N. Autologous Induced Pluripotent Stem Cell-Based Cell Therapies: Promise, Progress, and Challenges. Curr Protoc. 2021; 1: e88.
5. Zhang N, Bailus BJ, Ring KL, Ellerby LM. iPSC-based drug screening for Huntington's disease. Brain Res. 2016; 1638: 42–56.
6. Chang C-Y, Ting H-C, Liu C-A, Su H-L, Chiou T-W, Lin S-Z, et al. Induced Pluripotent Stem Cell (iPSC)-Based Neurodegenerative Disease Models for Phenotype Recapitulation and Drug Screening. Molecules. 2020; 25. DOI: 10.3390/molecules25082000.
7. Telias M. Neural differentiation protocols: how to choose the correct approach. Neural Regeneration Res. 2023; 18: 1273–4.
8. Chambers SM, Fasano CA, Papapetrou EP, Tomishima M, Sadelain M, Studer L. Highly efficient neural conversion of human ES and iPS cells by dual inhibition of SMAD signaling. Nat Biotechnol. 2009; 27: 275–80.
9. Zhang Y, Pak C, Han Y, Ahlenius H, Zhang Z, Chanda S, et al. Rapid single-step induction of functional neurons from human pluripotent stem cells. Neuron. 2013; 78: 785–98.
10. Ng AHM, Khoshakhlagh P, Rojo Arias JE, Pasquini G, Wang K, Swiersy A, et al. A comprehensive library of human transcription factors for cell fate engineering. Nat Biotechnol. 2021; 39: 510–9.

FEATURES OF CD163+ AND HLA-DR+ EXPRESSION ON BLOOD MONOCYTES ASSOCIATED WITH BREAST CANCER

Patysheva MR[1,2] ✉, Stakheyeva MN[1,2], Grigoryeva ES[2], Tarabanovskaya NA[1], Bragina OD[1], Kzhyshkowska JG[2,3], Cherdyntseva NV[1,2]

[1] Tomsk National Research Medical Center, Russian Academy of Sciences, Tomsk, Russia

[2] National Research Tomsk State University, Tomsk, Russia

[3] University of Heidelberg, Mannheim, Germany

Circulating monocytes are important actors of the tumor growth pathogenesis. It has been shown that some features of the monocyte populations expressing endocytosis receptors or the major histocompatibility complex components are observed in blood of patients with breast cancer. The study was aimed to assess the relationship of tumor parameters and blood cytokine profile with the composition of circulating monocyte populations in patients with localized and locally advanced breast cancer. The study has shown that the circulating monocytes' phenotypic characteristics are correlated to the clinical and morphological features of the neoplastic process. The content of populations with the CD14+CD16++CD163+ and CD14++CD16+CD163+ phenotypes positively correlates with the disease stage, while larger primary tumor size is associated with lower CD14+CD16++ monocyte levels. Elevated serum levels of IL8 and MCP-1 are observed in breast cancer patients. High IL6 levels in patients with breast cancer are associated with the reduced percentage of CD14++CD16-HLA-DR+, CD14+CD16++HLA-DR+ and CD14++CD16-CD163+ monocytes. Thus, CD163+ and HLA-DR+ monocytes are associated with the clinical and morphological parameters and blood levels of cytokines, which suggests that these populations are involved in breast cancer progression and indicates that further research is advisable for translation of the findings into clinical practice.

Keywords: monocytes, CD163, HLA-DR, breast cancer, IL6, IL8, MCP-1

Funding: the study was supported by the RSF grant (№ 22-25-00435).

Acknowledgements: we would like to express our gratitude to O. E. Savelieva, the lead researcher at the Institute of Personalized Psychiatry and Neurology, Bekhterev National Research Medical Center for Psychiatry and Neurology (Saint Petersburg), for assistance in conducting flow cytometry.

Author contribution: Patysheva MR — study design, flow cytometry, data analysis, manuscript writing; Stakheyeva MN — study concept, study design, data analysis, manuscript writing; Grigoryeva ES — flow cytometry; Tarabanovskaya NA — selection of patients, patient clinical data acquisition; Bragina OD — selection of patients, patient clinical data acquisition; Kzhyshkowska JG — study concept, search for funding, discussion; Cherdyntseva NV — study design, discussion.

Compliance with ethical standards: the study was approved by the Ethics Committee of the Cancer Research Institute, Tomsk National Research Medical Center (protocol № 10 dated 05 December 2019). All subjects submitted the informed consent to study participation.

✉ **Correspondence should be addressed:** Marina R. Patysheva
per. Kooperativnyi, 7/1, Tomsk, 634009, Russia; patysheva_mr@onco.tnimc.ru

Received: 14.09.2023 **Accepted:** 10.10.2023 **Published online:** 31.10.2023

DOI: 10.24075/brsmu.2023.043

ОСОБЕННОСТИ ЭКСПРЕССИИ CD163+ И HLA-DR+ НА МОНОЦИТАХ КРОВИ ПРИ РАКЕ МОЛОЧНОЙ ЖЕЛЕЗЫ

М. Р. Патышева[1,2] ✉, М. Н. Стахеева[1,2], Е. С. Григорьева[2], Н. А. Тарабановская[1], О. Д. Брагина[1], Ю. Г. Кжышковска[2,3], Н. В. Чердынцева[1,2]

[1] Томский национальный исследовательский медицинский центр Российской академии наук, Томск, Россия

[2] Национальный исследовательский Томский государственный университет, Томск, Россия

[3] Университет Гейдельберга, Мангейм, Германия

Циркулирующие моноциты — значимые участники патогенеза опухолевого роста. Показано, что в крови больных раком молочной железы наблюдаются особенности популяций моноцитов, экспрессирующих рецепторы эндоцитоза, либо компонентов главного комплекса гистосовместимости. Целью данной работы было проведение анализа взаимосвязи параметров опухоли и цитокинового профиля крови с популяционным составом циркулирующих моноцитов больных локализованными и местно-распространенными формами рака молочной железы. В исследовании было показано, что фенотипические характеристики циркулирующих моноцитов взаимосвязаны с клинико-морфологическими особенностями опухолевого процесса. Содержание популяций с фенотипом CD14+CD16++CD163+ и CD14++CD16+CD163+ имело положительную корреляцию со стадией заболевания, в то время как больший размер первичного опухолевого узла ассоциирован с более низким содержанием CD14+CD16++-моноцитов. У больных РМЖ увеличено содержание IL8 и MCP-1 в сыворотке крови. Высокий уровень содержания IL6 у больных РМЖ ассоциирован со снижением доли CD14++CD16-HLA-DR+-моноцитов, CD14+CD16++HLA-DR+-моноцитов и CD14++CD16-CD163+-моноцитов. Таким образом, CD163+ и HLA-DR+-моноциты связаны с клинико-морфологическими параметрами и уровнем цитокинов крови, что свидетельствует о вовлечении данных популяций в прогрессию рака молочной железы и говорит о целесообразности дальнейших исследований для трансляции полученных результатов в клиническую практику.

Ключевые слова: моноциты, CD163, HLA-DR, рак молочной железы, интерлейкин 8, интерлейкин 6, фактор миграции моноцитов

Финансирование: работа выполнена при поддержке гранта РНФ №22-25-00435.

Благодарности: благодарим ведущего научного сотрудника института персонализированной психиатрии и неврологии НМИЦ ПН имени В. М. Бехтерева (г. Санкт-Петербург) О. Е. Савельеву за помощь в проведении проточной цитометрии.

Вклад авторов: М. Р. Патышева — дизайн исследования, проточная цитометрия, анализ данных, написание статьи; М. Н. Стахеева — разработка концепции работы, дизайн исследования, анализ данных, написание статьи; Е. С. Григорьева — проточная цитометрия; Н. А. Тарабановская — подбор пациентов, сбор клинических данных о пациентах; О. Д. Брагина — подбор пациентов, сбор клинических данных о пациентах; Ю. Г. Кжышковска — разработка концепции работы, поиск грантовой поддержки работы, обсуждение результатов; Н. В. Чердынцева — дизайн исследования, обсуждение результатов.

Соблюдение этических стандартов: исследование одобрено этическим комитетом НИИ онкологии Томского НИМЦ (протокол № 10 от 05 декабря 2019 г.). Все участники подписали информированное согласие об участии в исследовании.

✉ **Для корреспонденции:** Марина Ринатовна Патышева
пер. Кооперативный, д. 7/1, г. Томск, 634009, Россия; patysheva_mr@onco.tnimc.ru

Статья получена: 14.09.2023 **Статья принята к печати:** 10.10.2023 **Опубликована онлайн:** 31.10.2023

DOI: 10.24075/vrgmu.2023.043

Monocytes are the most important effectors of nonspecific immunity involved in numerous disease processes associated with chronic inflammation. The malignant neoplasm emergence and development is one of such processes characterized by monocyte involvement in all phases of tumor pathogenesis. To date, it is known that the monocyte pool consists of three major populations: classical monocytes with the $CD14^{++}CD16^{-}$ phenotype, non-classical monocytes with the $CD14^{+}CD16^{++}$ phenotype, and intermediate $CD14^{++}CD16^{+}$ monocytes [1]. Furthermore, $CD14^{++}CD16^{-}$ monocytes are the source to replenish the pool of tumor-associated macrophages, dendrite cells and myeloid-derived suppressor cells in the tumor tissue [2]. The capability of maintaining endothelial integrity and absorbing foreign particles is typical for $CD14^{+}CD16^{++}$ cells [2, 3]. The role of intermediate population is poorly understood, however, it is assumed that this population occupies an intermediate position between the other two populations [4].

In addition to division into three major populations, monocytes are distinguished by expression of protein receptors related to certain cell functions. Thus, the monocyte capability of endocytosis involving the haptoglobin-hemoglobin complex uptake via CD163 receptor reflects the capability of absorbing particles and is enhanced under monocyte exposure to mediators reducing pro-inflammatory activity of such cells [5]. It is also known that cells of the macrophage-monocyte lineage possess functional plasticity and express the receptors related to the antigen-presenting function of monocytes and macrophages [6]. The increase in the counts of monocytes showing low HLA-DR expression is considered to be associated with immunosuppression observed in individuals with cancer and infectious diseases [7]. Thus, it is worthwhile to investigate the population structure of monocytes not only based on markers of the classical, intermediate, and non-classical population, but also considering additional functional markers.

The dynamics of malignant neoplasm development are considered to be closely related to two major factors: individual characteristics of the organism and biological properties of the tumor. In particular, it has been shown that the age of BC manifestation, genetic predisposition, and the presence of germline mutations can determine the clinical course of the disease in the patient [8]. Since biological processes in breast tissue largely depend on the woman's hormonal health, BC is often associated with impaired sex hormone regulation and, therefore, is correlated to menstrual status [9]. Furthermore, it has been confirmed that endocrine disorders and body's metabolic status are associated with production of biological factors, cytokines and chemokines, regulating the immune cell functional activity, by the tumor [10]. Body mass index (BMI), one of the metabolic status criteria, can be also associated with the course of BC [11]. The relationship between body weight increase and adult-onset BC has been demonstrated, where the increase by 5 kg/m^2 corresponds to the increase in the risk of breast cancer by 2% in women [11, 12].

In addition to the patient's individual characteristics, clinical and morphological parameters, such as primary tumor size, regional neoplastic process extension and tumor molecular subtype, are important factors associated with the BC clinical course [13, 14].

Cytokines and the major immune response regulators [15]. The circulating blood cytokine profile reflects body's systemic homeostasis [15]. In individuals with malignant neoplasms, the tumor itself can contribute to the body's abnormal homeostasis by affecting the immune system components [15]. It has been found that monocyte programming under exposure to interleukin 6 (IL6) and interleukin 8 (IL8) is an essential step of inducing their inflammatory phenotype [16]. Migration of monocytes from the bone marrow or spleen being the site of monocyte deposition is controlled by the major monocyte migration factor (MCP-1 or CCL2). Identification of the association of monocyte population structure with the disease stage and the patients' individual characteristics makes it possible to describe monocyte involvement in BC pathogenesis.

Given the fact that cells of the macrophage-monocyte lineage are important for BC development, the study was aimed to assess the association of $CD163^{+}$ and $HLA\text{-}DR^{+}$ monocyte counts with clinical and morphological characteristics of the disease and blood cytokine profile in individuals with BC.

METHODS

A total of 50 patients with stage I–III primary breast cancer, T1-3N0-3M0, aged 52.0 [46.0–63.0] years were enrolled. The diagnosis was confirmed by morphological assessment. The histologic tumor type corresponded to invasive carcinoma of no special type in all cases. A conventional panel of ERα, PR and HER2 immunohistochemical markers was used for breast tumor classification in accordance with molecular subtypes. The clinical and anamnestic data were acquired by analysis of the patients' medical history and outpatient charts. The characteristics of patients enrolled are provided in Table 1. BMI was calculated for each patient according to the following formula: square of the ratio of body weight (kg) to body length (m). Exclusion criteria were as follows: patients having multiple primary malignant tumors, history of cancer of other localization, previous breast surgery.

The control group included healthy women (average age 61.0 [50.0–69.0] years). Exclusion criteria were as follows: history of cancer, exacerbation of chronic disorder.

Determining the tumor molecular subtype

Expression of estrogen receptors (ER), progesterone receptors (PR), HER2/neu status (HER2), proliferative activity (Ki-67 expression) were estimated to determine the BC molecular subtype by immunohistochemistry performed using the standard method. Antibodies (Dako; Denmark) against estrogen receptors (clone 1D5, RTU, mouse), progesterone receptors (clone PgR636, RTU, mouse), c-erbB-2 protein (HER2/neu, working dilution 1:500, rabbit), Ki-67 (clone MIB-1, RTU, mouse) were used. Expression of the sex hormone receptors was assessed by quantitative Histo-Score method. Ki-67 expression was estimated as a percentage of positively stained cells of invasive breast carcinoma of no special type (in 10 fields of view per 1000 cells at 400x magnification). Molecular DC subtypes were determined based on the combination of estrogen and progesterone receptor expression, HER2/neu status and Ki-67: luminal B HER2– (ER+ and/or PR+, HER2– and Ki-67 ≥ 20%), luminal B HER2+ (ER+ and/or PR+, HER2+), triple negative (ER–, PR– and HER2–), and HER2/neu-overexpressing subtype (ER–, PR–, $HER2^{+}$).

Peripheral blood monocyte phenotyping

The $CD163^{+}$ (a scavenger receptor) and $HLA\text{-}DR^{+}$ expression on monocytes of classical $CD14^{++}CD16^{-}$, non-classical $CD14^{+}CD16^{++}$ and intermediate $CD14^{++}CD16^{+}$ populations in blood of patients of the BC group was assessed. For that venous blood was collected from patients and donors into the K3-EDTA vacuum blood sampling systems. A total of 100 μL

Table 1. Clinical and morphological parameters of patients with breast cancer

Clinical and pathological parameters	N (%) (n = 50)
Age	59.3 ± 10.4
BMI	27.2 ± 5.54
Menstrual status:	
preserved	24 (48.2)
menopause	26 (51.8)
Stage	
I	7 (14.0)
II	23 (46)
III	20 (40)
Molecular subtype	
Luminal B	25 (50.0)
Triple-negative subtype	19 (38.0)
HER2-positive	6 (12)
Lymph node metastasis	
present	22 (46.5)
absent	28 (53.5)

of white blood cell fraction were collected to determine the population structure of blood monocytes. Then the cells were suspended in 150 µL of the staining buffer (Cell Staining Buffer, Sony; Japan). Cells were counted with the Luna II cell counter (Logos Biosystems, Inc.; Korea). After that the cell concentrate was added 5 µL of Human TruStain FcX™ (Biolegend; USA) to block nonspecific binding and incubated for 10 min. Then it was stained using the set of labeled antibodies against markers CD45, CD14, CD16, CD163 and HLA-DR. The following antibodies were used in the study: CD45–APC-Cy7 (BD Bioscience, catalogue number 557833; USA), CD56–PE-Cy7 (eBioscience, Thermo Fisher Scientific; USA), CD14–FITC (BD Bioscience, catalogue number 345784; USA), CD16 –APC (BD Bioscience, USA, catalogue number 561248), CD163–PE (BD Bioscience, USA, catalogue number 556018), HLA-DR–PE-Cy5 (BD Bioscience, catalogue number 555813; USA), Isotype PE-Cy™5 (BD Bioscience, catalogue number 555750; USA), Isotype PE (BD Bioscience, catalogue number 556018; USA). Cell viability was assessed using the 7-AAD nucleic acid dye (BD Bioscience; USA). Staining was performed by adding antibodies to a ratio of 5 µL per 10^6 cells. The samples supplemented with the same concentration of appropriate isotopic control were used as negative controls. These samples were incubated at room temperature in the dark for 20 min. Then each stained or unstained sample was added 900 µL of VersaLyse Lysing Solution (Beckman Coulter; USA). Samples were analyzed in the NovoCyte cytometer (ACEA Bioscience; USA). The gating tactics is provided in Fig. 1. The data obtained were processed using the NovoExpress SoftWare (Acea; USA).

Assessment of serum cytokine levels

Serum cytokine levels were assessed using the Bio-Plex multiplex magnetic bead immunoassays (Bio-Rad, Hercules, CA; USA). The Human Milliplex MAG panel was used for analysis of three analytes: IL6, IL8 and MCP-1; 50 µL of serum from each case and control were analyzed using the Luminex 200 analyzer with the MasterPlex CT software for control and MasterPlex QT software for analysis (MiraiBio; USA). The calibration curves were plotted using the manufacturer's standards. Serum samples of patients with BC and healthy individuals were inactivated by heating prior to analysis. During the study we assessed the effects of heat inactivation on the cytokine stability; impossibility of normalization was the criterion for exclusion from the analysis.

Statistical data processing methods

Statistical processing was performed with the Statistica 8.0 software for Windows (StatSoft Inc.; USA). The pattern of the studied variables distribution was tested for normality using the Kolmogorov–Smirnov test. The numeric data obtained were presented in the following format based on the testing results: Me [LQu–UQu]. The Mann–Whitney U test was used to determine significant differences in independent groups. The correlation analysis involved calculation of the Spearman's rank correlation coefficient. The results for serum cytokine concentrations were presented in the GraphPad Prism 8 SoftWare (GraphPad Soft Inc; USA). In all tests, significant differences were reported at the following significance levels: $p < 0.001$, $p < 0.01$ and $p < 0.05$.

RESULTS

In the studied group, the patients' age was not associated with the blood monocyte population structure. At the same time, a moderate correlation between BMI and the percentage of $CD14^{++}CD16^{+}HLA\text{-}DR^{+}$ cells with the correlation coefficient of 0.409, $p \leq 0.05$, was reported (Table 2).

It is well-known that preservation or loss of menstrual function in individuals with BC is directly related to the patients' hormonal status and body's homeostasis. The levels of $CD14^{++}CD16^{+}CD163^{+}$ monocytes were slightly decreased in women with preserved menstrual function compared to the menopausal/postenopausal group: 96.01 [83.29–98.46]% vs. 99.49 [89.79–100.00]% at the trend level, $p = 0.056$.

The population structure of monocytes in affected individuals was correlated to the tumor clinical and morphological characteristics. The increase in the neoplastic process clinical stage positively correlated with the levels of classical $CD14^{++}CD16^{-}CD163^{+}$ cells (moderate correlation), while weak correlation was reported for the intermediate $CD14^{++}CD16^{+}CD163^{+}$ population (r = 0.52 and 0.356, respectively, $p < 0.05$). In contrast, T (tumor size) showed a weak negative correlation with the content of cells of the non-classical $CD14^{+}CD16^{++}$ population (r = –0.389 and $p < 0.05$). As for N parameter reflecting the regional lymph node metastasis, no significant correlations with the characteristics of the phenotype pattern of blood monocytes (Table 2).

When comparing two groups of patients with the tumor size of T1–2 and T3–4, it was found that the $CD14^{-}CD16^{+}$ monocyte counts significantly decreased with increasing tumor size (Table 3).

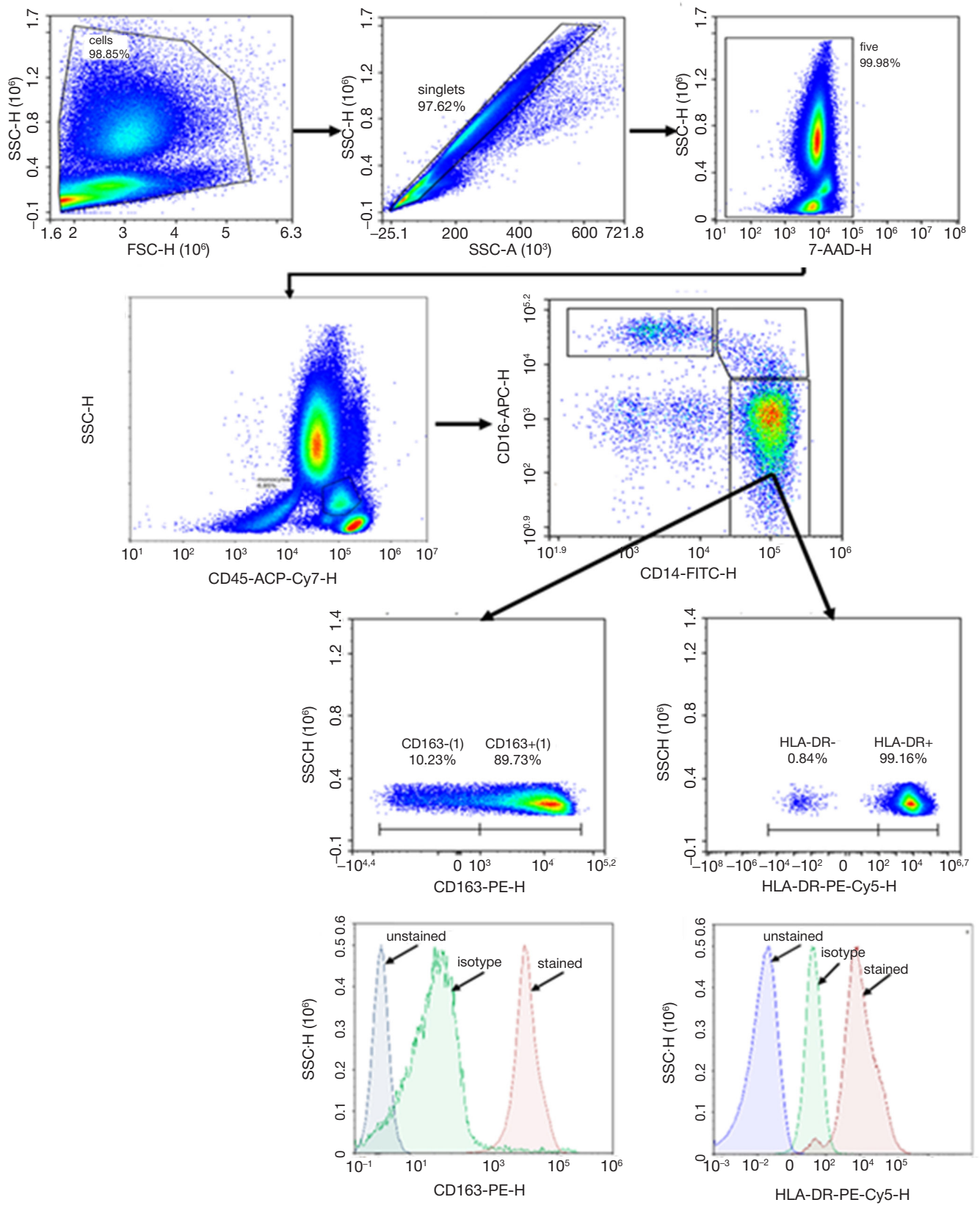

Fig. 1. Cytometry gating strategy for identification of monocyte subpopulations

At the same time, the $CD14^{+}CD16^{++}CD163^{+}$ monocyte counts decreased at the trend level from 98.77 [77.94–99.97]% at T1–2 to 69.81 [41.36–99.1]% at T3–4 (p = 0.09). The monocyte population structure was also associated with the degree of regional lymph node involvement. The content of $CD14^{++}CD16^{-}HLA\text{-}DR^{+}$ reported for patients with N0-1 was higher than that reported for the group with N2–3 by more than 4%. The disease stage as an integral indicator of the neoplastic process extent was associated with the monocyte distribution across the major populations. We compared the group of patients with the neoplastic process showing no regional lymph node involvement (cancer stage I–IIA) with the group showing tumor extension to the regional lymph nodes (stage IIB–IIIC). Thus, in the group of patients with stage I–IIA cancer, the share

Table 2. Correlation of individual features and tumor clinical and morphological parameters with the monocyte subpopulations in patients with BC

	Age	BMI	Stage	T	N
$CD14^+16^-$, %	$r = 0.135$ $p \geq 0.05$	$r = -0.073$ $p \geq 0.05$	$r = 0.228$ $p \geq 0.05$	$r = 0.206$ $p \geq 0.05$	$r = 0.149$ $p \geq 0.05$
$CD14^-16^+$, %	$r = -0.123$ $p \geq 0.05$	$r = 0.120$ $p \geq 0.05$	$r = -0.087$ $p \geq 0.05$	**$r = -0.389$ $p \leq 0.05$**	$r = -0.129$ $p \geq 0.05$
$CD14^+16^+$, %	$r = -0.122$ $p \geq 0.05$	$r = -0.043$ $p \geq 0.05$	$r = -0.028$ $p \geq 0.05$	$r = -0.026$ $p \geq 0.05$	$r = -0.036$ $p \geq 0.05$
$CD14^+16^-163^+$, %	$r = 0.038$ $p \geq 0.05$	$r = -0.017$ $p \geq 0.05$	**$r = 0.521$ $p \leq 0.05$**	$r = -0.082$ $p \geq 0.05$	$r = 0.198$ $p \geq 0.05$
$CD14^+16^-HLA\text{-}DR^+$, %	$r = -0.127$ $p \geq 0.05$	$r = 0.211$ $p \geq 0.05$	$r = 0.301$ $p \geq 0.05$	$r = -0.114$ $p \geq 0.05$	$r = -0.196$ $p \geq 0.05$
$CD14^-16^+163^+$, %	$r = 0.027$ $p \geq 0.05$	$r = -0.061$ $p \geq 0.05$	$r = 0.153$ $p \geq 0.05$	$r = -0.272$ $p \geq 0.05$	$r = -0.021$ $p \geq 0.05$
$CD14^-16^+HLA\text{-}DR^+$, %	$r = 0.069$ $p \geq 0.05$	$r = 0.082$ $p \geq 0.05$	$r = 0.093$ $p \geq 0.05$	$r = 0.159$ $p \geq 0.05$	$r = -0.085$ $p \geq 0.05$
$CD14^+16^+163^+$, %	$r = -0.250$ $p \geq 0.05$	$r = 0.195$ $p \geq 0.05$	**$r = 0.356$ $p \leq 0.05$**	$r = -0.171$ $p \geq 0.05$	$r = 0.217$ $p \geq 0.05$
$CD14^+16^+HLA\text{-}DR^+$, %	$r = 0.082$ $p \geq 0.05$	**$r = -0.409$ $p \leq 0.05$**	$r = 0.091$ $p \geq 0.05$	$r = 0.106$ $p \geq 0.05$	$r = 0.079$ $p \geq 0.05$

Note: BMI — body mass index.

of $CD14^{++}CD16^-$ cells was 89.4 [83.48–94.18]%, while in the group with stage IIB-IIIC cancer it was 94.2 [92.4–96.69]%, $p = 0.05$. These indicators for monocytes with the CD14-$CD16^+$ phenotype were higher in individuals with stage I-IIA compared to individuals with stage IIB–IIIC. The levels of $CD14^{++}CD16^-$ $CD163^+$ cells in patients with stage I–IIA were also higher than that of patients with stage IIB-IIIC, $p = 0.03$.

Parameters of $CD163^+$ and $HLA\text{-}DR^+$ expression on various monocyte populations were associated with the tumor molecular subtypes (Table 4). Thus, patients with triple-negative subtype (TNBC) were distinguished from the group of patients with luminal B and $Her2^+$ subtypes by reduced $CD14^+CD16^{++}HLA\text{-}DR^+$ cell counts. $Her2^+$ subtype, in turn, was characterized by elevated levels of $CD14^{++}CD16\text{-}CD163^+$ and $CD14^{++}CD16^+CD163^+$ cells compared to the same indicators of the joint group of patients with luminal/TNBC subtype ($p < 0.05$). The $CD14^+CD16^{++}HLA\text{-}DR^+$ content was also significantly higher in patients with $Her2^+$ tumors than in patients with luminal B and TNBC subtypes ($p < 0.05$). The group of patients with luminal B tumor subtype was distinguished from patients with luminal B and $Her2^+$ subtypes only by the reduced $CD14^{++}CD16^+CD163^+$ monocyte levels associated with luminal B cancer ($p < 0.05$).

The circulating blood cytokine profile is among important characteristics of the body determining its system-level functioning. Initially, serum levels of IL6, IL8 and MCP-1 cytokines were assessed in patients and healthy women. The analysis of MCP-1, IL6 and IL8 levels in blood serum showed that the group with BC was distinguished by elevated MCP-1 levels, specifically 0.32 [0.07–0.41] μg/mL, relative to the values of healthy women, 0.14 [0.12–0.27] μg/mL, $p = 0.002$ (Fig. 2).

The serum IL8 level of patients with BC was 70.1 [25.6–300.0] pg/μL, this value exceeded the value reported for the group of healthy women, 46.0 [16.3–113.0] pg/μL, $p =$

Table 3. Association of the disease stage with phenotypic characteristics of monocytes in patients with BC

	T1–2 ($n = 29$)	T3–4 ($n = 21$)	N0–1	N2–3	Stage I–IIA	Stage IIB–IIIC
$CD14^+16^-$, %	92.2 [83.7–94.58]	94.2 [92.1–96.88]	92.85 [83.7–96.69]	93.21 [89.28–96.13]	89.4 [83.48–94.18]	94.2 [92.4–96.69]
	$p = 0.15$		$p = 0.55$		$p = 0.05$	
$CD14^-16^+$, %	4.63 [1.3–10.23]	2.01 [1.24–2.41]	2.56 [1.3–9.13]	4.1 [1.51–5.8]	4.7 [2.56–11.41]	2.01 [1.44–2.44]
	$p = 0.04$		$p = 0.6$		$p = 0.01$	
$CD14^+16^+$, %	2.42 [1.3–10.23]	1.5 [1.24–5.49]	2.01 [1.24–5.16]	2.05 [0.48–5.6]	2.42 [1.13–5.6]	2.01 [1.28–3.42]
	$p = 0.63$		$p = 0.79$		$p = 0.54$	
$CD14^+16^-163^+$, %	94.63 [89.23–99.67]	96.74 [76.9–99.73]	94.63 [89.23–99.85]	96.74 [55.35–99.67]	92.94 [89.12–98.34]	97.98 [94.9–99.99]
	$p = 0.92$		$p = 0.65$		$p = 0.03$	
$CD14^+16^-$ $HLA\text{-}DR^+$, %	99.26 [97.34–99.9]	99.01 [96.65–99.81]	99.6 [98.08–99.9]	95.09 [87.7–99.01]	99.26 [97.34–99.99]	99.26 [98.09–99.93]
	$p = 0.48$		$p = 0.02$		$p = 0.93$	
$CD14^-16^+163^+$, %	98.77 [77.94–99.97]	69.81 [41.36–99.1]	99.6 [98.08–99.9]	50.0 [25.6–99.21]	89.89 [65.41–99.29]	98.08 [50.0–99.86]
	$p = 0.09$		$p = 0.15$		$p = 0.64$	
$CD14^-16^+$ $HLA\text{-}DR^+$, %	68.92 [54.06–87.73]	79.32 [55.08–93.31]	96.87 [69.81–99.97]	60.03 [37.0–79.32]	69.58 [54.06–85.91]	76.15 [60.03–93.13]
	$p = 0.37$		$p = 0.55$		$p = 0.36$	
$CD14^+16^+163^+$, %	98.0 [89.79–99.9]	98.7 [77.86–99.81]	76.15 [55.12–93.31]	98.7 [31.27–99.81]	96.19 [83.79–99.9]	99.18 [94.58–99.9]
	$p = 0.44$		$p = 0.16$		$p = 0.23$	
$CD14^+16^+$ $HLA\text{-}DR^+$, %	93.04 [80.43–98.44]	96.88 [89.85–98.47]	95.24 [88–98.47]	84.51 [55.0–97.5]	93.04 [86.99–98.28]	96.88 [84.51–98.44]
	$p = 0.48$		$p = 0.74$		$p = 0.86$	

Table 4. Phenotypic characteristics of blood monocytes depending on the tumor molecular subtype

	TNBC	Lum B/Her2+	*p*
CD14+16-, %	89.28 [79.79–96.13]	93.21 [92.1–96.69]	0.09
CD14-16+, %	4.1 [1.04–11.41]	2.41 [1.44–5.45]	0.1
CD14+16+, %	2.05 [1.39–6.43]	2.01 [1.13–3.89]	0.31
CD14+16-163+, %	94.63 [89.15–99.67]	95.34 [90.87–99.85]	0.76
CD14+16-HLA-DR+, %	99.26 [90.5–100.00]	99.26 [98.08–99.9]	0.23
CD14-16+163+, %	84.28 [50.00–99.29]	98.77 [53.47–100.0]	0.15
CD14-16+HLA-DR+, %	62.6 [53.4–84.06]	84.51 [60.03–96.33]	0.02
CD14+16+163+, %	98.06 [87.6–100.0]	98.00 [83.79–99.97]	0.19
CD14+16+HLA-DR+, %	95.67 [80.43–99.03]	93.14 [84.51–98.28]	0.54
	Her2+	Lum B/TNBC	
CD14+16-, %	94.2 [92.1–96.88]	92.4 [83.7–96.13]	0.63
CD14-16+, %	2.01 [0.15–4.7]	3.8 [1.51–9.13]	0.09
CD14+16+, %	1.28 [1.00–5.49]	2.05 [1.33–5.16]	0.08
CD14+16-163+, %	**99.67 [99.48–100.00]**	**94.3 [89.12–98.34]**	**0.04**
CD14+16-HLA-DR+, %	99.6 [99.26–99.00]	99.01 [96.65–99.99]	0.33
CD14-16+163+, %	99.86 [69.81–100.00]	91.28 [50.00–99.29]	0.62
CD14-16+HLA-DR+, %	**93.31 [60.03–98.81]**	**68.92 [54.06–85.91]**	**0.03**
CD14+16+163+, %	**100.00 [98.86–100.00]**	**96.19 [82.79–99.81]**	**0.02**
CD14+16+HLA-DR+, %	96.88 [80.43–99.71]	93.14 [84.51–98.44]	0.08
	Lum B	TNBC/Her2+	
CD14+16-, %	93.09 [88.64–94.58]	92.1 [86.7–96.13]	0.24
CD14-16+, %	2.56 [1.69–5.8]	3.65 [1.04–8.3]	0.55
CD14+16+, %	2.01 [1.24–3.3]	2.05 [1.28–5.6]	0.86
CD14+16-163+, %	94.3 [89.08–96.74]	98.34 [90.74–99.73]	0.09
CD14+16-HLA-DR+, %	99.01 [97.34– 99.93]	99.6 [98.09–99.99]	0.71
CD14-16+163+, %	98.08 [53.47–99.78]	89.89 [65.4–99.86]	0.65
CD14-16+HLA-DR+, %	76.15 [55.12–93.01]	69.58 [55.08–90.5]	0.09
CD14+16+163+, %	**95.83 [82.79–98.1]**	**99.81 [92.79–100.00]**	**0.04**
CD14+16+HLA-DR+, %	93.04 [84.51–98.06]	96.79 [86.99–99.03]	0.35

Note: TNBC — triple-negative breast cancer, Lum B — luminal B breast cancer, Her2+ –Her2neu-positive breast cancer

0.01. In contrast, blood levels of IL6 in patients were reduced from that of healthy individuals (23.3 [17.2–30.4] vs. 28.3 [24.3–33.4] pg/μL), but just at the trend level with $p = 0.06$.

The group of patients was divided into two subgroups with low (< Me) and high (≥ Me) biological factor levels in order to assess the nature of the relationship between serum MCP-1, IL8, IL6 levels and phenotypic features of monocytes associated with BC. No significant differences were revealed for MCP-1 and IL8, however, serum levels of IL6 were correlated to the monocyte phenotype. High IL6 levels were associated with the reduced share of CD14++CD16-CD163+, CD14++CD16-HLA-DR+ and CD14+CD16++HLA-DR+ monocytes, these were 91.29 [75.03–97.89]% vs. 99,12 [94.3–100.0]%, 98.09 [95,65–99,43]% vs. 99.93 [99.34–100.0]% and 48.06 [32.1–78.3]% vs. 93,01 [75.41–98.81]%, respectively. Thus, reduced HLA-DR expression on monocytes was typical for individuals with the decreased serum IL6 levels (Fig. 2B).

DISCUSSION

The neoplastic process extension (tumor size increase, regional lymph node or other organ metastasis) is a criterion of cancer progression. In our study the counts of CD14+CD16++ monocytes belonging to the non-classical population negatively correlated with the tumor size (Table 2). When assessing the association between the population structure and the stage we noted that a more advanced disease stage was characterized by lower CD14+CD16++ cell counts. An opposite trend was reported for the CD14++CD16- population predominating in blood: the CD14++CD16- counts increased with increasing disease stage (Table 3). Thus, the levels of CD163+ and HLA-DR+ monocytes were associated with a number of BC progression key factors, specifically with the disease stage and the presence of regional lymph node metastasis. Noteworthy is the fact that the levels of CD14+CD16++ cells potentially possessing antitumor activity are reduced. Thus, non-classical monocytes demonstrate the ability to suppress metastasis in murine models of lung cancer [17]. At the same time, the counts of CD14+CD16- cells being the source for replenishment of the tumor-associated macrophage pool increase [2, 4].

The CD14++CD16-HLA-DR+ monocyte population was associated with the regional lymph node involvement in the neoplastic process (Table 3). It is well-known that the CD14++CD16- population is recruited to perform the function of antigen-presenting cells in inflammatory response [18]. In individuals with BC, the regional lymph node involvement

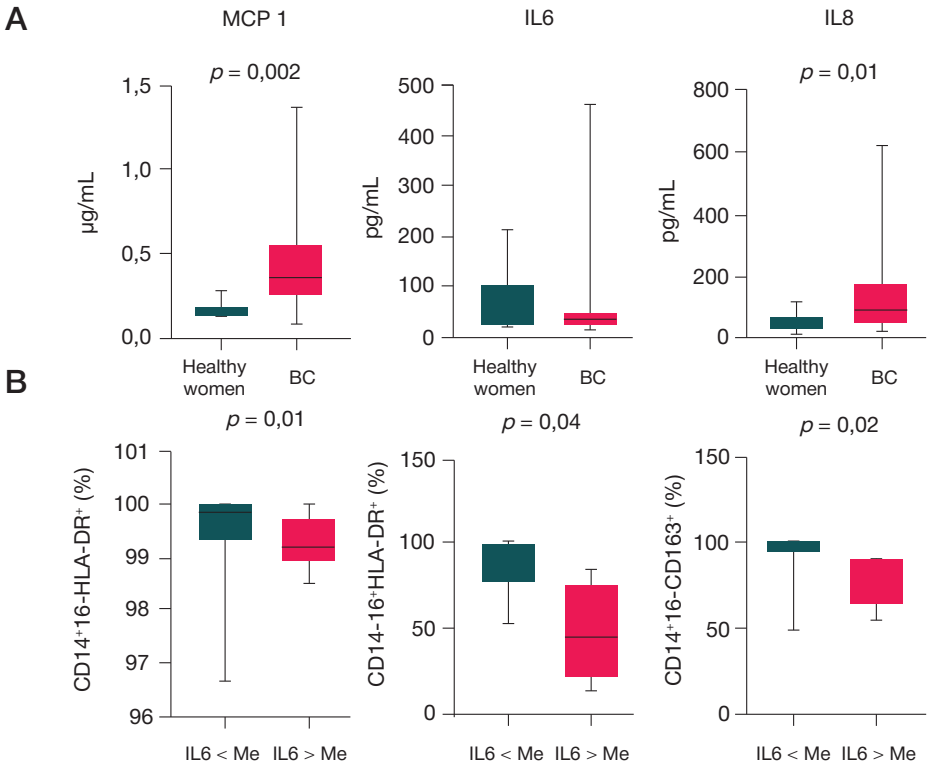

Fig. 2. Association of blood cytokine levels with circulating monocyte phenotype in breast cancer. **A**. Serum cytokine levels in patients with breast cancer and healthy women. **B**. Correlation of serum IL6 levels with the CD163+ and HLA-DR+ monocyte counts in breast cancer

is likely to stimulate generation of the $CD14^{++}CD16^{-}HLA\text{-}DR^{+}$ monocytes capable of maintaining the antitumor immune response. At the same time the disease progression expressed in the increase in malignancy stage is associated with the increase in the percentage of $CD14^{++}CD16^{-}CD163^{+}$ and $CD14^{++}CD16^{+}CD163^{+}$ cells, while the $CD14^{+}CD16^{++}CD163^{+}$ monocyte counts decrease with increasing tumor size (Tables 2, 3). It is noteworthy that the levels of $CD14^{++}CD16^{-}$ monocytes also positively correlate with the disease stage. We have earlier shown that the CD163 molecule expression is increased in monocytes of patients with BC, while in macrophages of the breast tumor this indicator increases in response to chemotherapy [19]. Furthermore, redistribution of monocyte counts between the $CD14^{++}CD16^{-}$ and $CD14^{+}CD16^{++}$ populations can be critical, which determines multidirectional changes in the counts of cells of these populations with increasing disease stage and tumor size. Among monocytes of classical population, the CD163 receptor-expressing cells have shown the association with clinical and morphological parameters. The latter suggest a pivotal role in BC pathogenesis played by the CD163 receptor-mediated mechanisms.

It has been shown that BC molecular subtypes show different immunogenicity [20]. Thus, the vast majority of TNBC subtypes are characterized by the increased mutational load and the content of tumor infiltrating lymphocytes being the criteria for prescription of immunotherapy drugs [21]. We have noted that monocyte population structure is correlated to the tumor molecular subtype. Thus, TNBC was characterized by the 1.4-fold decrease in the $CD14^{++}CD16^{-}HLA\text{-}DR^{+}$ cell counts (Table 4). At the same time, the $Her2^{+}$ subtype was characterized by the increased $CD14^{++}CD16^{-}HLA\text{-}DR^{+}$ monocyte counts. Thus, the differences between BC subtypes can be detected at the blood monocyte population level.

The soluble factors circulating in blood create a certain information environment capable of ensuring functional polarization of effectors and regulators of the immune system [22]. Assessment of the relationship between the serum levels of certain cytokines (IL6, IL8 and MCP-1) and the characteristics of monocyte population structure was performed for this purpose. Noteworthy is the increase in the concentration of the major MCP-1 monocyte migration factor in affected individuals, which is possibly associated with activation of monocyte recruitment to the tumor tissue (Fig. 2A). Despite the fact that we have noted no changes in blood levels of IL6 associated with BC, the relationship between the IL6 levels and the monocyte population structure has been revealed (Fig. 2A). It is interesting that the CD163 receptor expression on the $CD14^{++}CD16^{-}$ cells decreased along with the HLA-DR molecule expression, which had not been earlier reported in patients with BC and required further research. Patients with high IL6 levels had reduced $CD14^{++}CD16^{-}HLA\text{-}DR^{+}$ and $CD14^{+}CD16^{++}HLA\text{-}DR^{+}$ counts (Fig. 2B). IL6 exerts multidirectional effects on malignant neoplasms, it can both promote and inhibit tumor growth [23]. It has been shown that elevated serum levels of IL6 are a negative prognostic factor in patients with BC [23, 24]. Perhaps, the association between the levels of this cytokine and the decrease in the levels of monocytes performing antitumor functions can represent a possible explanation of the IL6 negative impact on the BC course (Fig. 2B). There is some evidence that monocytes showing low HLA-DR expression can differentiate into myeloid-derived suppressor cells suppressing the immune response [25]. The association of IL6 levels with the $HLA\text{-}DR^{+}$ monocyte counts is likely to be one of the mechanisms underlying the development of breast tumors and requires further research.

CONCLUSIONS

Thus, the study has shown that the disease progression is followed by redistribution of the major monocyte populations towards an increase in the classical population. Furthermore, elevated CD163 receptor expression on monocytes of the

classical population is typical for the advanced disease stage, while elevated HLA-DR expression, by contrast, is observed in individuals with no or minimal regional lymph node metastasis. The breast tumor molecular subtype is also related to the $CD163^{+}$ and $HLA\text{-}DR^{+}$ monocyte distribution across classical, intermediate, and non-classical populations. The decrease in HLA-DR expression on the $CD14^{++}CD16^{-}$ and $CD14^{+}CD16^{++}$ monocytes and CD163 expression on the $CD14^{++}CD16$ monocytes is associated with elevated serum IL6 levels in affected individuals. We believe that determination of monocyte population structure in patients with BC can contribute to the development of additional criteria for treatment tactics shaping. Further translational research focused on assessing the possibility of using the indicators of monocyte population characteristics in clinical practice for patients with BC is appropriate.

References

1. Ziegler-Heitbrock L. Blood monocytes and their subsets: established features and open questions. Frontiers in immunology. 2015; 6: 423.
2. Xin Fu MY. Monocytes in tumor: The perspectives of single-cell analysis. Tumor Discovery. 2022; 1 (1): 4.
3. Mildner A, Schönheit J, Giladi A, David E, Lara-Astiaso D, Lorenzo-Vivas E, et al. Genomic Characterization of Murine Monocytes Reveals C/EBPβ Transcription Factor Dependence of Ly6C(-) Cells. Immunity. 2017; 46 (5): 849–62.e7.
4. Kapellos TS, Bonaguro L, Gemünd I, Reusch N, Saglam A, Hinkley ER, et al. Human monocyte subsets and phenotypes in major chronic inflammatory diseases. Frontiers in immunology. 2019; 10: 2035.
5. Skytthe MK, Graversen JH, Moestrup SK. Targeting of CD163(+) Macrophages in Inflammatory and Malignant Diseases. International journal of molecular sciences. 2020; 21 (15).
6. Joshi I, Carney WP, Rock EP. Utility of monocyte HLA-DR and rationale for therapeutic GM-CSF in sepsis immunoparalysis. Frontiers in immunology. 2023; 14: 1130214.
7. Veglia F, Perego M, Gabrilovich D. Myeloid-derived suppressor cells coming of age. Nature immunology. 2018; 19 (2): 108–19.
8. Wang YA, Jian JW, Hung CF, Peng HP, Yang CF, Cheng HS, et al. Germline breast cancer susceptibility gene mutations and breast cancer outcomes. BMC cancer. 2018; 18 (1): 315.
9. Olsson HL, Olsson ML. The menstrual cycle and risk of breast cancer: a review. Frontiers in oncology. 2020; 10: 21.
10. Brown KA. Metabolic pathways in obesity-related breast cancer. Nature reviews Endocrinology. 2021; 17 (6): 350–63.
11. Byun D, Hong S, Ryu S, Nam Y, Jang H, Cho Y, et al. Early-life body mass index and risks of breast, endometrial, and ovarian cancers: a dose-response meta-analysis of prospective studies. British journal of cancer. 2022; 126 (4): 664–72.
12. Liu K, Zhang W, Dai Z, Wang M, Tian T, Liu X, et al. Association between body mass index and breast cancer risk: evidence based on a dose-response meta-analysis. Cancer management and research. 2018; 10: 143–51.
13. Koh J, Kim MJ. Introduction of a New Staging System of Breast Cancer for Radiologists: An Emphasis on the Prognostic Stage. Korean journal of radiology. 2019; 20 (1): 69–82.
14. Urru SAM, Gallus S, Bosetti C, Moi T, Medda R, Sollai E, et al. Clinical and pathological factors influencing survival in a large cohort of triple-negative breast cancer patients. BMC cancer. 2018; 18 (1): 56.
15. Morris RM, Mortimer TO, O'Neill KL. Cytokines: can cancer get the message? Cancers. 2022; 14 (9).
16. Niraula A, Sheridan JF. IL6 signaling in monocytes: a potential therapeutic avenue for stress-induced mood impairments. Chronic stress (Thousand Oaks, Calif). 2019; 3.
17. Hanna RN, Cekic C, Sag D, Tacke R, Thomas GD, Nowyhed H, et al. Patrolling monocytes control tumor metastasis to the lung. Science (New York, NY). 2015; 350 (6263): 985–90.
18. Lee J, Tam H, Adler L, Ilstad-Minnihan A, Macaubas C, Mellins ED. The MHC class II antigen presentation pathway in human monocytes differs by subset and is regulated by cytokines. PloS one. 2017; 12 (8): e0183594.
19. Patysheva M, Larionova I, Stakheyeva M, Grigoryeva E, Iamshchikov P, Tarabanovskaya N, et al. Effect of early-stage human breast carcinoma on monocyte programming. Frontiers in oncology. 2021; 11: 800235.
20. Stenmark Tullberg A, Sjöström M, Niméus E, Killander F, Chang SL, Feng FY, et al. Integrating Tumor-Intrinsic and Immunologic Factors to Identify Immunogenic Breast Cancers from a Low-Risk Cohort: Results from the Randomized SweBCG91RT Trial. Clinical cancer research : an official journal of the American Association for Cancer Research. 2023; 29 (9): 1783–93.
21. Loizides S, Constantinidou A. Triple negative breast cancer: Immunogenicity, tumor microenvironment, and immunotherapy. Frontiers in genetics. 2022; 13: 1095839.
22. Kartikasari AER, Huertas CS, Mitchell A, Plebanski M. Tumor-Induced Inflammatory Cytokines and the Emerging Diagnostic Devices for Cancer Detection and Prognosis. Frontiers in oncology. 2021; 11: 692142.
23. Knüpfer H, Preiss R. Significance of interleukin-6 (IL6) in breast cancer. Breast cancer research and treatment. 2007; 102 (2): 129–35.
24. Chen J, Wei Y, Yang W, Huang Q, Chen Y, Zeng K, et al. IL6: the link between inflammation, immunity and breast cancer. Frontiers in oncology. 2022; 12: 903800.
25. Chen J, Wei Y, Yang W, Huang Q, Chen Y, Zeng K, et al. IL6: the link between inflammation, immunity and breast cancer. Frontiers in oncology. 2022; 12: 903800.

Литература

1. Ziegler-Heitbrock L. Blood monocytes and their subsets: established features and open questions. Frontiers in immunology. 2015; 6: 423.
2. Xin Fu MY. Monocytes in tumor: The perspectives of single-cell analysis. Tumor Discovery. 2022; 1 (1): 4.
3. Mildner A, Schönheit J, Giladi A, David E, Lara-Astiaso D, Lorenzo-Vivas E, et al. Genomic Characterization of Murine Monocytes Reveals C/EBPβ Transcription Factor Dependence of Ly6C(-) Cells. Immunity. 2017; 46 (5): 849–62.e7.
4. Kapellos TS, Bonaguro L, Gemünd I, Reusch N, Saglam A, Hinkley ER, et al. Human monocyte subsets and phenotypes in major chronic inflammatory diseases. Frontiers in immunology. 2019; 10: 2035.
5. Skytthe MK, Graversen JH, Moestrup SK. Targeting of CD163(+) Macrophages in Inflammatory and Malignant Diseases. International journal of molecular sciences. 2020; 21 (15).
6. Joshi I, Carney WP, Rock EP. Utility of monocyte HLA-DR and rationale for therapeutic GM-CSF in sepsis immunoparalysis. Frontiers in immunology. 2023; 14: 1130214.
7. Veglia F, Perego M, Gabrilovich D. Myeloid-derived suppressor cells coming of age. Nature immunology. 2018; 19 (2): 108–19.
8. Wang YA, Jian JW, Hung CF, Peng HP, Yang CF, Cheng HS, et al. Germline breast cancer susceptibility gene mutations and breast cancer outcomes. BMC cancer. 2018; 18 (1): 315.
9. Olsson HL, Olsson ML. The menstrual cycle and risk of breast cancer: a review. Frontiers in oncology. 2020; 10: 21.

10. Brown KA. Metabolic pathways in obesity-related breast cancer. Nature reviews Endocrinology. 2021; 17 (6): 350–63.
11. Byun D, Hong S, Ryu S, Nam Y, Jang H, Cho Y, et al. Early-life body mass index and risks of breast, endometrial, and ovarian cancers: a dose-response meta-analysis of prospective studies. British journal of cancer. 2022; 126 (4): 664–72.
12. Liu K, Zhang W, Dai Z, Wang M, Tian T, Liu X, et al. Association between body mass index and breast cancer risk: evidence based on a dose-response meta-analysis. Cancer management and research. 2018; 10: 143–51.
13. Koh J, Kim MJ. Introduction of a New Staging System of Breast Cancer for Radiologists: An Emphasis on the Prognostic Stage. Korean journal of radiology. 2019; 20 (1): 69–82.
14. Urru SAM, Gallus S, Bosetti C, Moi T, Medda R, Sollai E, et al. Clinical and pathological factors influencing survival in a large cohort of triple-negative breast cancer patients. BMC cancer. 2018; 18 (1): 56.
15. Morris RM, Mortimer TO, O'Neill KL. Cytokines: can cancer get the message? Cancers. 2022; 14 (9).
16. Niraula A, Sheridan JF. IL6 signaling in monocytes: a potential therapeutic avenue for stress-induced mood impairments. Chronic stress (Thousand Oaks, Calif). 2019; 3.
17. Hanna RN, Cekic C, Sag D, Tacke R, Thomas GD, Nowyhed H, et al. Patrolling monocytes control tumor metastasis to the lung. Science (New York, NY). 2015; 350 (6263): 985–90.
18. Lee J, Tam H, Adler L, Ilstad-Minnihan A, Macaubas C, Mellins ED. The MHC class II antigen presentation pathway in human monocytes differs by subset and is regulated by cytokines. PloS one. 2017; 12 (8): e0183594.
19. Patysheva M, Larionova I, Stakheyeva M, Grigoryeva E, Iamshchikov P, Tarabanovskaya N, et al. Effect of early-stage human breast carcinoma on monocyte programming. Frontiers in oncology. 2021; 11: 800235.
20. Stenmark Tullberg A, Sjöström M, Niméus E, Killander F, Chang SL, Feng FY, et al. Integrating Tumor-Intrinsic and Immunologic Factors to Identify Immunogenic Breast Cancers from a Low-Risk Cohort: Results from the Randomized SweBCG91RT Trial. Clinical cancer research : an official journal of the American Association for Cancer Research. 2023; 29 (9): 1783–93.
21. Loizides S, Constantinidou A. Triple negative breast cancer: Immunogenicity, tumor microenvironment, and immunotherapy. Frontiers in genetics. 2022; 13: 1095839.
22. Kartikasari AER, Huertas CS, Mitchell A, Plebanski M. Tumor-Induced Inflammatory Cytokines and the Emerging Diagnostic Devices for Cancer Detection and Prognosis. Frontiers in oncology. 2021; 11: 692142.
23. Knüpfer H, Preiss R. Significance of interleukin-6 (IL6) in breast cancer. Breast cancer research and treatment. 2007; 102 (2): 129–35.
24. Chen J, Wei Y, Yang W, Huang Q, Chen Y, Zeng K, et al. IL6: the link between inflammation, immunity and breast cancer. Frontiers in oncology. 2022; 12: 903800.
25. Chen J, Wei Y, Yang W, Huang Q, Chen Y, Zeng K, et al. IL6: the link between inflammation, immunity and breast cancer. Frontiers in oncology. 2022; 12: 903800.

CYP2D6*3, *4, *6 GENOTYPES AND ENDOMETRIAL THICKNESS IN PATIENTS WITH BREAST CANCER DURING TAMOXIFEN THERAPY

Goryainova AYu[1,2] ✉, Usman NYu[3], Rubanovich AV[4], Borinskaya SA[4], Meshcheryakov AA[5]

[1] Clinical Oncologic Dispensary № 1, Krasnodar, Russia
[2] Kuban State Medical University, Krasnodar, Russia
[3] Kulakov National Medical Research Center for Obstetrics, Gynecology and Perinatology, Moscow, Russia
[4] Vavilov Institute of General Genetics Russian Academy of Sciences, Moscow, Russia
[5] Lopukhin Federal Research and Clinical Center of Physical-Chemical Medicine of Federal Medical Biological Agency, Moscow, Russia

Tamoxifen therapy results in endometrial thickening in some patients with hormone-sensitive breast cancer (HSBC). The data on the impact of polymorphic variants of the *CYP2D6* gene encoding the CYP2D6 enzyme of the cytochrome P450 family on the efficacy and safety of treatment with tamoxifen are controversial. A prospective cohort study was aimed to explore the association of *CYP2D6*3, *4, *6* polymorphisms with the risk of endometrial thickness during adjuvant tamoxifen therapy for HSBC. A total of 145 patients with resectable HSBC, who received 20 mg of oral tamoxifen per day, were enrolled. The *CYP2D6*3, *4, *6* polymorphisms were identified by real-time PCR. Endometrial thickness was measured by ultrasonography after 3, 6 and 9 months of endocrine therapy. The study showed that endometrial hyportrophy was more often found in patients having no alternative alleles after 3 months of follow-up (40% against 23.2% in the group of "poor" metabolizers; $p = 0.034$). Meta-analysis of all follow-up periods has revealed that "normal" metabolizers show a significantly higher rate of endometrial thickness than "poor" metabolizers (OR = 1.88; 95% CI = 1.27–2.79; $p = 0.002$). A lack of significant differences in indicators of the state of endometrium between groups of patients with different *CYD2D6* genotypes and menopausal status requires further investigation.

Keywords: breast cancer, tamoxifen, endometrial thickness, CYP2D6, endocrine therapy

Funding: medical piece of research was conducted without sponsor's support as part of the Inter-organization agreement concerning non-profit scientific collaboration. Molecular genetic testing and statistical analysis were conducted as part of the publicly funded project "Study of Polymorphism at the Cellular, Organism and Population Levels as a Basis for Genetic Technology Development" (№ 122022600161-3).

Author contribution: Goryainova AYu — study design, data acquisition, statistical processing of the results, review of papers on the subject, manuscript writing; Usman NYu — selection of genotyping method and molecular genetic analysis; Rubanovich AV — statistical processing of the results; Borinskaya SA — literature review, molecular genetic testing, interpretation of the results, manuscript editing; Meshcheryakov AA — study concept and design, manuscript editing.

Compliance with ethical standards: the study was approved by the Ethics Committee of the Blokhin National Medical Research Center of Oncology (protocol № 10 dated 26 December 2019). Anonymized patient information was acquired and processed. Personal and medical data were not subject to transfer to a third party or to disclosure in the study results. All patients submitted the informed consent to study participation.

✉ **Correspondence should be addressed:** Alla Yu. Goryainova
Dimitrov, 146, Krasnodar, 350040, Russia; mashelueva@yandex.ru

Received: 28.09.2023 **Accepted:** 20.10.2023 **Published online:** 29.10.2023

DOI: 10.24075/brsmu.2023.041

ГЕНОТИПЫ CYP2D6*3, *4, *6 И ГИПЕРТРОФИЯ ЭНДОМЕТРИЯ У БОЛЬНЫХ РАКОМ МОЛОЧНОЙ ЖЕЛЕЗЫ НА ФОНЕ ТЕРАПИИ ТАМОКСИФЕНОМ

А. Ю. Горяинова[1,2] ✉, Н. Ю. Усман[3], А. В. Рубанович[4], С. А. Боринская[4], А. А. Мещеряков[5]

[1] Клинический онкологический диспансер № 1 Министерства здравоохранения Краснодарского края, Краснодар, Россия
[2] Кубанский государственный медицинский университет Министерства здравоохранения РФ, Краснодар, Россия
[3] Национальный медицинский исследовательский центр акушерства, гинекологии и перинатологии имени В. И. Кулакова, Москва, Россия
[4] Институт общей генетики имени Н. И. Вавилова Российской академии наук, Москва, Россия
[5] Федеральный научно-клинический центр физико-химической медицины имени академика Ю. М. Лопухина Федерального медико-биологического агентства, Москва, Россия

Терапия тамоксифеном у части пациенток с гормоночувствительным раком молочной железы (ГР+РМЖ) приводит к увеличению толщины эндометрия. Данные о влиянии полиморфных вариантов в гене *CYP2D6*, кодирующем фермент CYP2D6 семейства цитохрома Р450, на эффективность и безопасность лечения тамоксифеном противоречивы. Целью проспективного когортного исследования было изучение ассоциации полиморфизмов *CYP2D6*3, *4, *6* с риском развития гипертрофии эндометрия в процессе адъювантной терапии тамоксифеном по поводу ГР+РМЖ. В исследование включено 145 больных операбельным ГР+РМЖ, получавших тамоксифен в дозировке 20 мг в сутки перорально. Полиморфизмы *CYP2D6*3, *4, *6* определены методом ПЦР в режиме реального времени. Проводили измерение толщины эндометрия ультразвуковым методом через 3, 6 и 9 месяцев гормонотерапии. В исследовании показано, что гипертрофию эндометрия чаще наблюдали у больных без альтернативных аллелей на этапе 3 месяцев наблюдения (40% по сравнению с 23,2% в группе «слабых метаболизаторов»; $p = 0,034$). Метаанализ всех периодов наблюдения показал, что среди «нормальных метаболизаторов» наблюдается значимо более высокая частота случаев гипертрофии эндометрия по сравнению со «слабыми метаболизаторами» (ОШ = 1,88; 95%ДИ = 1,27–2,79; $p = 0,002$). Отсутствие статистически значимых различий в показателях состояния эндометрия между группами пациенток с различным *CYD2D6*-генотипом в зависимости от менопаузального статуса требуют проведения дополнительных исследований.

Ключевые слова: рак молочной железы, тамоксифен, гипертрофия эндометрия, CYP2D6, гормонотерапия

Финансирование: медицинская часть исследования проведена без спонсорской поддержки в рамках межцентрового соглашения о некоммерческом научном сотрудничестве. Молекулярно-генетическая и статистическая часть исследования проведена в рамках темы бюджетного финансирования «Исследования полиморфизма на клеточном, организменном и популяционном уровне как основа создания генетических технологий» № 122022600161-3.

Вклад авторов: А. Ю. Горяинова — разработка дизайна исследования, сбор полученных данных, статистическая обработка результатов, обзор публикаций по теме статьи, написание текста рукописи; Н. Ю. Усман — выбор методики генотипирования и проведение молекулярно-генетического анализа; А. В. Рубанович — статистическая обработка результатов; С. А. Боринская — анализ литературы, молекулярно-генетическое тестирование, интерпретация результатов, редактирование рукописи статьи; А. А. Мещеряков — разработка концепции и дизайна исследования, редактирование рукописи статьи.

Соблюдение этических стандартов: исследование одобрено этическим комитетом при ФГБУ «НМИЦ онкологии имени Н. Н. Блохина» Минздрава России (протокол № 10 от 26 декабря 2019 г.). Информация о больных была собрана и обработана в обезличенном виде. Персональные и медицинские данные не подлежали передаче третьим лицам, а также разглашению в результатах исследования. Все пациентки подписали информированное согласие на участие в исследовании.

✉ **Для корреспонденции:** Алла Юрьевна Горяинова
ул. Димитрова, д. 146, г. Краснодар, 350040, Россия; mashelueva@yandex.ru

Статья получена: 28.09.2023 **Статья принята к печати:** 20.10.2023 **Опубликована онлайн:** 29.10.2023

DOI: 10.24075/vrgmu.2023.041

Reduction of the hormone-sensitive breast cancer (HSBC) relapse risk by more than a third, significant decrease in the probability of death from this disease, and cost-effectiveness make tamoxifen hold a leading position in adjuvant endocrine therapy [1–3]. However, prolonged use of tamoxifen is associated with the risk of pathological processes in the reproductive organs [4–7].

Some studies consider tamoxifen as an independent risk factor of endometrial abnormalities, explaining this by partly estrogen-like effects of the drug, identify obesity as an inducing factor, and do not fully disclose biological mechanisms of this phenomenon [8–12]. There is an opinion that hyperestrogenism associated with obesity contributes to the development of endometrial disorder by creating low-grade inflammation in the reproductive system tissue and modulating endometrial microenvironment, thereby promoting carcinogenesis [13].

The role of tamoxifen effects on the currently known estrogen receptors (ERα, ERβ, GPER or 7-transmembrane G protein-coupled estrogen receptor) is actively discussed in the literature, along with activation and blocking of the mechanisms underlying the estrogen receptor signal transmission, since the lack of selectivity towards all types of receptors results in the emergence of multiple pharmacoterapeutic problems and severe side effects of therapy [14].

A number of studies focused on the role of tamoxifen metabolism involving the cytochrome P450 system enzymes in the development of endometrial disorders yielded ambiguous results [15, 16]. We have assumed that the development of disorder in the form of endometrial thickness during tamoxifen therapy for HSBC can be due to the features of metabolic profile of each specific patient related to different allele variants of the *CYP2D6* gene. To date, more than 40 alleles of this gene determining the decreased or no enzyme activity have been reported. Of the latter, the *CYP2D6 *4* allele is most often found in the populations of Caucasoid origin (frequency 20%), the next most common alleles are *3 and *6 (2 and 0.9%, respectively) [17].

The study was aimed to explore the association of the *CYP2D6* polymorphic variants for alleles **3, *4 *6* with endometrial thickness in patients receiving tamoxifen adjuvant endocrine therapy for HSBC.

METHODS

The study was conducted at Clinical Oncologic Dispensaru № 1 between January 2020 and September 2022. The molecular genetic part of the study was conducted in Vavilov Institute of General Genetics Russian Academy.

A total of 145 patients with resectable HSBC, who received combination or complex therapy followed by prescription of standard tamoxifen endocrine therapy (20 mg of oral tamoxifen per day every day), were enrolled. Inclusion criteria: the patients enrolled had no history of endocrine therapy, they did not use concomitant medications, including CYP2D6 inhibitors. Exclusion criteria: patients, who missed scheduled check-up, stopped using tamoxifen due to any reasons, refused to participate in the study during any phase, were excluded. Clinical protocols of patient management were compliant with the guidelines of the Ministry of Health of the Russian Federation on the diagnosis and treatment of breast cancer [18]. All patients were subjected to gynecological examination that included pelvic ultrasound scan before breast cancer treatment to rule out abnormalities of the reproductive organs. All patients were characterized in terms of anthropometric, anamnestic, clinical, morphological, and immunohistochemical parameters. Buccal epithelial samples were collected from the fasting patients before the start of tamoxifen therapy in accordance with the general rules of collecting biomaterial for genetic tests with mandatory labeling of each sample with the specific code reproducing the data from the roster. DNA was isolated by phenol–chloroform extraction in accordance with the general rules [19]. Genotyping by *CYP2D6*3, *4, *6* alleles was performed by real-time polymerase chain reaction (PCR) using the reagent kit for identification of the *CYP2D6* allele variants (catalogue number RUO-R1-H990-N3/4, DNA Technology TC; Russia) in accordance with the manufacturer's instructions. To perform statistical data processing, carriers of the *CYP2D6* alleles associated with normal enzyme activity were allocated to the group referred to as "normal" metabolizers, while carriers of *CYP2D6* alleles associated with reduced enzyme activity (homo- and heterozygotes) were allocated to the group referred to as "poor" metabolizers; the groups were relatively balanced.

The patients receiving tamoxifen therapy were examined on the milestone dates 3, 6 and 9 month after the start of therapy. In addition to common tests performed in accordance with the guidelines, transvaginal ultrasound involving measurement of endometrial thickness was performed in all patients with preserved menstrual cycle on days 5–7 of the cycle; in patients with amenorrhea, ultrasonography was performed routinely at the end of the 3-month interval. Eight millimeters in premenopausal patients and 5 mm in patients with amenorrhea were considered to be threshold values in accordance with the recommended standards of the endometrial disorder diagnosis [20, 21]. When forming subgroups based on the menstrual function status, patient with regular or irregular menorrhagia during endocrine therapy with tamoxifen were allocated to the premenopausal group, while patients receiving therapy, who had no menstruation throughout the follow-up period, including postmenopausal patients, were allocated to the amenorrhea group.

Statistical analysis and data visualization were performed using the R 4.2.2 environment for statistical computing (R Foundation for Statistical Computing; Austria). Descriptive statistics were presented as relative frequency of observations for qualitative variables and the mean (standard deviation) and median (1st and 3rd quartiles) for quantitative ones. When

Table 1. Frequencies of *CYP2D6* genotypes and alleles in the studied group of patients

Polymorphism	Genotype frequency, % (*n*)			Allele frequency (%) and statistical error (± se)		χ^2 (*p*)*
CYP2D6*3 (c.2549delA / rs35742686)	A/A	A/del	del/del	A	del	
	98.6 (143)	1.4% (2)	0	99.7 ± 0.7	0.7 ± 0.7	0.01 (0.933)
CYP2D6*4 (c.1846G > A / rs3892097)	A/A	A/G	G/G	A	G	
	4.8 (7)	39.3 (57)	55.9 (81)	24.5 ± 3.6	75.5 ± 3.6	0.58 (0.447)
CYP2D6*6 (c.1707delT / rs5030655)	T/T	T/del	del/del	T	del	
	97.2 (141)	2.8 (4)	0	98.6 ± 1.0	1.4 ± 1.0	0.03 (0.866)

Note: * — chi-squared test for deviations from Hardy–Weinberg equilibrium.

Table 2. Characteristics of the studied group of patients considering *CYP2D6* genotype

Characteristics	All patients *n* = 145	"Normal" metabolizers *n* = 76	"Poor" metabolizers *n* = 69	*p**
Demographic and anthropometric characteristics. The upper row contains the mean (SD), the lower row contains the mediana (1st–3rd quartiles)				
Age (years)	47.4 (6.2) 47 (44–51)	47.6 (5.9) 47 (44–52)	47.1 (6.5) 47 (43–51)	0.511
Body weight (kg)	73 (15.6) 72 (62–80)	72.9 (12.9) 72 (64–80)	73 (18.2) 72 (61–80)	0.602
Body length (cm)	164.6 (7.9) 164 (162–169)	164.4 (6.1) 164 (160–168)	164.7 (9.5) 164 (162–169)	0.19
Body mass index (kg/m^2)	27.6 (13.1) 25.6 (22.7–30.1)	27.1 (5.5) 25.9 (23–30.1)	28.2 (18.2) 25 (22.1–30.1)	0.576
Anamnestic characteristics				
Smoking				0.396
Never-smokers	101 (69.7%)	56 (73.7%)	45 (65.2%)	
Former smokers	28 (19.3%)	11 (14.5%)	17 (24.6%)	
Current smokers	16 (11%)	9 (11.8%)	7 (10.1%)	
Clinical, morphological and immunohistochemical characteristics				
T. primary tumor size				0.231
1	82 (56.6%)	47 (61.8%)	35 (50.7%)	
2	46 (31.7%)	21 (27.6%)	25 (36.2%)	
3	5 (3.4%)	2 (2.6%)	3 (4.3%)	
4	12 (8.3%)	6 (7.9%)	6 (8.7%)	
N, presence, absence and prevalence of regional lymph node metastasis				0.963
	76 (52.4%)	39 (51.3%)	37 (53.6%)	
1	54 (37.2%)	30 (39.5%)	24 (34.8%)	
2	13 (9%)	6 (7.9%)	7 (10.1%)	
3	2 (1.4%)	1 (1.3%)	1 (1.4%)	
G, tumor grade				0.974
Grade 1	28/143 (19.6%)	15/74 (20.3%)	13/69 (18.8%)	
Grade 2	88/143 (61.5%)	45/74 (60.8%)	43/69 (62.3%)	
Grade 3	27/143 (18.9%)	14/74 (18.9%)	13/69 (18.8%)	
Estrogen receptor expression in tumor tissue showing its sensitivity to endocrine therapy, %				0.864
1–20	6 (4.1%)	3 (3.9%)	3 (4.3%)	
21–30	1 (0.7%)	0 (0.0%)	1 (1.4%)	
≥ 31	138 (95.2%)	73 (96.1%)	65 (94.2%)	
Progesterone receptor expression in tumor tissue showing its sensitivity to endocrine therapy, %				0.37
1–20	30 (20.7%)	17 (22.4%)	13 (18.8%)	
21–30	2 (1.4%)	1 (1.3%)	1 (1.4%)	
≥ 31	113 (77.9%)	58 (76.3%)	55 (79.7%)	
Human epidermal growth factor receptor 2 (HER-2/neu) expression status				0.069
0	74 (51%)	36 (47.4%)	38 (55.1%)	
1	52 (35.9%)	28 (36.8%)	24 (34.8%)	
2	6 (4.1%)	2 (2.6%)	4 (5.8%)	
3	13 (9%)	10 (13.2%)	3 (4.3%)	
Tumor proliferative activity (Ki-67 index) showing the percentage of actively dividing tumor cells, %				0.629
1–20	108 (74.5%)	57 (75.0%)	51 (73.9%)	
21–30	20 (13.8%)	9 (11.8%)	11 (15.9%)	
≥ 31	17 (11.7%)	10 (13.2%)	7 (10.1%)	
Chemotherapy				0.598
Not used	68 (46.9%)	37 (48.7%)	31 (44.9%)	
Used	77 (53.1%)	39 (51.3%)	38 (55.1%)	
Ovarian suppression				0.293
Not used	104 (72.2%)	57 (76%)	47 (68.1%)	
Used	40 (27.8%)	18 (24%)	22 (31.9%)	
Menstrual function before treatment				0.854
No	48 (33.1%)	26 (34.2%)	22 (31.9%)	
Preserved	97 (66.9%)	50 (65.8%)	47 (68.1%)	
Menstrual function during endocrine therapy				0.441
No	112 (77.2%)	56 (73.7%)	56 (81.2%)	
Preserved	33 (22.8%)	20 (26.3%)	13 (18.8%)	

Note: * — comparison of "normal" and "poor" metabolizer groups based on the Mann–Whitney U test (quantitative characteristics) and Fisher's exact test (nominal characteristics).

Table 3. Endometrial thickness (mm) based on ultrasonography data in the groups of patients considering the *CYP2D6* genotype

Period	"Normal" metabolizers	"Poor" metabolizers	*p***
All patients			
3 months	6.0 (4.0–10.0) *	5 (3.0–8.0)	0.131
6 months	7.0 (5.0–11.0)	6.0 (4.0–9.5)	0.122
9 months	8.0 (5.0–12.0)	6.0 (4.0–9.5)	0.088
*p****	0. 00045	0.005	
Premenopausal			
3 months	6 (3.75–10.25)	5 (4.0–8.0)	0.24
6 months	7 (5.0–11.25)	6 (4.0–9.0)	0.124
9 months	7 (4.75–12.25)	6 (4.0–9.0)	0.159
*p****	0.02	0.062	
Amenorrhea			
3 months	6 (4.0–8.5)	4.5 (3.0–8.5)	0.313
6 months	9 (5.0–11.0)	7 (4.0–12.25)	0.78
9 months	9 (5.0–11.5)	6.5 (3.75–11.25)	0.454
*p****	0.005	0.021	

Note: * — median values and qurtiles (25% and 75%) are provided; ** — comparison of "normal" and "poor" metabolizer groups based on the Mann–Whitney U test; *** — comparison of "3 months" and "9 months" groups for "normal" and "poor" metabolizers based on the Mann–Whitney U test.

comparing basic characteristics, the Mann–Whitney U test and Fisher's exact test were used for quantitative and qualitative variables, respectively. Comparative analysis of binary indicators involved the use of the mixed effects logistic regression models, which included the term of interaction between the group indicator and the follow-up period, as well as the odds ratio (OR) with appropriate 95% confidence interval (95% CI) as the effect size measure. Meta-analysis of all follow-up periods was conducted in accordance with the Mantel-Haenszel Fixed Effects model. The differences were considered significant at $p < 0.05$.

RESULTS

Genotypes for *CYP2D6* polymorphysms associated with reduced tamoxifen metabolism that are most common in the Russian population have been determined in the patients enrolled: alleles **3, *4* and **6* (Table 1) [22]. The determined allele frequencies are close to that reported for the population of Caucasoid origin [17].

Genotypes associated with reduced enzyme activity were found in eight individuals (5.5%): seven A/A *CYP2D6*4* homozygotes and one compound heterozygote (T/del *CYP2D6*6* / A/G *CYP2D6*4*). Other patients turned out to be homozygous for alleles determining normal enzyme activity (74 individuals, 51.0%) or heterozygous for one of the studied polymorphisms (63 individuals, 43.5%). Patients were divided into two balanced groups based on the presence/absence of nonfunctional CYP2D6 alleles.

No significant association of the risk of endometrial thickness with age 3 months (OR = 1.02 [95% CI: 0.97; 1.06], $p = 0.51$), 6 months (OR = 1.03 [95% CI: 0.98; 1.07],

Table 4. Rate of endometrial thickness in the groups of patients considering the *CYP2D6* genotype

Period	"Normal" metabolizers	"Poor" metabolizers	Comparison of "normal" and "poor" metabolizers: OR (*p*)
All patients *n* = 76 *n* = 69			
3 months	30 (40.0%)	16 (23.2%)	2.21 (0.034)
6 months	39 (52.0%)	26 (37.7%)	1.79 (0.096)
9 months	37 (49.3%)	25 (36.2%)	1.71 (0.131)
Comparison of 3 and 9 months: *OR* (*p*)	1.46 (0.324)	1.88 (0.136)	
Premenopausal *n* = 50 *n* = 47			
3 months	17 (34.0%)	9 (19.1%)	2.18 (0.114)
6 months	21 (42.0%)	12 (25.5%)	2.11 (0.133)
9 months	18 (36.0%)	12 (25.5%)	1.64 (0.282)
Comparison of 3 and 9 months: *OR* (*p*)	1.09 (1)	1.45 (0.621)	
Amenorrhea *n* = 26 *n* = 22			
3 months	13 (52.0%)	7 (31.8%)	2.32 (0.238)
6 months	18 (72.0%)	14 (63.6%)	1.47 (0.755)
9 months	19 (76.0%)	13 (59.1%)	2.19 (0.347)
Comparison of 3 and 9 months: *OR* (*p*)	2.92 (0.140)	3.1 (0.129)	

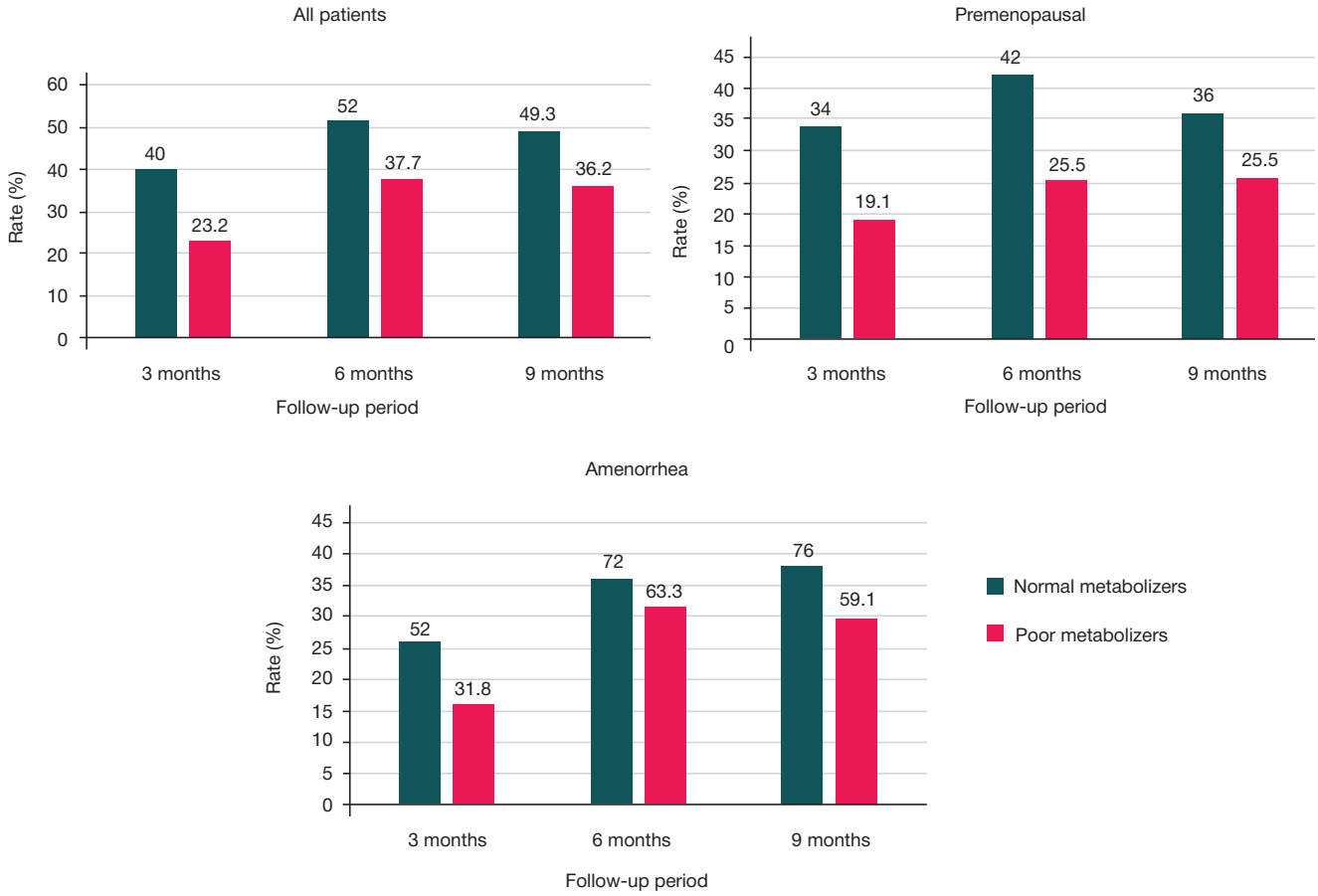

Fig. Rate of endometrial thickness in the general group and subgroups of patients depending on menopausal status and *CYP2D6* genotype

p = 0.292) and 9 months after using tamoxifen (OR = 1.0 [95% CI: 0.95; 1.04], *p* = 0.884), with body mass index after 3 months (OR = 1 [95% CI: 0.99; 1.02], *p* = 0.671), 6 months (OR = 1 [95% CI: 0.99; 1.02], *p* = 0.901) and 9 months of treatment (OR = 1 [95% CI: 0.99; 1.01], *p* = 0.99). Smoking status, clinical characteristics (primary tumor size, having or not having a history of chemotherapy, using ovarian suppression), as well as histological and immunohistochemical characteristics of breast tumor (primary lesion size, number of lymph nodes involved, estrogen and progesterone receptor expression, proliferative activity index, HER-2/neu status) were not considered to be significant predictors of endometrial hepertrophy in the studied cohort (Table 2).

Endometrial thickness was greater in "normal" metabolizers than in "poor" ones in all groups, however, the differences were non-significant (Table 3).

Among patients with amenorrhea, the increase in endometrial thickness after 9 months of tamoxifen therapy relative to that after 3 months of treatment was reported in both "normal" (the differences between mean values were 1.64 [95% CI: 0.269; 1.97] cm (*p* = 0.011) and 1.64 [95% CI: 0.683; 2.60] cm (*p* = 0.001), respectively) and "poor" metabolizers (the differences were 0.83 [95% CI: 0.01; 1.65] cm (*p* = 0.05) and 1.36 [95% CI: 0.46; 2.37] cm (*p* = 0.004), respectively).

No significant differences in the dynamics of thickening were revealed in the overall cohort (*p* = 0.052), premenopausal patients (*p* = 0.532) and patients with amenorrhea (*p* = 0,366) (Table 4; Fig.).

Higher rate of endometrial thickness cases in "normal" metabolizers relative to "poor" metabolizer was always reported in the studied cohort, however, the increase was significant only at around 3 months in all patients (OR = 2.21; *p* = 0.034). Regularity of these differences enables meta-analysis of three follow-up periods per group of patients (Table 5). The analysis has revealed a significant increase in the rate of endometrial thickness cases in "normal" metabolizers relative to "poor" ones (OR = 1.88; 95% CI = 1.27–2.79; *p* = 0.002).

DISCUSSION

Tamoxifen is a prodrug, the transformation of which into endoxifen, its most important metabolite, is ensured mainly by the CYP2D6 enzyme [23, 24]. Polymorphic variants of eponymous gene encoding the enzyme can cause changes in its enzyme activity associated with different tamoxifen efficacy in carriers of certain alleles [25]. However, the research data are ambiguous; the debate about the CYP2D6 genotyping clinical significance and interpretation of the results continues in the literature [26]. The impact of differences in tamoxifen metabolism on the treatment adherence is also discussed: early discontinuation of tamoxifen therapy decided by patient herself due to side effects affects the outcome of breast cancer treatment [27]. At the same time, little attention is paid to the issue of the association between the risk of side effects, including endometrial abnormalities, and the levels of CYP2D6 enzyme activity: sporadic small studies provide insufficient coverage of the issue [27–29].

In this paper we have tried to trace the risk of such adverse effect of tamoxifen therapy, as endometrial thickness in patients carrying various *CYP2D6* alleles found in the populations of Caucasoid origin and responsible for reduced tamoxifen metabolism [30]. There were no correlations between the *CYP2D6*3, *4, *6* alleles and such factors, as baseline tumor size, number of the lymph node involved, histological and

Table 5. Meta-analysis of differences in the rate of endometrial thickness between "normal" and "poor" metabolizers for all follow-up periods

Groups	OR (Mantel-Haenszel odds ratio)	95% CI	*p* (Fisher's exact test)
All patients	1.88	1.27–2.79	0.002
Premenopausal	1.95	1.17–3.26	0.014
Menopausal	1.96	0.97–3.97	0.089

immmunohistochemical characteristics of primary tumor, body mass index, smoking, in the studied group of patients. However, as for the association of the studied alleles with endometrial thickness and the rate of thickness, the findings suggest that patients with amenorrhea having no enzyme activity reducing alleles show a more frequent and prominent endometrial thickening depending on the endocrine therapy duration. Therefore, a cumulative effect of high endoxifen concentration is observed in the postmenopausal "normal" metabolizers.

Endometrial thickness was more often found in patients, who had no enzyme activity reducing alleles, after 3 months of follow-up (40% against 23.2% in the group of "poor" metabolizers; $p = 0.034$). Perhaps, three months of treatment with tamoxifen were enough for realization of the main estrogen-like effect of tamoxifen. The lack of data on endometrial thickness before the start of tamoxifen therapy is considered to be a problem of the study design. Future studies should involve conducting additional ultrasound examination of the uterus before using tamoxifen.

Premenopausal patients turned out to show minor dynamic changes in endometrial thickness, since endometrium was shed every time during menstruation. Ultrasonography enabled imaging of abnormal endometrium only, however, more time was probably required to form it. We performed ultrasound scan in the first phase of the menstrual cycle. In the future it is necessary to provide for ultrasound scan in the middle of the cycle in premenopausal patients, i.e. during the period characterized by maximum effects of estrogens and estrogen-like substances. This will enable a more precise investigation of estrogen-like tamoxifen activity. However, premenopausal patients having alternative alleles showed lesser endometrial thickness compared to premenopausal patients with no metabolism reduction. It can be assumed that tamoxifen exhibits temporary (within the menstrual cycle) estrogen-like effect in "normal" metabolizers.

The correlation between the *CYP2D6* genotype and endometrial thickness can be affected by endocrine factors, however, to date the impact of endoxifen concentrations on the ovarian, tissue steroidogenesis and regulation of the hypothalamic-pituitary axis is poorly understood. The lack of understanding of endocrine mechanisms along with trying to disconnect the interconnected factors may have been a limitation of the earlier studies yielding conflicting results. The role of hyperestrogenism in endometrial abnormalities has been proven [31], that is why it makes sense to clarify whether tamoxifen metabolism involving CYP2D6 is a factor contributing to formation of hyperestrogenic environment via stimulation of ovarial or tissue steroidogenesis.

CONCLUSIONS

The CYP2D6 enzyme metabolic activity alteration resulting from *CYP2D6*3, *4, *6* polymorphisms can modify the risk of endometrial thickness associated with tamoxifen therapy for HSBC, however, in these studies only trends have been revealed. The findings underscore the need for further study of the CYP2D6 enzyme activity with the better design and larger cohort of patients. The search for extraneous tamoxifen effects, primarily effects on ovarial steroidogenesis, and additional factors, with which pharmacogenetic testing will show maximum clinical significance, seems promising.

References

1. Protasova AE, Solntseva IA, Tsypurdeyeva AA, Semiglazova TYu, Stenina MB, Yureneva SV, et al. Substantiated approaches to the diagnosis and treatment of tamoxifen-induced endometrial conditions in patients with breast cancer.Journal of obstetrics and women s diseases. 2018; 67 (6): 69–78. Russian.
2. Krauss K, Stickeler E. Endocrine therapy in early breast cancer. Breast Care. 2020; 15 (4): 337–46.
3. Wijayabahu AT, Egan KM, Yaghjyan L. Uterine cancer in breast cancer survivors: A systematic review. Breast Cancer Research and Treatment. 2020; 180 (1): 1–9.
4. Shakhlamova MN, Isaeva EA, Pankratov VV. Eetiology and pathogenesis of hyperplastic processes of the endometrium in the postmenopause. Vopr. ginekol. akus. perinatol. (Gynecology, Obstetrics and Perinatology). 2011; 10 (4): 76–84. Russian.
5. Ferriss JS, Erickson BK, Shih IM, Fader AN. Uterine serous carcinoma: key advances and novel treatment approaches. International Journal of Gynecologic Cancer. 2021; 31 (8): 1165–74.
6. Emons G, Mustea A, Tempfer C. Tamoxifen and endometrial cancer: A janus-headed drug. Cancers. 2020; 12 (9): 2535.
7. Ignatov A, Ortmann O. Endocrine risk factors of endometrial cancer: polycystic ovary syndrome, oral contraceptives, infertility, tamoxifen. Cancers. 2020; 12 (7): 1766.
8. Bergman L, Beelen ML, Gallee MP, Hollema H, Benraadt J, van Leeuwen FE. Risk and prognosis of endometrial cancer after tamoxifen for breast cancer. Comprehensive Cancer Centres' ALERT Group. Assessment of Liver and Endometrial cancer Risk following Tamoxifen. Lancet. 2000; 356 (9233): 881–7. DOI: 10.1016/S0140-6736(00)02677-5.
9. Chlebowski R, Schottinger J, Shi J, Chung J, Haque, R. Aromatase inhibitor, tamoxifen and endometrial cancer in breast cancer survivors. Cancer. 2015; 121 (13): 2147–55. DOI: 10.1002/cncr.29332.
10. Hoogendoorn WE, Hollema H, van Boven HH, Bergman E, de Leeuw-Mantel G, Platteel I, et al. Comprehensive Cancer Centers TAMARISK-group. Prognosis of uterine corpus cancer after tamoxifen treatment for breast cancer. Breast Cancer Res Treat. 2008; 112 (1): 99–108. DOI: 10.1007/s10549-007-9823-1.
11. Vizzotto AO Jr, Nicolau SM, Lopes GM, Castelo Filho A. Risk factors for the development of endometrial lesions in breast cancer patients using tamoxyphen: a retrospective cohort study. Rev Col Bras Cir. 2023; 50: e20233442. DOI: 10.1590/0100-6991e-20233442-en.
12. Fleming CA, Heneghan HM, O'Brien D, McCartan DP, McDermott EW, Prichard RS. Meta-analysis of the cumulative risk of endometrial malignancy and systematic review of endometrial surveillance in extended tamoxifen therapy. Journal of British Surgery. 2018; 105 (9): 1098–106.
13. Dottino JA, Zhang Q, Loose DS, Fellman B, Melendez BD, Borthwick MS, et al. Endometrial biomarkers in premenopausal women with obesity: an at-risk cohort. Am J Obstet Gynecol. 2021; 224 (3): 278.e1–278.e14. DOI: 10.1016/j.ajog.2020.08.053.
14. Revankar CM, Bologa CG, Pepermans RA, Sharma G, Petrie WK,

Alcon SN, et al. A selective ligand for estrogen receptor proteins discriminates rapid and genomic signaling. Cell Chem Biol. 2019; 26 (12): 1692–1702.e5. DOI: 10.1016/j.chembiol.2019.10.009.
15. Dieudonné AS, et al. The rs1800716 variant in CYP2D6 is associated with an increased double endometrial thickness in postmenopausal women on tamoxifen. Ann Oncol. 2014; 25: 90–5.
16. Okishiro M, Taguchi T, Jin Kim S, Shimazu K, Tamaki Y, Noguchi S. Genetic polymorphisms of CYP2D6 10 and CYP2C19 2, 3 are not associated with prognosis, endometrial thickness, or bone mineral density in Japanese breast cancer patients treated with adjuvant tamoxifen. Cancer. 2009; 115: 952–61.
17. Bradford LD. CYP2D6 allele frequency in European Caucasians, Asians, Africans and their descendants. Pharmacogenomics. 2002; 3 (2): 229–43. DOI: 10.1517/14622416.3.2.229.
18. Rak molochnoy zhelezy. Klinicheskie rekomendatsii. Ministerstvo zdravookhraneniya RF, 2021; p. 93. Russian.
19. Maniatis T, Fritsch E, Sambrook J. Molecular Cloning. A Laboratory Manual. M.: Mir, 1984; p. 479.
20. Saveleva GM, Sukhikh GT, Serov VN, Radzinskiy VE, editors. Akusherstvo: natsional'noe rukovodstvo. 2nd ed., revised and additional. M.: GEOTAR-Media, 2019; p. 1080. ISBN 978-5-9704-4916-5. Russian.
21. Auclair MH, Yong PJ, Salvador S, Thurston J, Colgan TTJ, Sebastianelli A. Guideline No. 392-Classification and Management of Endometrial Hyperplasia. J Obstet Gynaecol Can. 2019; 41 (12): 1789–800. DOI: 10.1016/j.jogc.2019.03.025.
22. Korchagina RP, Osipova LP, Vavilova NA, et al. Polymorphisms of the GSTM1, GSTT1, and CYP2D6 xenobiotic biotransformation genes, which are possible risk markers of cancer in populations of indigenous ethnic groups and Russians of North Siberia. Russian Journal of Genetics: Applied Research. 2012; 2: 7–17. DOI: 10.1134/S2079059712010091. Russian.
23. Briest S, Stearns V. Tamoxifen metabolism and its effect on endocrine treatment of breast cancer. Clin Adv Hematol Oncol. 2009; 7 (3): 185–92. PMID: 19398943.
24. Goetz MP, Sangkuhl K, Guchelaar HJ, Schwab M, Province M, Whirl-Carrillo M, et al. Clinical Pharmacogenetics Implementation Consortium (CPIC) Guideline for CYP2D6 and Tamoxifen Therapy. Clin Pharmacol Ther. 2018; 103 (5): 770–7. DOI: 10.1002/cpt.1007.
25. Mulder TAM, de With M, Del Re M, Danesi R, Mathijssen RHJ, van Schaik RHN. Clinical CYP2D6 genotyping to personalize adjuvant tamoxifen treatment in ER-Positive breast cancer patients: current status of a controversy. Cancers (Basel). 2021; 13 (4): 771. DOI: 10.3390/cancers13040771.
26. Nardin JM, Schroth W, Almeida TA, Mürdter T, Picolotto S, Vendramini ECL, et al. The influences of adherence to tamoxifen and CYP2D6pharmacogenetics on plasma concentrations of the active metabolite (Z)-endoxifen in breast cancer. Clin Transl Sci. 2020; 13: 284–92. DOI: 10.1111/cts.12707.
27. Günaldı M, Erkisi M, Afşar CU, Erçolak V, Paydas S, Kara IO, et al. Evaluation of endometrial thickness and bone mineral density based on CYP2D6 polymorphisms in Turkish breast cancer patients receiving tamoxifen treatment. Pharmacology. 2014; 94 (3–4): 183–9. DOI: 10.1159/000363304.
28. Dieudonné AS, Lambrechts D, Smeets D, Belmans A, Wildiers H, Paridaens R, et al. The rs1800716 variant in CYP2D6 is associated with an increased double endometrial thickness in postmenopausal women on tamoxifen. Ann Oncol. 2014; 25 (1): 90–5. DOI: 10.1093/annonc/mdt399.
29. Okishiro M, Taguchi T, Jin Kim S, Shimazu K, Tamaki Y, Noguchi S. Genetic polymorphisms of CYP2D6 10 and CYP2C19 2, 3 are not associated with prognosis, endometrial thickness, or bone mineral density in Japanese breast cancer patients treated with adjuvant tamoxifen. Cancer. 2009; 115 (5): 952–61. DOI: 10.1002/cncr.24111.
30. Marez D, Legrand M, Sabbagh N, Lo Guidice JM, Spire C, Lafitte JJ, et al. Polymorphism of the cytochrome P450 CYP2D6 gene in a European population: characterization of 48 mutations and 53 alleles, their frequencies and evolution. Pharmacogenetics. 1997; 7 (3): 193–202. DOI: 10.1097/00008571-199706000-00004.
31. Hecht JL, Mutter GL. Molecular and pathologic aspects of endometrial carcinogenesis. J Clin Oncol. 2006; 24 (29): 4783–91. DOI: 10.1200/JCO.2006.06.7173.

Литература

1. Протасова А. Э., Солнцева И. А., Цыпурдеева А. А., Семиглазова Т. Ю., Стенина М. Б., Юренева С. В. и др. Обоснованные подходы к диагностике и лечению тамоксифен-индуцированных состояний эндометрия у больных раком молочной железы. Журнал акушерства и женских болезней. 2018; 67 (6): 69–78.
2. Krauss K, Stickeler E. Endocrine therapy in early breast cancer. Breast Care. 2020; 15 (4): 337–46.
3. Wijayabahu AT, Egan KM, Yaghjyan L. Uterine cancer in breast cancer survivors: A systematic review. Breast Cancer Research and Treatment. 2020; 180 (1): 1–9.
4. Шахламова М. Н., Исаева Э. А., Панкратов В. В. Этиология и патогенез гиперпластических процессов эндометрия в постменопаузе. Вопросы гинекологии, акушерства и перинатологии. 2011; 10 (4): 76–84.
5. Ferriss JS, Erickson BK, Shih IM, Fader AN. Uterine serous carcinoma: key advances and novel treatment approaches. International Journal of Gynecologic Cancer. 2021; 31 (8): 1165–74.
6. Emons G, Mustea A, Tempfer C. Tamoxifen and endometrial cancer: A janus-headed drug. Cancers. 2020; 12 (9): 2535.
7. Ignatov A, Ortmann O. Endocrine risk factors of endometrial cancer: polycystic ovary syndrome, oral contraceptives, infertility, tamoxifen. Cancers. 2020; 12 (7): 1766.
8. Bergman L, Beelen ML, Gallee MP, Hollema H, Benraadt J, van Leeuwen FE. Risk and prognosis of endometrial cancer after tamoxifen for breast cancer. Comprehensive Cancer Centres' ALERT Group. Assessment of Liver and Endometrial cancer Risk following Tamoxifen. Lancet. 2000; 356 (9233): 881–7. DOI: 10.1016/S0140-6736(00)02677-5.
9. Chlebowski R, Schottinger J, Shi J, Chung J, Haque, R. Aromatase inhibitor, tamoxifen and endometrial cancer in breast cancer survivors. Cancer. 2015; 121 (13): 2147–55. DOI: 10.1002/cncr.29332.
10. Hoogendoorn WE, Hollema H, van Boven HH, Bergman E, de Leeuw-Mantel G, Platteel I, et al. Comprehensive Cancer Centers TAMARISK-group. Prognosis of uterine corpus cancer after tamoxifen treatment for breast cancer. Breast Cancer Res Treat. 2008; 112 (1): 99–108. DOI: 10.1007/s10549-007-9823-1.
11. Vizzotto AO Jr, Nicolau SM, Lopes GM, Castelo Filho A. Risk factors for the development of endometrial lesions in breast cancer patients using tamoxyphen: a retrospective cohort study. Rev Col Bras Cir. 2023; 50: e20233442. DOI: 10.1590/0100-6991e-20233442-en.
12. Fleming CA, Heneghan HM, O'Brien D, McCartan DP, McDermott EW, Prichard RS. Meta-analysis of the cumulative risk of endometrial malignancy and systematic review of endometrial surveillance in extended tamoxifen therapy. Journal of British Surgery. 2018; 105 (9): 1098–106.
13. Dottino JA, Zhang Q, Loose DS, Fellman B, Melendez BD, Borthwick MS, et al. Endometrial biomarkers in premenopausal women with obesity: an at-risk cohort. Am J Obstet Gynecol. 2021; 224 (3): 278.e1–278.e14. DOI: 10.1016/j.ajog.2020.08.053.
14. Revankar CM, Bologa CG, Pepermans RA, Sharma G, Petrie WK, Alcon SN, et al. A selective ligand for estrogen receptor proteins discriminates rapid and genomic signaling. Cell Chem Biol. 2019; 26 (12): 1692–1702.e5. DOI: 10.1016/j.chembiol.2019.10.009.
15. Dieudonné AS, et al. The rs1800716 variant in CYP2D6 is associated with an increased double endometrial thickness in postmenopausal women on tamoxifen. Ann Oncol. 2014; 25: 90–5.
16. Okishiro M, Taguchi T, Jin Kim S, Shimazu K, Tamaki Y, Noguchi S. Genetic polymorphisms of CYP2D6 10 and CYP2C19 2, 3 are

not associated with prognosis, endometrial thickness, or bone mineral density in Japanese breast cancer patients treated with adjuvant tamoxifen. Cancer. 2009; 115: 952–61.
17. Bradford LD. CYP2D6 allele frequency in European Caucasians, Asians, Africans and their descendants. Pharmacogenomics. 2002; 3 (2): 229–43. DOI: 10.1517/14622416.3.2.229.
18. Рак молочной железы. Клинические рекомендации. Министерство здравоохранения РФ, 2021; 93 с.
19. Маниатис Т., Фрич Э., Сэмбрук Д. Молекулярное клонирование. Монография. М.: Мир, 1984; 479 с.
20. Савельева Г. М., Сухих Г. Т., Серов В. Н., Радзинский В. Е., редакторы. Акушерство: национальное руководство. 2-е изд., перераб. и доп. М.: ГЭОТАР-Медиа; 2019. 1080 с. ISBN 978-5-9704-4916-5.
21. Auclair MH, Yong PJ, Salvador S, Thurston J, Colgan TTJ, Sebastianelli A. Guideline No. 392-Classification and Management of Endometrial Hyperplasia. J Obstet Gynaecol Can. 2019; 41 (12): 1789–800. DOI: 10.1016/j.jogc.2019.03.025.
22. Корчагина Р. П., Осипова Л. П., Вавилова Н. А. и др. Полиморфизмы генов биотрансформации ксенобиотиков GSTM1, GSTT1 и CYP2D6, которые являются возможными маркерами риска развития рака в популяциях коренных этносов и русских Северной Сибири. Russian Journal of Genetics: Applied Research. 2012; 2: 7–17. DOI: 10.1134/S2079059712010091.
23. Briest S, Stearns V. Tamoxifen metabolism and its effect on endocrine treatment of breast cancer. Clin Adv Hematol Oncol. 2009; 7 (3): 185–92. PMID: 19398943.
24. Goetz MP, Sangkuhl K, Guchelaar HJ, Schwab M, Province M, Whirl-Carrillo M, et al. Clinical Pharmacogenetics Implementation Consortium (CPIC) Guideline for CYP2D6 and Tamoxifen Therapy. Clin Pharmacol Ther. 2018; 103 (5): 770–7. DOI: 10.1002/cpt.1007.
25. Mulder TAM, de With M, Del Re M, Danesi R, Mathijssen RHJ, van Schaik RHN. Clinical CYP2D6 genotyping to personalize adjuvant tamoxifen treatment in ER-Positive breast cancer patients: current status of a controversy. Cancers (Basel). 2021; 13 (4): 771. DOI: 10.3390/cancers13040771.
26. Nardin JM, Schroth W, Almeida TA, Mürdter T, Picolotto S, Vendramini ECL, et al. The influences of adherence to tamoxifen and CYP2D6pharmacogenetics on plasma concentrations of the active metabolite (Z)-endoxifen in breast cancer. Clin Transl Sci. 2020; 13: 284–92. DOI: 10.1111/cts.12707.
27. Günaldı M, Erkisi M, Afşar CU, Erçolak V, Paydas S, Kara IO, et al. Evaluation of endometrial thickness and bone mineral density based on CYP2D6 polymorphisms in Turkish breast cancer patients receiving tamoxifen treatment. Pharmacology. 2014; 94 (3–4): 183–9. DOI: 10.1159/000363304.
28. Dieudonné AS, Lambrechts D, Smeets D, Belmans A, Wildiers H, Paridaens R, et al. The rs1800716 variant in CYP2D6 is associated with an increased double endometrial thickness in postmenopausal women on tamoxifen. Ann Oncol. 2014; 25 (1): 90–5. DOI: 10.1093/annonc/mdt399.
29. Okishiro M, Taguchi T, Jin Kim S, Shimazu K, Tamaki Y, Noguchi S. Genetic polymorphisms of CYP2D6 10 and CYP2C19 2, 3 are not associated with prognosis, endometrial thickness, or bone mineral density in Japanese breast cancer patients treated with adjuvant tamoxifen. Cancer. 2009; 115 (5): 952–61. DOI: 10.1002/cncr.24111.
30. Marez D, Legrand M, Sabbagh N, Lo Guidice JM, Spire C, Lafitte JJ, et al. Polymorphism of the cytochrome P450 CYP2D6 gene in a European population: characterization of 48 mutations and 53 alleles, their frequencies and evolution. Pharmacogenetics. 1997; 7 (3): 193–202. DOI: 10.1097/00008571-199706000-00004.
31. Hecht JL, Mutter GL. Molecular and pathologic aspects of endometrial carcinogenesis. J Clin Oncol. 2006; 24 (29): 4783–91. DOI: 10.1200/JCO.2006.06.7173.

GENE GEOGRAPHY OF PHARMACOGENETICALLY SIGNIFICANT CYP2C19 CYTOCHROME SUPERFAMILY DNA MARKERS IN THE POPULATIONS OF RUSSIA AND NEIGHBORING COUNTRIES

Balanovska EV[1] ✉, Abdulaev ShP[2], Gorin IO[1], Belov RO[1], Mukatdarova EA[1], Pylev VYu[1,3]

[1] Research Centre for Medical Genetics, Moscow, Russia
[2] Russian Medical Academy of Continuous Professional Education, Moscow, Russia
[3] Biobank of North Eurasia, Moscow, Russia

Genetic testing of each patient aimed at detecting the pharmacogenetic marker carrier state is challenging for healthcare system. However, knowledge about the frequencies of pharmacogenetically important genes enables making decisions about treatment based on the patient's ethnicity. The *CYP2C19* cytochrome gene involved in biotransformation of a broad spectrum of drugs is one of the most important. The study was aimed to determine the frequencies of major *CYP2C19* variants and the patterns of their spatial variability in the population of Russia. The database Pharmacogenetics of the Population of Russia and Neighboring Countries created by the research team was used to determine frequencies of the *CYP2C19 *1, *2, *3, *17* variants and their genotypes: *1 – 53 populations, *n* = 2261 samples; *2 — 79 populations, *n* = 6346; *3 — 92 populations, *n* = 7517; *17 — 35 populations, *n* = 3313. We have created a cartographic atlas that includes the *1, *2, *3, *17 frequency maps, correlation maps, and genotype frequency maps. Specific data on the frequencies of *CYP2C19* variants and their pharmacogenetically significant genotypes in the major ethnic groups of Russia are provided. The cartographic atlas enables prediction of frequencies of significant *CYP2C19* variants and their genotypes in the peoples, information about which is currently missing. The *1 and *2 variants gene geography is characterized by similar pattern: the combination of longitudinal trend of frequency increase from west to southeast and latitudinal variability of frequency increase from north to south in the Asian part of the region. Variant *3 is characterized by the clear longitudinal vector of frequency increase from 0 in the west to the world's maximum in the Amur region. Variant *17 shows a pronounced longitudinal trend with the oppositely directed vector of frequency decrease from west to southeast. The correlation maps indicate regions, where the similarity between core patterns is disrupted.

Keywords: pharmacogenetics, *CYP2C19*, DNA markers, gene pool, gene geography, cartographic atlas, Russia, North Eurasia, populations

Funding: the study was supported by the Russian Science Foundation grant № 21-14-00363 (bioinformatics, statistical and cartographic analysis), State Assignment of the Ministry of Science and Higher Education of the Russian Federation for the Research Centre for Medical Genetics (genealogical analysis, interpretation of the results).

Acknowlegements: the authors would like to thank all sample donors, who took part in the study, and Biobank of North Eurasia for access to DNA collections.

Author contribution: Balanovska EV — data analysis, manuscript writing, research management; Abdulaev ShP — discriptions of pharmacogenetic markers; Gorin IO — bioinformatics analysis; Belov RO — manuscript formatting; Mukatdarova EA — working with genealogical database; Pylev VYu — statistical analysis, cartographic analysis.

Compliance with ethical standards: the study was approved by the Ethics Commitee of the Research Centre for Medical Genetics (protocol № 1 of 29 June 2020); all subjects submitted the informed consent to study participation.

✉ **Correspondence should be addressed:** Elena V. Balanovska
Moskvorechye, 1, 115522, Moscow, Russia; balanovska@mail.ru

Received: 18.09.2023 **Accepted:** 18.10.2023 **Published online:** 31.10.2023

DOI: 10.24075/brsmu.2023.039

ГЕНОГЕОГРАФИЯ ФАРМАКОГЕНЕТИЧЕСКИ ЗНАЧИМЫХ ДНК-МАРКЕРОВ CYP2C19 СУПЕРСЕМЕЙСТВА ЦИТОХРОМОВ В НАРОДОНАСЕЛЕНИИ РОССИИ И СОПРЕДЕЛЬНЫХ СТРАН

Е. В. Балановская[1] ✉, Ш. П. Абдулаев[2], И. О. Горин[1], Р. О. Белов[1], Е. А. Мукатдарова[1], В. Ю. Пылёв[1,3]

[1] Медико-генетический научный центр имени Н. П. Бочкова, Москва, Россия
[2] Российская медицинская академия непрерывного профессионального образования Минздрава России, Москва, Россия
[3] Биобанк Северной Евразии, Москва, Россия

Генетическое тестирование каждого пациента для выявления носительства фармакогенетических маркеров проблемно для системы здравоохранения. Но знание частоты встречаемости фармакогенетически важных генов позволяет принимать решение о терапии в зависимости от этнической принадлежности пациента. Одним из наиболее значимых является ген цитохрома *CYP2C19*, участвующий в биотрансформации широкого спектра лекарственных препаратов. Целью работы было выявить частоты встречаемости основных вариантов *CYP2C19* и паттерны их пространственной изменчивости в народонаселении России. На основе созданной коллективом базы данных «Фармакогенетика популяций России и сопредельных стран» получены частоты вариантов *CYP2C19 *1, *2, *3, *17* и частоты их генотипов: *1 — 53 популяции, *n* = 2261 образец; *2 — 79 популяций, *n* = 6346; *3 — 92 популяции, *n* = 7517; *17 — 35 популяций, *n* = 3313. Создан картографический атлас, включающий карты частоты вариантов *1, *2, *3, *17, их корреляционные карты и карты частоты их генотипов. Представлены конкретные данные о частотах вариантов *CYP2C19* и их фармакогенетически значимых генотипах в основных этнических группах России. Картографический атлас дает прогноз частоты значимых вариантов *CYP2C19* и их генотипов для народов, информация о которых пока отсутствует. Геногеография *1 и *2 характеризуется схожим паттерном: совмещение долготного тренда роста частоты с запада на юго-восток и широтного роста частоты с севера на юг в азиатской части региона. Вариант *3 отличается четкостью долготного вектора роста частоты от 0 на западе до мирового максимума частоты в Приамурье. Вариант *17 имеет выразительный долготный тренд с противоположным вектором падения частоты с запада на юго-восток. Корреляционные карты указывают регионы, в которых нарушено сходство между основными паттернами.

Ключевые слова: фармакогенетика, *CYP2C19*, ДНК-маркеры, генофонд, геногеография, картографический атлас, Россия, Северная Евразия, популяции

Финансирование: РНФ №21-14-00363 (биоинформатический, статистический и картографический анализ) и Государственного задания Министерства науки и высшего образования РФ для Медико-генетического научного центра имени академика Н. П. Бочкова (генеалогический анализ, интерпретация результатов).

Благодарности: авторы благодарят всех доноров образцов, принимавших участие в исследовании, и АНО «Биобанк Северной Евразии» за предоставление коллекций ДНК.

Вклад авторов: Е. В. Балановская — анализ данных, написание текста, руководство исследованием; Ш. П. Абдулаев — описание фармакогенетических маркеров; И. О. Горин — биоинформатический анализ; Р. О. Белов — оформление статьи; Е. А. Мукатдарова — работа с базой генеалогических данных; В. Ю. Пылёв — статистический анализ, картографический анализ.

Соблюдение этических стандартов: исследование одобрено этическим комитетом ФГБНУ «Медико-генетический научный центр имени Н. П. Бочкова» (протокол № 1 от 29 июня 2020 г.); все участники подписали добровольное информированное согласие на участие в исследовании.

✉ **Для корреспонденции:** Елена Владимировна Балановская
ул. Москворечье, д. 1, 115522, г. Москва, Россия balanovska@mail.ru

Статья получена: 18.09.2023 **Статья принята к печати:** 18.10.2023 **Опубликована онлайн:** 31.10.2023

DOI: 10.24075/vrgmu.2023.039

Drug therapy efficacy and safety depend largely on individual differences between patients. This is a pressing issue of modern pharmacotherapy, since the body's genetic status accounts for up to 50% of the pharmacological response individual variability. Selection of the drug and dosage considering the patient's molecular genetic features is the subject of pharmacogenetics [1, 2] aiming to search for the drug dose that would be effective and safe for this particular patient [3].

The CYP450 cytochrome superfamily, in which the *CYP2C19* gene is highly polymorphic, represents one of the pharmacogenes extensively studied from clinical perspective. The *CYP2C19* enzyme is involved in biotransformation of the wide range of drugs, such as clopidogrel, omeprazole, lansoprazole, propranolol, diazepam, imipramine and some other antidepressants [4]. It has been shown that *CYP2C19*2* and *CYP2C19*3* are associated with the enzyme reduced metabolic activity [5], while *CYP2C19*17* (*rs12248560*) is associated with enchanced metabolism of the enzyme substrates [5]. Clopidogrel is a prime example of the drug, for which the guidelines on the treatment regimen and dose adjustment have been developed. In individuals with "normal" *1/*1 genotype, it is used in accordance with the instructions. The *1/*2, *1/*3, *2/*17, *3/*17 genotypes are characterized by smaller decline in platelet aggregation relative to normal, higher residual platelet aggregation, and increased risk of cardiovascular events. Accumulation of "slow" alleles (*2/*2, *2/*3, *3/*3) in the genotype is associated with low clopidogrel efficacy and high residual platelet reactivity. The group of "ultrafast" metabolizers (*1/*17, *17/*17) is characterized by the increased antiplatelet activity and decreased residual platelet aggregation, which can be due to the risk of hemorrhage [5]. The carrier frequency for various *CYP2C19* SNP markers and the associated clopidogrel resistance are characterized by the pronounced ethnoracial heterogeneity [6]: *CYP2C19*2* is found in 15% of Caucasoids, 17% of Negroids and is far more frequent in Mongoloids living in East Asia (31%). The opposite trend has been revealed for *CYP2C19*17*: it is common in Caucasoids (22%) and rare (1.5%) in Mongoloids of East Asia [6]. The *CYP2C19*3* variant is rare: it averagely accounts for 1.4% of global population [6]. In the Russian population the rate of *CYP2C19*2* is about 11%, the rate of *CYP2C19*3* is about 0.34%, and that of *CYP2C19*17* is about 27% [7].

The principles of precision, preventive, and personalized medicine envision using genetic information to make clinical decisions. However, extensive use of pharmacogenetic testing (PGT) in clinical practice has a number of limitations. PGT remains an option that is not available in the regions with inadequate funding of the health sector. An important role is also played by the time of obtaining PGT results, which can be relevant when providing emergency care [8].

The population gene geography that reveals the patterns in pharmacogenetic biomarker distribution provides one of the solutions [9–13]. The gene geography data can play an important role in clinical decision-making in such multi-ethnic country as Russia. That is why assessment of polymorphic genes' carrier frequency in Russia is essential for development and implementation of the personalized medicine principles. Exploration and identification of the distribution patterns of important pharmacogenetic markers in the population of Russia make it possible to identify ethnic groups and regions, in which PGT of the large population of patients can be a clinically and economically advantageous solution: in these regions the decision that PGT is essential for therapy personalization can be made based on the patient's ethnicity.

The study was aimed to determine frequencies of major *CYP2C19* cytochrome superfamily DNA markers (*1, *2, *3, *17) in the population of Russia and determine the trends in their gene geographical variability.

METHODS

The study involved analysis of frequencies of the *CYP2C19*1*, *CYP2C19*2*, *CYP2C19*3*, *CYP2C19*17* variants (hereinafter *1, *2, *3, *17) and their genotypes in indigenous peoples of North Eurasia and other regions. These four variants (*1, *2, *3, *17) belong to different *CYP2C19* gene SNP markers and are not alleles of the same SNP; their frequencies were calculated using the PLINK 1.9 tool [14] and Python 3. The *1 variant is the sum of 11 SNPs of "normal" variants. Among them 7 SNPs were found in the databases and had representative frequencies, and the *1 frequency was calculated as the square root of the frequency of the combination of seven homozygotes. The genotype frequencies were calculated based on the *1, *2, *3, *17 variant frequencies in accordance with the Hardy–Weinberg equilibrium.

The analysis involved the use of the database "Pharmacogenetics of Population of Russia and Neighboring Countries" created by the research team and the GG-base (world's populations) [15] compiled in accordance with [16] and assessed using various panels of SNP markers [9–13]. Populations with the sample size of $n < 25$ samples were included in large metapopulations together with other populations based on the commonality of ethnogenesis and region. The data on the peoples of the Caucasus on the scale of North Eurasia were represented by four subregional samples. The total samples for the *CYP2C19* gene SNP variants were as follows: *1 — n = 2261 samples; *2 — n = 6346; *3 — n = 7517; *17 — n = 3313. The results were presented as tables (frequencies of SNP variants and their genotypes in 53 metapopulations of 13 world's regions) and as the gene geographical atlas including maps showing spatial variability of frequencies of SNP markers and their genotypes, as well as correlation maps demonstrating the association of geographical variability of frequencies of all SNP markers. The following SNP variant variability parameters were provided; $\bar{q}$ — average frequency; G_{ST} — interpopulation differences based on certain variant (G_{ST} is the F_{ST} analog for biallelic cases); H_S — heterozygosity level.

The *CYP2C19* gene geographic maps were plotted using the GeneGeo software [17] by the weighted average interpolation with the 2nd degree weighting function, range radius of 1500 km for North Eurasia and 5000 km for the world. In the tables each population was assigned a number that was shown on the maps, which made it possible to clearly identify and distinguish all the studied populations on the maps. As for metapopulations, the trait frequency value was projected onto all coordinates of input local populations. The genotype frequency maps were calculated for each node of the map based on the frequency value in each node of the maps for the *1, *2*, *3, *17 variants in accordance with the Hardy–Weinberg equilibrium. Statistical parameters of the map are shown in specific box of the legend of each map: K — number of input populations for map plotting; min — minimum trait frequency; max — maximum trait frequency; avr — average trait frequency; G_{ST} — interpopulation differences based on this trait; H_S —heterozygosity level.

The correlation maps were created by the 1100 km floating window method using the Kendall rank correlation coefficient. Correlation between two traits was calculated for all nodes falling into the specified window and assigned to the central node. Then this window was moved one node, and calculation was repeated. Thus, correlations were calculated for all nodes

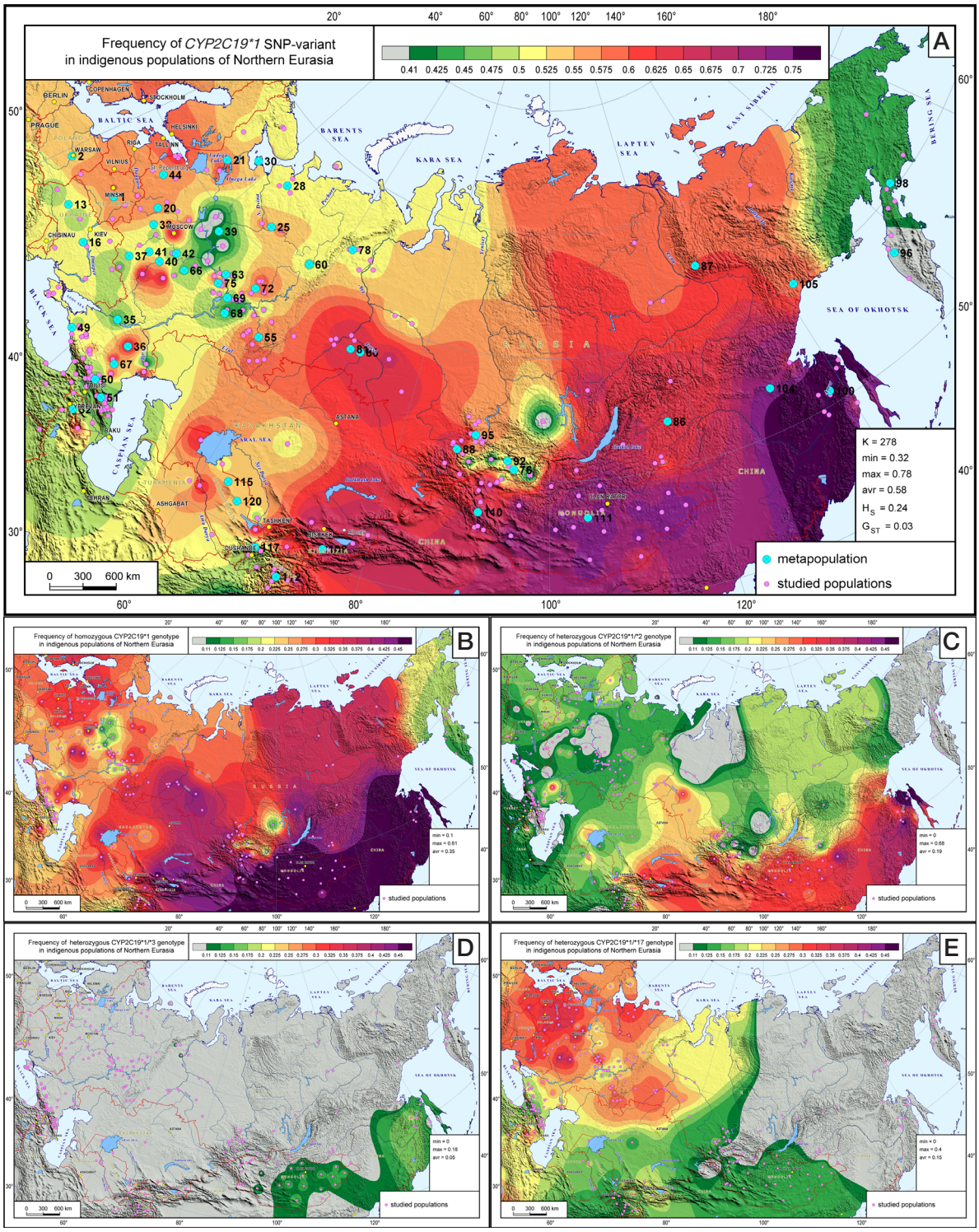

Fig. 1. Spatial *CYP2C19*1* variability in indigenous population of Russia and neighboring countries. **A**. Gene geography of *CYP2C19*1* SNP variant frequency. **B**. Gene geography of *1/*1 genotype frequency. **C**. Gene geography of *1/*2 genotype frequency. **D**. Gene geography of *1/*3 genotype frequency. **E**. Gene geography of *1/*17 genotype frequency

of digital mesh model of the map (81259 nodes) providing the basis for correlation pattern visualization.

RESULTS

Gene geography of *CYP2C19*1* (Fig. 1; Tables 1, 2)

Understanding the *1 "normal" variant gene geography (Fig. 1) is beneficial for identification of patterns in variability of genotypes that are important for pharmacotherapy.

The main longitudinal trend represented by the *1 frequency increase from west to southeast is combined with latitudinal variability in the Asian part of the region. The average *1 frequency ($\bar{q}$ = 0.58) is much higher than that of variants *2, *3, *17 (0.04 < $\bar{q}$ < 0.15). That is why a common frequency interval (0.125) was used in all maps for variant *1 to make all maps comparable (Fig. 1–4), however it was within another frequency range (0.41 < q < 0.75).

The longitudinal trend of frequency decrease from west to southeast is associated with many irregularities. Low

Table 1. Frequencies of CYP2C19*1, *2, *3, 17 SNP variant in indigenous population of Russia and the world

Region	№ on the map	Population	*CYP2C19*1*		*CYP2C19*2*		*CYP2C19*3*		*CYP2C19*17*	
			-		rs4244285		rs4986893		rs12248560	
			n	$\bar{q}$	*n*	$\bar{q}$	*n*	$\bar{q}$	*n*	$\bar{q}$
FOREIGN EUROPE	1	Belarusians	33	0.577	50	0.170	50	0.020	19	0.290
	2	Eastern Europe (Gagauz, Lithuanians, Macedonians)	21	0.535	-	-	-	-	-	-
	3	Northern peoples of Balkans (Hungarians, Romanians, Slovenes)	-	-	-	-	51	0	-	-
	4	Central peoples of Balkans (Bosnians, Kosovars, Serbs, Croats, Montenegrins)	-	-	-	-	80	0.013	-	-
	5	Southern peoples of Balkans (Bulgarians, Greeks, Macedonians)	-	-	70	0.171	129	0	-	-
	6	Peoples of Europe	-	-	503	0.145	503	0	-	-
	7	Peoples of Moldova (Gagauz, Moldovans)	-	-	20	0.175	20	0	-	-
	8	Peoples of Northern Europe (Latvians, Lithuanians, Swedes)	-	-	-	-	34	0	-	-
	9	Peoples of Central Europe (Germans, Poles, Slovaks)	-	-	-	-	45	0	-	-
	10	Peoples of Southern Europe (Spaniards, Italians)	-	-	-	-	36	0	-	-
	11	Peoples of Southern Europe (Macedonians)	-	-	-	-	-	-	49	0.153
	12	Ukrainians (eastern)	-	-	-	-	-	-	64	0.320
	13	Ukrainians (western)	31	0.475	58	0.103	58	0	-	-
	14	Ukrainians (western, central)	-	-	-	-	-	-	37	0.284
	15	Ukrainians (northeastern)	-	-	65	0.154	70	0.043	-	-
	16	Ukrainians (central, eastern)	47	0.505	-	-	-	-	-	-
	17	Ukrainians (central, southeastern)	-	-	70	0.114	72	0	-	-
NORTH OF EUROPEAN PART OF RUSSIA	18	Vepsians	-	-	37	0.189	38	0.013	-	-
	19	Vod, Izhora	-	-	46	0.141	47	0	-	-
	20	Western finnish-speaking peoples (Vepsians, Vod, Izhora, Ingrian Finns)	32	0.612	-	-	-	-	70	0.236
	21	Karelians (North, Tver, South)	26	0.519	-	-	-	-	103	0.238
	22	Karelians (Tver)	-	-	78	0.108	78	0	-	-
	23	Karelians (North), Sami	-	-	20	0.200	21	0	-	-
	24	Karelians (South)	-	-	50	0.100	53	0	-	-
	25	Russians of Arkhangelsk region (Krasnoborsky, Lensky districts)	29	0.557	-	-	-	-	-	-
	26	Russians of Arkhangelsk region (Krasnoborsky district)	-	-	57	0.114	57	0	-	-
	27	Russians of Arkhangelsk region (Leshukonsky, Mezensky districts)	-	-	31	0.177	34	0	-	-
	28	Russians of Arkhangelsk region (Leshukonsky, Pinezhsky, Mezensky districts)	36	0.500	-	-	-	-	-	-
	29	Russians of Arkhangelsk region (Pinezhsky district)	-	-	65	0.115	65	0	-	-
	30	Russians of Arkhangelsk region (Pomors of the Winter, Summer, Onega coasts)	27	0.544	52	0.183	55	0.027	-	-
	31	Northern Russians (Arkhangelsk, Kostroma regions)	-	-	-	-	-	-	46	0.272
	32	Northern Russians (Pinezhsky district of Arkhangelsk region)	-	-	-	-	-	-	45	0.322
	33	Northern Russians (Pomors, Mezensky, Leshukonsky districts of Arkhangelsk region)	-	-	-	-	-	-	40	0.300
	34	Ingrian Finns	-	-	29	0.207	33	0	-	-
CENTER AND SOUTH OF EUROPEAN PART OF RUSSIA	35	Cossacks (Don, Kuban, Nekrasov, Terek)	37	0.435	59	0.085	59	0	-	-
	36	Kalmyks	36	0.667	36	0.264	36	0.028	-	-
	37	Russians of Belgorod, Kursk, Oryol regions	28	0.500	59	0.093	59	0.008	-	-
	38	Russians of Bryansk, Smolensk, Tver regions	42	0.577	62	0.177	62	0	-	-
	39	Russians of Vologda and Kostroma regions	35	0.378	53	0.075	54	0	-	-
	40	Russians of Voronezh and Tambov regions	24	0.677	42	0.143	42	0	-	-
	41	Russians of Kaluga and Ryazan regions	32	0.468	47	0.096	47	0	-	-
	42	Russians of Yaroslavl region	29	0.322	-	-	-	-	-	-
	43	Russians of Nizhny Novgorod region	-	-	28	0.018	28	0	-	-
	44	Russians of Novgorod and Pskov regions	43	0.550	71	0.127	72	0	-	-
	45	Russians of the Yaroslavl region	-	-	68	0.132	68	0.015	-	-

	46	Russians of North-West (Novgorod, Pskov regions)	-	-	-	-	-	-	34	0.309
	47	Central Russians (Nizhny Novgorod, Smolensk, Tver, Yaroslavl regions)	-	-	-	-	-	-	59	0.314
	48	Southern Russians (Belgorod, Voronezh, Kaluga, Kursk, Oryol, Ryazan, Tambov regions)	-	-	-	-	-	-	70	0.293
NORTH CAUCASUS, CRIMEA, TRANSCAUCASIA	49	Western Caucasus and Crimea (Adygea, Kabardino-Balkaria, Karachay-Cherkessia, peoples of Crimea)	107	0.502	390	0.112	390	0.001	264	0.178
	50	Central Caucasus (Ossetia, Ingushetia, Chechnya)	78	0.464	328	0.136	328	0.020	244	0.158
	51	Eastern Caucasus (Dagestan)	129	0.452	655	0.079	1003	0.004	648	0.201
	52	Transcaucasia (Azerbaijan, Armenia, Georgia)	123	0.494	181	0.124	202	0.007	45	0.300
VOLGA-URAL REGION	53	Bashkirs (northern, western)	-	-	63	0.127	63	0.016	-	-
	54	Bashkirs (southeastern)	-	-	37	0.135	37	0.014	-	-
	55	Bashkirs (total)	44	0.584	-	-	-	-	52	0.240
	56	Komi-Permyaks (northern)	-	-	76	0.145	80	0.006	-	-
	57	Komi-Permyaks (southeastern)	-	-	80	0.144	81	0	-	-
	58	Komi-Permyaks (southwestern)	-	-	51	0.137	51	0	-	-
	59	Komi-Permyaks (total)	-	-	-	-	-	-	141	0.252
	60	Komi (Komi-Permyaks, Komi-Zyrians)	49	0.495	-	-	-	-	-	-
	61	Mari (Hill)	-	-	52	0.106	52	0.038	-	-
	62	Mari (Meadow)	-	-	76	0.059	77	0.006	-	-
	63	Mari (total)	31	0.440	-	-	-	-	83	0.313
	64	Peoples of Mordovia (Moksha, Shoksha)	-	-	72	0.125	72	0	-	-
	65	Peoples of Mordovia (Erzya)	-	-	86	0.099	90	0	-	-
	66	Peoples of Mordovia (total)	56	0.463	-	-	-	-	-	-
	67	Nogais (Astrakhan, Kuban, Stavropol, Kara-Nogai people)	34	0.642	34	0.191	35	0.043	-	-
	68	Volga Tatars (Kazan, Astrakhan)	26	0.392	83	0.157	84	0.054	-	-
	69	Volga Tatars (Mishars, Kryashens)	29	0.455	79	0.127	79	0.006	-	-
	70	Volga Tatars (Kazan, Kryashens, Mishars)	-	-	-	-	-	-	95	0.221
	71	Udmurts	-	-	-	-	-	-	47	0.170
	72	Udmurts, Besermyan	51	0.594	112	0.121	113	0.018	-	-
	73	Chuvash (anat jenchi)	-	-	79	0.089	79	0.006	-	-
	74	Chuvash (anatri, virjal)	-	-	55	0.109	55	0	-	-
	75	Chuvash (total)	34	0.594	-	-	-	-	89	0.281
WESTERN AND CENTRAL SIBERIA	76	Buryats (Buryatia, Transbaikal region, Irkutsk region)	32	0.661	41	0.171	41	0.061	-	-
	77	Mansi	-	-	40	0.180	40	0.125	-	-
	78	Peoples of Western Siberia (Mansi, Nenets, Khanty)	59	0.521	-	-	-	-	-	-
	79	Nenets	-	-	21	0.119	21	0	-	-
	80	Siberian Tatars (Baraba, Tobol, Zabolotnie)	48	0.661	49	0.235	49	0.051	-	-
	81	Siberian Tatars (Tyumen-Turin)	35	0.609	45	0.144	45	0.033	-	-
	82	Ugrians (Mansi, Khanty)	-	-	-	-	-	-	40	0.200
	83	Khanty	-	-	56	0.054	56	0.009	-	-
	84	Chukchi people	-	-	35	0	35	0.057	15	0.033
	85	Evenks (Baikal)	-	-	-	-	-	-	29	0.052
	86	Evenks (Baikal), Hamnigan	25	0.566	50	0.060	51	0.088	-	-
	87	Yakuts	39	0.599	41	0.159	41	0.037	-	-
SOUTH SIBERIA	88	Altai people, Shors	56	0.655	-	-	-	-	50	0.120
	89	Nothern Altai people, Shors	-	-	59	0.220	59	0.068	-	-
	90	Southern Altai people	-	-	48	0.156	48	0.042	-	-
	91	Tofalar people	-	-	29	0.052	29	0	-	-
	92	Tuvans, Tofalar people	62	0.381	-	-	-	-	53	0.075
	93	Tuvans (northern)	-	-	43	0.047	43	0.047	-	-
	94	Tuvans (central, southern)	-	-	41	0.049	41	0.024	-	-
	95	Khakas	32	0.559	32	0.141	32	0.063	-	-
FAR EAST	96	Itelmens	29	0.371	29	0.069	29	0	-	-
	97	Koryaks	-	-	60	0.075	60	0.042	-	-
	98	Koryaks, Chukchi people	35	0.447	-	-	-	-	-	-

	99	Nanai people	-	-	73	0.185	74	0.115	47	0
	100	Peoples of Amur (Nanai people, Nivkh people, Ulchis, Negidals)	49	0.782	-	-	-	-	-	-
	101	Peoples of Amur (Nivkh people, Ulchis, Negidals)	-	-	30	0.433	30	0.083	-	-
	102	Peoples of Kamchatka	-	-	-	-	-	-	36	0.028
	103	Evenks, Evens (Okhotsk)	-	-	-	-	-	-	25	0
	104	Evenks (Okhotsk), Oroch people	25	0.693	34	0.177	35	0.057	-	-
	105	Evens (Okhotsk, Kamchatka)	31	0.596	58	0.112	58	0.078	-	-
CENTRAL AND EAST ASIA	106	Dungan people, Uyghurs	-	-	34	0.250	34	0.059	-	-
	107	Kazakhs	-	-	55	0.164	55	0.045	46	0.141
	108	Kyrgyz	43	0.682	51	0.245	51	0.049	-	-
	109	Peoples of East Asia	-	-	504	0.312	504	0.056	504	0.015
	110	Peoples of Mongolia (other than Khalkha)	70	0.655	94	0.218	94	0.032	-	-
	111	Peoples of Mongolia (Khalkha)	58	0.731	67	0.224	68	0.088	-	-
	112	Peoples of Pamirs (Wakhans, Ryns, Gorans, Shugnans, Rushans, Bartangs Wanchs, Shahdarins, Yazgulyamites)	30	0.548	-	-	-	-	45	0.133
	113	Peoples of Pamirs (northern)	-	-	44	0.159	44	0	-	-
	114	Peoples of Pamirs (southern)	-	-	33	0.106	33	0	-	-
	115	Peoples of Middle Asia (Kazakhs, Karakalpaks, Turkmens)	30	0.516	-	-	-	-	-	-
	116	Peoples of Middle Asia (Karakalpaks, Kyrgyz, Tajiks, Uzbeks)	-	-	-	-	-	-	24	0.146
	117	Peoples of Tajikistan (Tajiks, Yagnobis)	41	0.469	50	0.140	50	0	-	-
	118	Peoples of Central Asia (Dungan people, Mongols, Uyghurs)	-	-	-	-	-	-	55	0.100
	119	Turkmens, Karakalpaks	-	-	30	0.133	30	0.033	-	-
	120	Uzbeks	38	0.628	40	0.200	40	0.038	-	-
SOUTH ASIA	121	Peoples of South Asia (Paniya, Pashtuns, Sakilli, North Kannadi, Hazaras)	-	-	-	-	26	0	-	-
	122	Peoples of South Asia (Ladakh, Tibetans, Farsi)	15	0.365	15	0.067	15	0	-	-
WEST ASIA	123	Arabs	-	-	-	-	50	0		
	124	Ashkenazi Jews	-	-	-	-	29	0	-	-
	125	Jews	-	-	-	-	176	0.003	-	-
	126	Peoples of Anatolia and Levant	-	-	-	-	55	0	-	-
AFRICA	127	Peoples of Africa	-	-	-	-	41	0	-	-
AMERICA	128	Peoples of America	-	-	-	-	39	0	-	-
	129	Peoples of Greenland	-	-	-	-	39	0	-	-

frequencies ($q < 0.44$) are concentrated not in the west of the region, but in the plain stretching from the Russian Vologda and Kostroma regions to peoples of the Volga-Ural region, then to southern Russian populations and after that to peoples of Central and Eastern Caucasus. The second low frequency center is found in the north of the Far East ($0.37 < q < 0.45$). However, when moving southwards from the latter, frequency increases rapidly to maximum values ($0.70 < q < 0.78$) found in Evenks of the Okhotsk Coast and peoples living along Amur. Siberian peoples are characterized by great *1 genetic diversity: high frequencies ($0.61 < q < 0.66$) prevail in Eastern Siberia (Yakut) and in the south of Western Siberia (Siberian Tatars), which decrease ($0.52 < q < 0.56$) in the north of Western Siberia and in Southern Siberia.

The combination of *1 longitudinal and latitudinal variability is even more prominent on the map of "normal" *1/*1 homozygous genotype (Fig. 1B) and the map of "slow" *1/*2 heterozygote (Fig. 1C). An "ultrafast" *1/*17 heterozygote (Fig. 1E) associated with the risk of hemorrhage is characterized by clear, but oppositely directed vector: frequency dropping from west ($q = 0.40$) to east ($q = 0$).

Gene geography of *CYP2C19*2* (Fig. 2; Tables 1, 2)

The gene geographic variability of *2 variant is similar to that of *1. At significantly lower frequencies ($0 < q < 0.43$, $\bar{q} = 0.15$; Fig. 2A) overlapping of two trends is found again. The main trend is longitudinal once again, with the *2 frequency increase from west to southeast, where the primary maximum falls on Central Asia ($0.20 < q < 0.31$) with frequency surge in the Amur region ($q = 0.43$). The latitudinal trend is observed in Siberia: the *2 frequency increases from north to Central Asia. Both trends demonstrate numerous irregularities.

As for European part of the assessed range, additional *2 frequency maximum ($0.19 < q < 0.24$) is found in the northwest in the Veps, Sami, North Karelians, Ingrian Finns. Frequencies above the average ($0.17 < q < 0.18$) are also found in peoples speaking Indo-European languages: in the Russian North and in the west of the European part of the region (Balkans, Belarus, west of Russia, Moldova, Ukraine).

In the Russian populations, the *2 frequency varies within a broad range ($0.02 < q < 0.18$, $\bar{q} = 0.12$). In the Cis-Urals area at $\bar{q} = 0.11$ it varies within a narrower range ($0.06 < q < 0.15$).

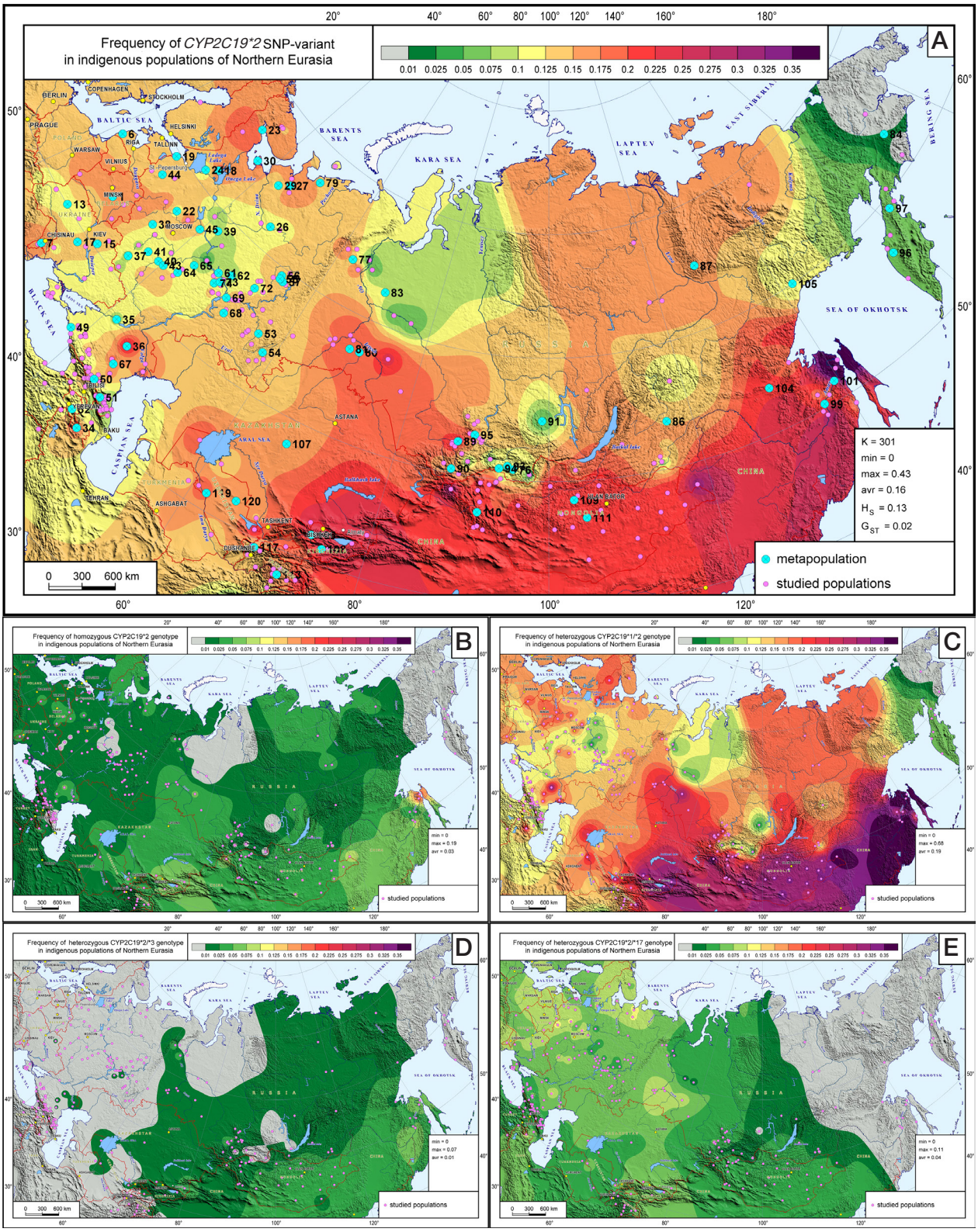

Fig. 2. Spatial *CYP2C19*2* variability in indigenous population of Russia and neighboring countries. **A**. Gene geography of *CYP2C19*2* SNP variant frequency. **B**. Gene geography of **2/*2* genotype frequency. **C**. Gene geography of **2/*1* genotype frequency. **D**. Gene geography of **2/*3* genotype frequency. **E**. Gene geography of **2/*17* genotype frequency.

In the Trans-Urals region, in Ob-Ugrians, the unexpectedly large differences between Khanty (q = 0.05) and Mansi (q = 0.18) have been revealed. In the North Caucasus the **2* frequency varies within a very broad range: between q = 0.08 in Dagestan and q = 0.19 in the Chechens and Ingush. The quite expected frequency increase in the Kalmyks (q = 0.26) results from preserving the memory of their Central Asian ancestral homeland.

The trend becomes latitudinal in the Asian part of the region: the frequency increases from north to south. The range of populations with low frequencies is huge: from Khanty in the west (q = 0.05) to Kamchatka (q = 0.07) and Chukotka (q = 0) in the east. Southwards, it extends to South Siberia (q = 0.05) and the Baikal region (q = 0.06). Increased frequencies are reported in Buryats and Yakuts (q = 0.16). The Central Asian maximum

Table 2. Frequencies of *CYP2C19* genotypes in indigenous population of Russia and the world

Region	Population	*CYP2C19* genotype																			
		*1/*1		*1/*2		*1/*3		*1/*17		*2/*2		*2/*3		*2/*17		*3/*3		*3/*17		*17/*17	
		n	$\bar{q}$	*n*	$\bar{q}$	*n*	$\bar{q}$	*n*	$\bar{q}$	*n*	$\bar{q}$	*n*	$\bar{q}$	*n*	$\bar{q}$	*n*	$\bar{q}$	*n*	$\bar{q}$	*n*	$\bar{q}$
Foreign Europe	Belarusians	33	0.333	33	0.196	33	0.023	19	0.334	50	0.029	50	0.007	19	0.098	50	0	19	0.012	19	0.084
	Eastern Europe	21	0.286	21	0.184	21	0	21	0.164	90	0.030	90	0	49	0.053	149	0	49	0	49	0.023
	Northern peoples of Balkans	-	-	-	-	-	-	-	-	-	-	-	-	-	-	51	0	-	-	-	-
	Central peoples of Balkans	-	-	-	-	-	-	-	-	-	-	-	-	-	-	80	0	-	-	-	-
	Peoples of Europe (total)	-	-	-	-	-	-	-	-	503	0.021	503	0	-	-	503	0	-	-	-	-
	Peoples of Northern Europe	-	-	-	-	-	-	-	-	-	-	-	-	-	-	34	0	-	-	-	-
	Peoples of Central Europe	-	-	-	-	-	-	-	-	-	-	-	-	-	-	45	0	-	-	-	-
	Peoples of Southern Europe	-	-	-	-	-	-	-	-	-	-	-	-	-	-	36	0	-	-	-	-
	Ukrainians	78	0.243	78	0.123	78	0.015	78	0.303	193	0.015	193	0.004	101	0.076	200	0	101	0.009	101	0.094
North of european part of Russia	Western finnish-speaking peoples	32	0.375	32	0.213	32	0.005	32	0.288	112	0.030	112	0.001	70	0.082	118	0	70	0.002	70	0.056
	Karelians, Sami	26	0.269	26	0.122	26	0	26	0.247	148	0.014	148	0	103	0.056	152	0	103	0	103	0.057
	Northern Russians	92	0.282	92	0.150	92	0.008	92	0.316	205	0.020	205	0.002	131	0.084	211	0	131	0.004	131	0.089
Center and south of european part of Russia	Cossacks	37	0.189	37	0.074	37	0	-	-	59	0.007	59	0	-	-	59	0	-	-	-	-
	Kalmyks	36	0.445	36	0.352	36	0.037	-	-	36	0.070	36	0.015	-	-	36	0.001	-	-	-	-
	Northeastern Russians	35	0.143	35	0.057	35	0	-	-	53	0.006	53	0	-	-	54	0	-	-	-	-
	Northwestern Russians	43	0.303	43	0.139	43	0	34	0.340	71	0.016	71	0	34	0.078	72	0	34	0	34	0.095
	Central Russians	71	0.224	71	0.123	71	0.006	59	0.297	158	0.017	158	0.002	59	0.081	158	0	59	0.004	59	0.098
	Southern Russians	84	0.290	84	0.116	84	0.004	70	0.315	148	0.012	148	0.001	70	0.063	148	0	70	0.002	70	0.086
North caucasus. crimea.trans-caucasia	Western Caucasus and Crimea	107	0.252	107	0.112	107	0.001	107	0.179	390	0.012	390	0	264	0.040	390	0	264	0	264	0.032
	Central Caucasus	78	0.215	78	0.126	78	0.018	78	0.146	328	0.018	328	0.005	244	0.043	328	0	244	0.006	244	0.025
	Eastern Caucasus	129	0.204	129	0.072	129	0.004	129	0.181	655	0.006	655	0.001	648	0.032	1003	0	648	0.002	648	0.040
	Transcaucasia	123	0.244	123	0.123	123	0.007	45	0.296	181	0.015	181	0.002	45	0.075	202	0	45	0.004	45	0.090
Volga-ural region	Bashkirs	44	0.341	44	0.152	44	0.018	44	0.281	100	0.017	100	0.004	52	0.063	100	0	52	0.007	52	0.058
	Komi	49	0.245	49	0.141	49	0.002	49	0.249	207	0.020	207	0.001	141	0.072	212	0	141	0.001	141	0.063
	Mari	31	0.194	31	0.069	31	0.017	31	0.276	128	0.006	128	0.003	83	0.049	129	0	83	0.012	83	0.098
	Peoples of Mordovia	56	0.214	56	0.103	56	0	-	-	158	0.012	158	0	-	-	162	0	-	-	-	-
	Nogais	34	0.412	34	0.246	34	0.055	-	-	34	0.037	34	0.016	-	-	35	0.002	-	-	-	-
	Volga Tatars	55	0.181	55	0.121	55	0.026	55	0.188	162	0.020	162	0.009	95	0.063	163	0.001	95	0.014	95	0.049
	Udmurts, Besermyan	51	0.353	51	0.143	51	0.021	47	0.202	112	0.015	112	0.004	47	0.041	113	0	47	0.006	47	0.029
	Chuvash	34	0.353	34	0.115	34	0.004	34	0.334	134	0.009	134	0.001	89	0.055	134	0	89	0.002	89	0.079
Western and central siberia	Buryats	32	0.437	32	0.226	32	0.081	-	-	41	0.029	41	0.021	-	-	41	0.004	-	-	-	-
	Peoples of the north of Western Siberia	59	0.271	59	0.113	59	0.049	40	0.208	117	0.012	117	0.010	40	0.043	117	0.002	40	0.019	40	0.040
	Siberian Tatars	83	0.409	83	0.254	83	0.056	-	-	94	0.039	94	0.017	-	-	94	0.002	-	-	-	-
	Yakuts	39	0.359	39	0.190	39	0.044	-	-	41	0.025	41	0.012	-	-	41	0.001	-	-	-	-
South siberia	Nothern Altai people, Shors	56	0.429	56	0.289	56	0.089	50	0.157	59	0.049	59	0.030	50	0.053	59	0.005	50	0.016	50	0.014
	Southern Altai people	-	-	-	-	-	-	-	-	48	0.024	48	0.013	-	-	48	0.002	-	-	-	-
	Tuvans, Tofalar people	62	0.145	62	0.037	62	0.007	53	0.058	113	0.002	113	0.001	53	0.007	113	0	53	0.001	53	0.006
	Khakas	32	0.312	32	0.157	32	0.070	-	-	32	0.020	32	0.018	-	-	32	0.004	-	-	-	-

Far east	Itelmens	29	0.138	29	0.051	29	0	-	-	29	0.005	29	0	-	-	29	0	-	-	-	-
	Koryaks, Chukchi people	35	0.200	35	0.042	35	0.115	35	0.026	95	0.002	95	0.012	51	0.003	95	0.017	51	0.008	51	0.001
	Peoples of Amur	49	0.612	49	0.402	49	0.165	47	0	103	0.066	103	0.054	47	0	104	0.011	47	0	47	0
	Evenki peoples	81	0.380	81	0.135	81	0.094	54	0.034	142	0.012	142	0.017	54	0.006	144	0.006	54	0.004	54	0.001
Central and east Asia	Peoples of East Asia	-	-	-	-	-	-	-	-	504	0.097	504	0.035	504	0.009	504	0.003	504	0.002	504	0
	Pamir peoples	30	0.300	30	0.149	30	0	30	0.146	77	0.019	77	0	45	0.036	77	0	45	0	45	0.018
	Peoples of Central Asia	152	0.334	152	0.207	152	0.038	70	0.165	226	0.032	226	0.012	70	0.051	226	0.001	70	0.009	70	0.020
	Peoples of Mongolia	128	0.475	128	0.311	128	0.077	55	0.138	195	0.051	195	0.025	55	0.045	196	0.003	55	0.011	55	0.010
South Asia	Peoples of South Asia	15	0.133	15	0.049	15	0	-	-	15	0.004	15	0	-	-	41	0	-	-	-	-
West Asia	Arabs	-	-	-	-	-	-	-	-	-	-	-	-	-	-	50	0	50	0	0	0
	Jews	-	-	-	-	-	-	-	-	-	-	-	-	-	-	205	0	-	-	-	-
	Peoples of Anatolia and Levant	-	-	-	-	-	-	-	-	-	-	-	-	-	-	55	0	-	-	-	-
Africa	Peoples of Africa	-	-	-	-	-	-	-	-	-	-	-	-	-	-	41	0	-	-	-	-
America	Peoples of America	-	-	-	-	-	-	-	-	-	-	-	-	-	-	39	0	-	-	-	-
	Peoples of Greenland	-	-	-	-	-	-	-	-	-	-	-	-	-	-	39	0	-	-	-	-

in the west spans the Dungan people, Kyrgyz and Uighurs (q = 0.25), Mongols, Northern Altai people and Shors (q = 0.22), Siberian Tatars and Uzbeks (q = 0.20). In the Amur region, the *2 frequency in the Nanai people, Oroch people and Evenks is lower (0.18 < q < 0.19), however, an unexpectedly sharp surge is observed in the combined population of the most ancient Far Eastern peoples: Negidals, Nivkh people and Ulchis (q = 0.43).

Gene geography of pharmacogenetically significant genotypes *2/*2 (Fig. 2B) and *2/*3 (Fig. 2D) is monotonous. The homozygote varying over a wide range (0 < q < 0.19) is spread across the region with low frequency ($\bar{q}$ = 0.03) showing a slight increase toward Central Asia and reaching its maximum in the Far East. There is almost no *2/*3 heterozygote in Europe, Urals and Western Siberia, low frequencies (q = 0.07) are reported in Mongolia and the Amur region.

Gene geography of *CYP2C19*3* (Fig. 3; Tables 1, 2)

Spatial variability of the *3 variant differs from previous variants showing a far stronger trend (Fig. 3A). That is why these have the same level of interpopulation differences (G_{ST} = 0.02), despite huge differences in heterozygosity of variants *3 (H_S = 0.04) and *2 (H_S = 0.13), as well as the range of their frequencies (*3 — 0 < q < 0.10; *2 — 0 < q < 0.40).

Furthermore, the maximum *3 frequencies are once again concentrated in the southeast (0.08 < q < 0.12) of Transbaikalia, in Khalkha Mongols and in the Amur region. Some frequency increase is observed in the Evenks of Okhotsk coast and the Chukchi people (q = 0.06) continuing west to the number of peoples of South Siberia (0.06 < q < 0.07) and Central Asia (0.05 < q < 0.06). A sharp frequency surge in the Mansi (q = 0.12) is the exception to this pattern.

In the European part of the region the *3 variant is missing or extremely rare. In Slavic populations, notable frequency have been found only in the Belarusians, Russians of Arkhangelsk region (q = 0.03), Russians of Yaroslavl region, as well as in the Central Caucasus (q = 0.02).

Gene geography of pharmacogenetically significant genotypes is discussed in other sections (Fig. 2D for *2/*3; Fig. 4D for 3/*17).

In general, the *3 variant is characterized by gradual frequency increase from zero values in the west of North Eurasia to low frequency (q = 0.12) in the east and southeast of the region. However, these low frequencies turn out to be maximum frequencies on a global scale (Fig. 5A): high world's frequencies are concentrated in East Asia with their maximum in the Amur region.

Gene geography of *CYP2C19*17* (Fig. 4; Tables 1, 2).

The trend of *17 variant variability is much stronger, and the vector is oppositely directed: the natural frequency drop from maximum values (q = 0.32) in the west of North Eurasia to zero frequency in the east and southeast of the region. This clear variability, even with low average frequency ($\bar{q}$ = 0.13), results in the interpopulation difference value (G_{ST} = 0,08) 4 times higher than that of other variants.

The maximum frequency range (0.27 < q < 0.32) included 12 populations out of 35 assessed using this SNP marker: all Slavic populations (Belarusians, Russians, Ukranians), Mari and Chuvash of the Ural region, peoples of Transcaucasia.

The next interval (0.20 < q < 0.25) brought together the Finnish-speaking peoples (all western Finnish-speaking populations and Komi-Permyaks), Ob-Ugrians, Urals Turkic (Bashkir and Volga Tatars), and peoples of Dagestan.

Only two European populations (Udmurts and peoples of South Europe) have been found among other populations showing above the average frequencies (0.13 < q < 0.18), and the trend is shifted southeastward: here peoples of Kazakhstan, Pamirs and Central Asia coexist with the populations of Western and Central Caucasus.

Only Asian peoples are found among populations showing below the average frequencies (0 < q < 0.12): South Siberia (Altai people, Tofalars, Tuvans, Shors), Baikal region (Evenks), Far East (Nanai people, peoples of Kamchatka, Evenks, Evens, Chukchi people), East and Central Asia.

Both genotypes of "ultrafast" metabolizers (*17/*17, Fig. 4B; *1/*17, Fig. 4C) are characterized by the same variability trend: obvious frequency drop from west to east. However, their variability ranges are different: the range of variant *17/*17 is small (0 < q < 0.10) and that of variant *1/*17 is 4 times larger (0 < q < 0.40).

The *3/*17 heterozygote (Fig. 4E) encoding intermediate metabolizers has been found showing extremely low frequencies

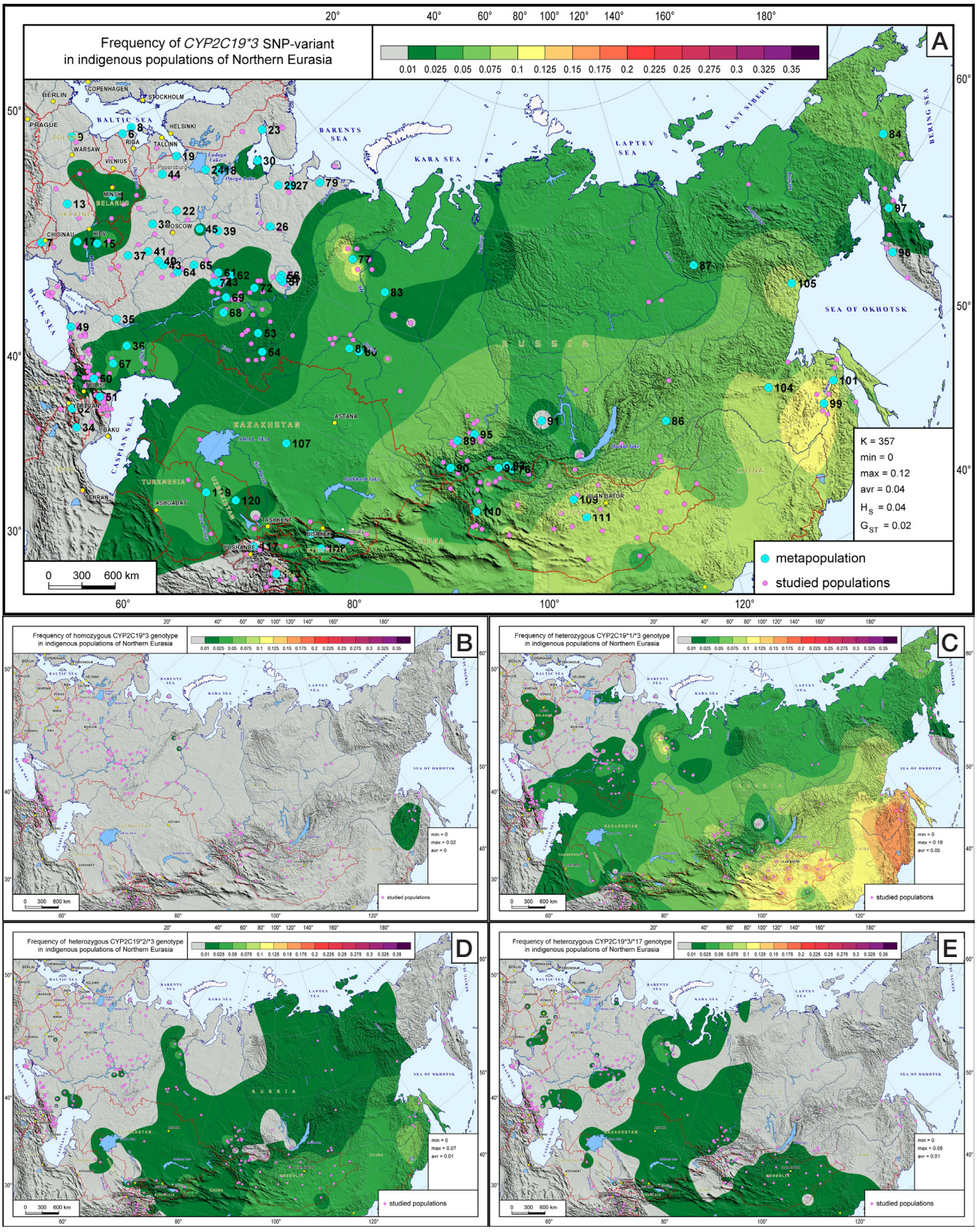

Fig. 3. Spatial *CYP2C19*3* variability in indigenous population of Russia and neighboring countries. **A**. Gene geography of *CYP2C19*3* SNP variant frequency. **B**. Gene geography of *3/*3 genotype frequency. **C**. Gene geography of *3/*1 genotype frequency. **D**. Gene geography of *3/*2 genotype frequency. **E**. Gene geography of *3/*17 genotype frequency

(0 < q < 0.05), it is almost absent in the west and east of North Eurasia. It has unique geography: the range where *3/*17 is present forms a continuous strip stretching from Ob-Ugrians in the north to peoples of Central Asia, then stretching to the east, to Mongolia and East Asia.

DISCUSSION

The population of North Eurasia is the area of most ancient (since Paleolithic times) interactions between major racial branches of the humankind: western (Caucasoids) and eastern

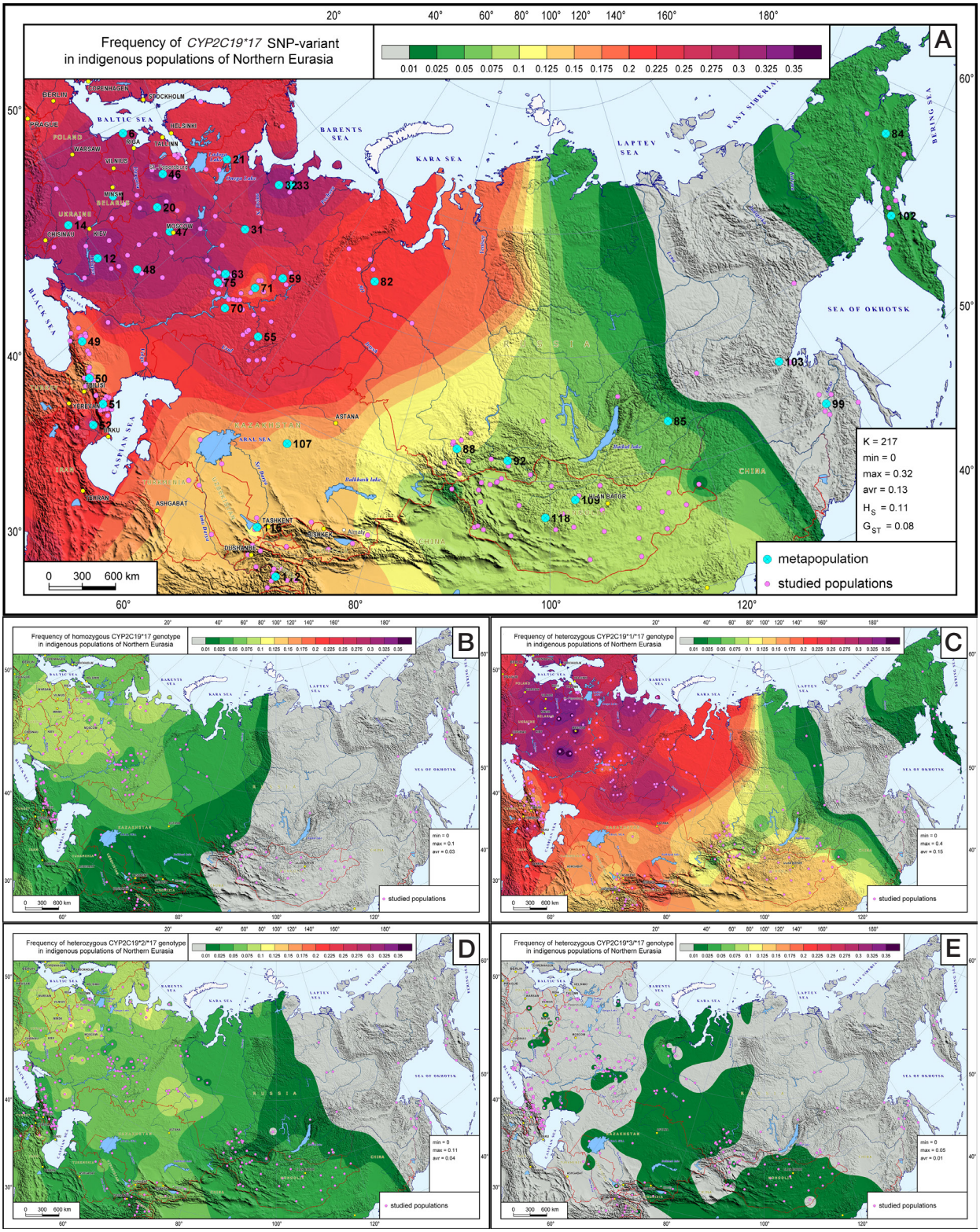

Fig. 4. Spatial *CYP2C19*17* variability in indigenous population of Russia and neighboring countries. **A**. Gene geography of *CYP2C19*17* SNP variant frequency. **B**. Gene geography of *17/*17 genotype frequency. **C**. Gene geography of *17/*1 genotype frequency. **D**. Gene geography of *17/*2 genotype frequency. **E**. Gene geography of *17/*3 genotype frequency

(Mongoloids). These interactions are clearly reflected by the *CYP2C19* SNP marker maps (Fig. 1–4). However, it has been no less convincingly shown how tough and imprecise is confining the real picture showing variability of these variants to the straightforward scheme of two racial poles.

Information about the fact that *CYP2C19*2* is two times less often found in Caucasoids (15%) than in Mongoloids of East Asia (31%) [5] is obviously insufficient. True situation is much more complex: the actual *2 variability (Fig. 2) represents the imposition of the latitudinal vector and additional maximum in Europe on the common longitudinal vector in Siberia. That is why the use of specific data on the peoples of Russia and neighboring countries in pharmacogenetics is so popular. Such data on the frequencies of four *CYP2C19* variants in multiple

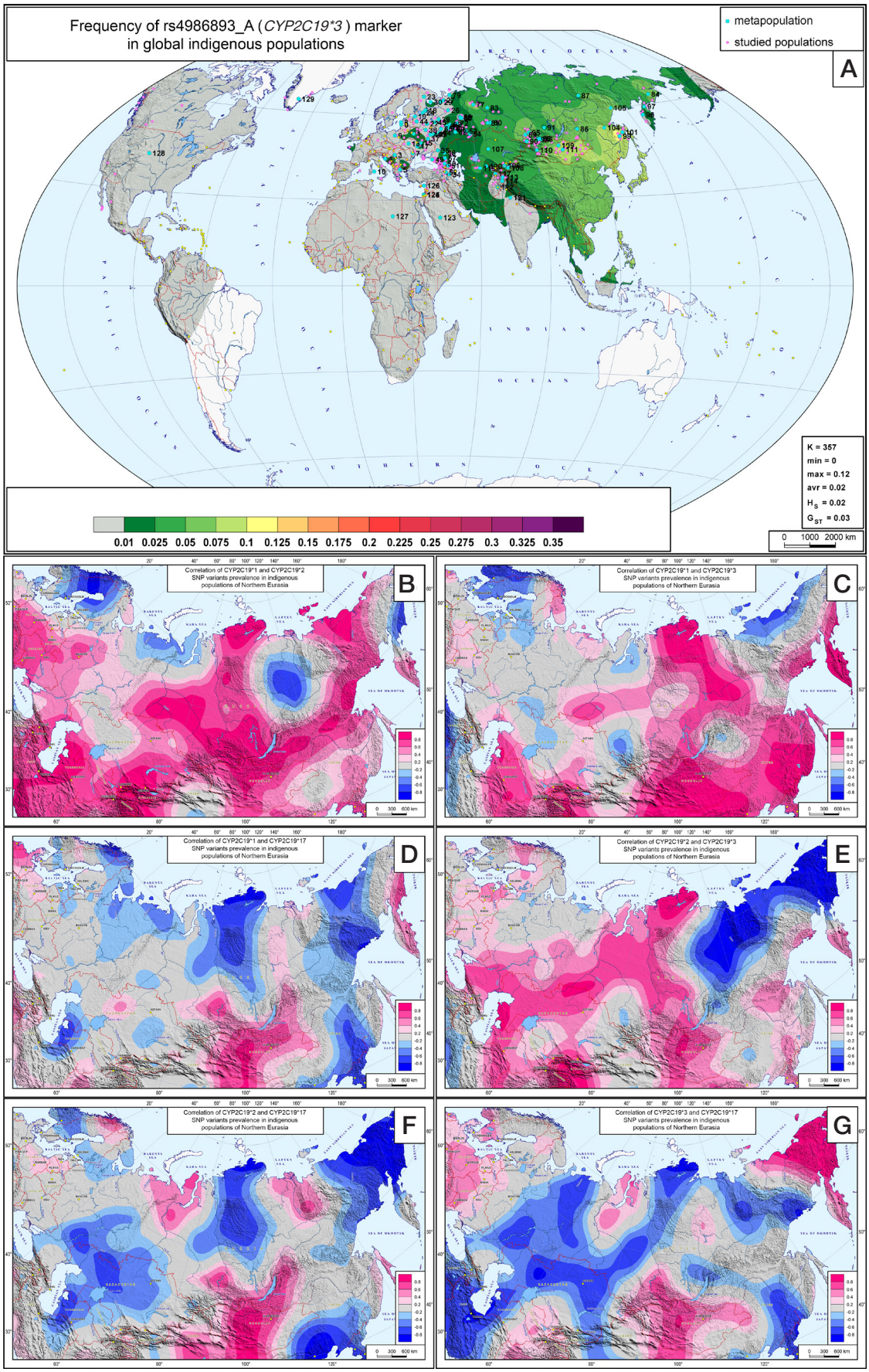

Fig. 5. Maps of correlations between patterns of *1, *2, *3, *17 variant frequency variability and gene geography of *CYP2C19*3* in indigenous population of the world. **A**. Spatial *CYP2C19*3* variability in indigenous population of the world. B. Correlation map for patterns of *1 and *2 variant frequencies. **C**. Correlation map for patterns of *1 and *3 variant frequencies. **D**. Correlation map for patterns of *1 and *17 variant frequencies. **E**. Correlation map for patterns of *2 and *3 variant frequencies. **F**. Correlation map for patterns of *2 and *17 variant frequencies. **G**. Correlation map for patterns of *3 and *17 variant frequencies.

ethnic groups or their sets are provided in Table 1: information about the *2 variant spans 79 populations with the total sample of 6346 individuals. With the *2 frequency variability span between q = 0 and q = 0.43, both its minimum (Chukchi people, q = 0) and maximum (Negidals, Nivkh people, Ulchis, q = 0.43) are in the same region, in the Far East of Russia. This precedent demonstrates that it is impossible to think in terms of generalized ethnoracial categories and there is a need for a differentiated approach. The *CYP2C19*2* frequency in the Russian populations is about 11% [6], but it varies over a very broad range: between q = 0.02 in the Nizhny Novgorod region and q = 0.18 in the Arkhangelsk, Bryansk and Smolensk regions.

The sharper ethnoracial differences are reported for *17 variant in literature: between q = 0.22 in Caucasoids and q = 0.02 in Mongoloids of East Asia [5]. As for European populations, the papers report the increase in *17 frequency in Central and Eastern Europe ($0.25 < q < 0.33$) with the decrease in the north ($0.19 < q < 0.22$), south (up to q = 0.18) and west (q = 0.17) of Europe [18, 19]. Our data on the frequency of *17 variant provided in Table 1 for 35 populations with the total sample of 3313 individuals demonstrate a similar Eurasian*17 frequency range ($0 < q < 0.32$). Furthermore, in Caucasoids, frequency varies within the range between q = 0.15 in peoples of South Europe and q = 0.32 in the north in Russians of Arkhangelsk region. A wide variety of populations conditionally classified as Mongoloids has an equally large span: from 0 in the Far East to q = 0.31 in Mari of the Cis-Urals region. That is why it is necessary to assess the real picture of geographical variability instead of using the straightforward Caucasoid-Mongoloid scheme.

The data reported (Tables 1, 2) provide important information about many ethnic groups of Russia and neighboring countries, populations of which have migrated en masse to Russia. However, these data cover only a part of the genetic diversity of peoples of our countries. That is why the knowledge of the gene geographical variability (Fig. 1–5) predicting frequencies of the *CYP2C19* clinically significant variants for peoples, information about which is currently missing in the databases and published papers, is so important.

Given the common patterns, first of all, it is necessary to emphasize that the geographical trend clarity is not dependent on the abundance of this or that *CYP2C19* variant or its variability span (Fig. 1–4).

Variants *2 and *17 are characterized by similar variability span ($0 < q < 0.4$) and similar average heterozygosity ($0.11 < H_S < 0.12$). However, while *17 demostrates a strong trend of frequency decrease from west to east (Fig. 4), the *2 variability is much more complex (Fig. 2). This apparent difference between *2 and *17 is also indicated by the interpopulation variability (G_{ST}) value: *2 shows interpopulation differences ($G_{ST} = 0.02$) that are 4 times lower than that of *17 ($G_{ST} = 0.08$). However, a less frequent ($0 < q < 0.1$) marker *3 shows a very strong trend (Fig. 3), which results in the same interpopulation difference span ($G_{ST} = 0.02$) as in *2.

The correlation maps (Fig. 5) demonstrate similarity zones in the patterns of the *1, *2, *3, *17 frequency variability (positive correlations are highlighted in red) and in the area of the oppositely directed vectors of their variability (negative correlations are highlighted in blue). The set of six correlation maps (Fig. 5B–G) demonstrates that, given overall similarity of the *1, *2, *3, *17 frequency variability patterns, there are always regions, in which the general pattern is replaced by the correlation with opposite sign. The combination of longitudinal and latitudinal trends (red color) makes similarity of the *1 and *2 gene geography obvious (Fig. 5B), however, a number of exceptions are found in the north showing negative correlation between maps of variants *1 and *2 (blue color). The pronounced similarity of the patterns of maps for *2 and *3 (Fig. 5E) is disrupted in the northeast of the region (negative correlation highlighted in blue). Despite the fact that the *3 and *17 frequency change vectors are generally oppositely directed (negative correlation), but not always alternative to each other, in some regions (foreign Europe, Ob-Ugrians, Middle Asia, South Siberia, north of the Far East) there is a positive correlation between these two maps (Fig. 5G). In general, the correlation maps convincingly show that even when the common trends in pharmacogenetic biomarker variability have been found, it is necessary to continue studying each of the peoples living in multi-ethnic Russia. The upcoming publication will show how high such variability can be on the example of peoples of the Caucasus region. That is why it is necessary to get closer to the real picture of the pharmacogenetic biomarker gene geographical variability and create cartographic atlases for various regions of Russia.

Study limitations

Certain study limitations are related to limited sample sizes of assessed biomaterial samples from some populations (sample sizes are provided in Tables 1, 2).

CONCLUSIONS

The paper provides data in the *CYP2C19*1, *2, *3, *17* SNP marker frequencies and pharmacogenetically significant genotypes in the major ethnic groups of Russia and neighboring countries. The gene geographical variability of *CYP2C19*1* (based on the data on 2261 individuals of 53 populations) combines a longitudinal trend of frequency increase from west to southeast of North Eurasia and latitudinal variability of frequency increase from north to south in the Asian part of the region. The *CYP2C19*2* spatial variability (6346 individuals, 79 populations) is characterized by variability similar to that of *1, however, both trends, longitudinal and latitudinal, are interrupted by local extrema. Gene geography of *CYP2C19*3* (7517 individuals, 92 populations) shows a stronger longitudinal trend of natural frequency increase from 0 in the west to 12% in the east and southeast of North Eurasia. This is a world's maximum: the high frequency area is located in East Asia with the peak frequency in the Amur region. The *CYP2C19*17* gene geographical variability (3313 individuals, 35 populations) is different from that of previous variants, it shows a strong oppositely directed longitudinal trend of frequency decrease from west to southeast. The correlation maps of the *CYP2C19*1, *2, *3, *17* variant frequencies demonstrate regions, in which there is no similarity between the main frequency variability patterns of these *CYP2C19* gene variants. The fact is important for practical use in pharmacogenomics. So long as the currently available data do not cover all peoples of Russia, the gene geographical variability maps are first to predict the *CYP2C19*1, *2, *3, *17* variant frequency and pharmacogenetically significant genotypes for the populations, information about which is missing.

References

1. Mini E, Nobili S. Pharmacogenetics: implementing personalized medicine. Clinical cases in mineral and bone metabolism. 2009; 6 (1):17.
2. Samani NJ, Tomaszewski M, Schunkert H. The personal genome — the future of personalised medicine? The Lancet. 2010; 375 (9725): 1497–8.
3. Collins FS, Varmus H. A new initiative on precision medicine. New England journal of medicine. 2015; 372 (9): 793–5.
4. Sinitsina II, Boyarko AV, Temirbulatov II, Sychev DA, Akmalova KA, Sozaeva ZA, et al. CYP2C9 gene polymorphisms influence on antihypertensive effectiveness and hypouricemic effect of losartan among patients with arterial hypertension: an observational study. Drug Metabolism and Personalized Therapy. 2022; 38 (2): 163–8.
5. Lee CR, Luzum JA, Sangkuhl K, Gammal RS, Sabatine MS, Stein CM, et al. Clinical pharmacogenetics implementation consortium guideline for CYP2C19 genotype and clopidogrel therapy: 2022 update. Clinical Pharmacology & Therapeutics. 2022; 112 (5): 959–67.
6. Niu X, Mao L, Huang Y, Baral S, Li JY, Gao Y, et al. CYP2C19 polymorphism and clinical outcomes among patients of different races treated with clopidogrel: a systematic review and meta-analysis. Journal of Huazhong University of Science and Technology [Medical Sciences]. 2015; 35 (2): 147–56.
7. Gaikovitch EA, Cascorbi I, Mrozikiewicz PM, Brockmöller J, Frötschl R, Köpke K, et al. Polymorphisms of drug-metabolizing enzymes CYP2C9, CYP2C19, CYP2D6, CYP1A1, NAT2 and of P-glycoprotein in a Russian population. European journal of clinical pharmacology. 2003; 59: 303–12.
8. Johnson JA, Caudle KE, Gong L, Whirl–Carrillo M, Stein CM, Scott SA, et al. Clinical Pharmacogenetics Implementation Consortium (CPIC) guideline for pharmacogenetics–guided warfarin dosing: 2017 update. Clinical Pharmacology & Therapeutics. 2017; 102 (3): 397–404.
9. Pyljov VJu, Agdzhojan AT, Gorin IO, Petrushenko VS, Pocheshhova JeA, Balanovskaja EV i dr. Populjacionnyj biobank kak osnova dlja vyjavlenija prostranstvennoj izmenchivosti klinicheski znachimyh farmakogeneticheskih biomarkerov serdechno-sosudistyh zabolevanij. Kardiovaskuljarnaja terapija i profilaktika. 2022; 21 (11): 114–34. Russian.
10. Balanovska EV, Petrushenko VS, Koshel SM, Pocheshkhova EA, Chernevskiy DK, Mirzaev KB, Abdullaev ShP, Balanovsky OP, et al. Cartographic atlas of frequency variation for 45 pharmacogenetic markers in populations of Russia and its neighbor states. Bulletin of RSMU. 2020 (6): 38–51.
11. Balanovska EV, Gorin IO, Ponomarev GYu, Pylev VYu, Petrushenko VS, Markina NV, Mamaeva AD, Larin AK, Agdzhoyan AT et al. Footprints of interaction among Finnic-speaking, Slavic, and Turkic-speaking populations in modern gene pool and their reflection in pharmacogenetics. Bulletin of RSMU. 2022; 2: 20–9.
12. Balanovska EV, Napolskih VV, Churakov VS, Pislegin NV, Zapiseckaja YuS, Balanovsky OP, i dr. Genofondy udmurtov i besermjan v kontekste finno-ugorskih i drugih okruzhajushhih narodov: polnogenomnye i farmakogeneticheskie dannye. Ezhegodnik finno-ugorskih issledovanij. 2022; 2: 328–46. Russian.
13. Balanovsky O, Petrushenko V, Gorin I, Agdzhoyan A, Balanovska E, Sychev D, et al. Variation of genomic sites associated with severe Covid-19 across populations: global and national patterns. Pharmacogenomics and Personalized Medicine. 2021: 1391–402.
14. Chang CC, Chow CC, Tellier LC, Vattikuti S, Purcell SM, Lee JJ. Second-generation PLINK: rising to the challenge of larger and richer datasets. Gigascience. 2015; 4 (1): s13742–015.
15. GG-base [cited 2022 Sep 10]. Available from: https://gg-base.org/.
16. Balanovska EV, Zhabagin MK, Agdzhoyan AT, Chuhryaeva MI, Markina NV, Asylguzhin RR, i dr. Populjacionnye biobanki: principy organizacii i perspektivy primenenija v genogeografii i personalizirovannoj medicine. Genetika. 2016; 52 (12): 1371–87. Russian.
17. Koshel SM. Geoinformacionnye tehnologii v genogeografii. Sovremennaja geograficheskaja kartografija. 2012; c. 158–8. Russian.
18. Petrović J, Pešić V, Lauschke VM. Frequencies of clinically important CYP2C19 and CYP2D6 alleles are graded across Europe. European journal of Human Genetics. 2020; 28 (1): 88–94.
19. Pedersen RS, Brasch-Andersen C, Sim SC, et al. Linkage disequilibrium between the CYP2C19*17 allele and wildtype CYP2C8 and CYP2C9 alleles: identification of CYP2C haplotypes in healthy Nordic populations. European journal of clinical pharmacology. 2010; 66: 1199–1205.20.

Литература

1. Mini E, Nobili S. Pharmacogenetics: implementing personalized medicine. Clinical cases in mineral and bone metabolism. 2009; 6 (1):17.
2. Samani NJ, Tomaszewski M, Schunkert H. The personal genome — the future of personalised medicine? The Lancet. 2010; 375 (9725): 1497–8.
3. Collins FS, Varmus H. A new initiative on precision medicine. New England journal of medicine. 2015; 372 (9): 793–5.
4. Sinitsina II, Boyarko AV, Temirbulatov II, Sychev DA, Akmalova KA, Sozaeva ZA, et al. CYP2C9 gene polymorphisms influence on antihypertensive effectiveness and hypouricemic effect of losartan among patients with arterial hypertension: an observational study. Drug Metabolism and Personalized Therapy. 2022; 38 (2): 163–8.
5. Lee CR, Luzum JA, Sangkuhl K, Gammal RS, Sabatine MS, Stein CM, et al. Clinical pharmacogenetics implementation consortium guideline for CYP2C19 genotype and clopidogrel therapy: 2022 update. Clinical Pharmacology & Therapeutics. 2022; 112 (5): 959–67.
6. Niu X, Mao L, Huang Y, Baral S, Li JY, Gao Y, et al. CYP2C19 polymorphism and clinical outcomes among patients of different races treated with clopidogrel: a systematic review and meta-analysis. Journal of Huazhong University of Science and Technology [Medical Sciences]. 2015; 35 (2): 147–56.
7. Gaikovitch EA, Cascorbi I, Mrozikiewicz PM, Brockmöller J, Frötschl R, Köpke K, et al. Polymorphisms of drug-metabolizing enzymes CYP2C9, CYP2C19, CYP2D6, CYP1A1, NAT2 and of P-glycoprotein in a Russian population. European journal of clinical pharmacology. 2003; 59: 303–12.
8. Johnson JA, Caudle KE, Gong L, Whirl–Carrillo M, Stein CM, Scott SA, et al. Clinical Pharmacogenetics Implementation Consortium (CPIC) guideline for pharmacogenetics–guided warfarin dosing: 2017 update. Clinical Pharmacology & Therapeutics. 2017; 102 (3): 397–404.
9. Пылёв В. Ю., Агджоян А. Т., Горин И. О., Петрушенко В. С., Почешхова Э. А., Балановская Е. В., и др. Популяционный биобанк как основа для выявления пространственной изменчивости клинически значимых фармакогенетических биомаркеров сердечно-сосудистых заболеваний. Кардиоваскулярная терапия и профилактика. 2022; 21 (11): 114–34.
10. Балановская Е. В., Петрушенко В. С., Кошель С. М., Почешхова Э. А., Черневский Д. К., Балановский О. П., и др. Картографический атлас распространения 45 фармакогенетических маркеров в народонаселении России и сопредельных стран. Вестник Российского государственного медицинского университета. 2020 (6): 39–52.
11. Балановская Е. В., Горин И. О., Пономарев Г. Ю., Пылёв В. Ю., Петрушенко В. С., Агджоян А. Т., и др. Следы взаимодействия финноязычного, славянского и тюркоязычного населения в современном генофонде и их отражение в фармакогенетике. Вестник Российского государственного медицинского университета. 2022; 2: 20–9.

12. Балановская Е. В., Напольских В. В., Чураков В. С., Пислегин Н. В., Записецкая Ю. С., Балановский О. П., и др. Генофонды удмуртов и бесермян в контексте финно-угорских и других окружающих народов: полногеномные и фармакогенетические данные. Ежегодник финно-угорских исследований. 2022; 2: 328–46.
13. Balanovsky O, Petrushenko V, Gorin I, Agdzhoyan A, Balanovska E, Sychev D, et al. Variation of genomic sites associated with severe Covid-19 across populations: global and national patterns. Pharmacogenomics and Personalized Medicine. 2021: 1391–402.
14. Chang CC, Chow CC, Tellier LC, Vattikuti S, Purcell SM, Lee JJ. Second-generation PLINK: rising to the challenge of larger and richer datasets. Gigascience. 2015; 4 (1): s13742–015.
15. GG-base [cited 2022 Sep 10]. Available from: https://gg-base.org/.
16. Балановская Е. В., Жабагин М. К., Агджоян А. Т., Чухряева М. И., Маркина Н. В., Асылгужин Р. Р., и др. Популяционные биобанки: принципы организации и перспективы применения в геногеографии и персонализированной медицине. Генетика. 2016; 52 (12): 1371–87.
17. Кошель С. М. Геоинформационные технологии в геногеографии. Современная географическая картография. 2012; с. 158–8.
18. Petrović J, Pešić V, Lauschke VM. Frequencies of clinically important CYP2C19 and CYP2D6 alleles are graded across Europe. European journal of Human Genetics. 2020; 28 (1): 88–94.
19. Pedersen RS, Brasch-Andersen C, Sim SC, et al. Linkage disequilibrium between the CYP2C19*17 allele and wildtype CYP2C8 and CYP2C9 alleles: identification of CYP2C haplotypes in healthy Nordic populations. European journal of clinical pharmacology. 2010; 66: 1199–1205.20.

ISCHEMIC STROKE WITH AND WITHOUT BRACHIOCEPHALIC ARTERY DISSECTIONS: RESULTS OF COMPREHENSIVE EXAMINATION OF PATIENTS

Orlova EV ✉, Berdalin AB, Reshetarov ID, Lelyuk VG

Federal Center for Brain and Neurotechnology of the Federal Medical Biological Agency of Russia, Moscow, Russia

Currently, there are no clearly defined optimal diagnostic strategies of detection of dissections. This study aimed to analyze and compare the results of comprehensive examinations of people who suffered an ischemic stroke (IS) with and without brachiocephalic artery (BCA) dissections. Dissections group, formed based on the results of multispiral computed tomography angiography that confirmed dissections, included 53 patients, and control group — patients without BCA dissections — comprised 1451 people; examination of all patients involved duplex scanning (DS) of BCA and transcranial part, transthoracic echocadiography (TTE), multispiral computed tomography angiography (msCTA) and/or magnetic resonance imaging (MRI). Patients with dissection were younger ($p < 0.0005$) and had a lower body mass index ($p < 0.0005$) than participants from the control group; according to echocadiography, they were less likely to have left ($p = 0.014$) and right ($p = 0.018$) atrial dilation and aortic stenosis ($p = 0.017$). Also, dissections were significantly less often associated with atherosclerotic plaques in the common carotid artery (CCA) ($p < 0.002$), and BCA deformations ($p < 0.05$). Duplex scanning of BCA revealed that in patients with dissections, differentiation of the intima-media complex in CCA was compromised significantly less often, and signs of thrombosis of the internal carotid artery were registered significantly more often ($p = 0.021$ and $p = 0.004$); according to MRI, such patients had less pronounced changes in the periventricular and deep white matter of the brain ($p < 0.0005$ and $p = 0.001$) and never suffered strategic infarcts affecting the thalamus area ($p < 0.0005$). Comparison of the results of examinations of IS patients with and without BCA dissections revealed differences that are probably conditioned by the younger age of those who had said dissections.

Keywords: dissection, duplex scanning, brachiocephalic arteries, CT angiography, ischemic stroke

Funding: the study was carried out as part of the State Task № 388-00083-22-00 of 30.12.2021, research project № 122022100113-7 of February 21, 2022.

Author contribution: Orlova EV — study planning, article review authoring, analysis of the results; Berdalin AB — database compilation, information collection, statistical processing, analysis and participation in recounting of the results of discussion; Reshetarov ID — article review authoring, analysis and interpretation of the results of statistical processing; Lelyuk VG — study planning, article editing, search for sources of funding.

Compliance with ethical standards: the study was approved by the Ethics Committee of the Federal Center for Brain and Neurotechnology of FMBA of Russia (Minutes № 09/03-07-23 of July 03, 2023). All study participants signed the voluntary informed consent form.

✉ **Correspondence should be addressed:** Ekaterina Vladimirovna Orlova
Ostrovityanova, 1, str. 10, Moscow, 117513, Russia; ekaterina.shlyk@gmail.com

Received: 04.08.2023 **Accepted:** 30.09.2023 **Published online:** 20.10.2023

DOI: 10.24075/brsmu.2023.037

ИШЕМИЧЕСКИЙ ИНСУЛЬТ С НАЛИЧИЕМ И ОТСУТСТВИЕМ ДИССЕКЦИЙ БРАХИОЦЕФАЛЬНЫХ АРТЕРИЙ: РЕЗУЛЬТАТЫ КОМПЛЕКСНОГО ОБСЛЕДОВАНИЯ ПАЦИЕНТОВ

Е. В. Орлова ✉, А. Б. Бердалин, И. Д. Решетаров, В. Г. Лелюк

Федеральный центр мозга и нейротехнологий Федерального медико-биологического агентства России, Москва, Россия

Актуальность исследования обусловлена наличием неопределенности в оптимальных диагностических стратегиях при выявлении диссекций. Целью исследования были анализ и сопоставление результатов комплексного обследования лиц, перенесших ишемический инсульт (ИИ), с диссекциями брахиоцефальных артерий (БЦА) и без них. Основная группа пациентов с наличием диссекций по данным мультиспиральной компьютерно-томографической ангиографии включала 53 пациента, группа без диссекций — 1451 человек; все пациенты обследованы с проведением дуплексного сканирования (ДС) БЦА и транскраниального ДС, трансторакальной эхокадиографии (ЭхоКГ), мсКТА и/или магнитно-резонансной томографии (МРТ). Пациенты с диссекцией были моложе ($p < 0,0005$) и имели меньший индекс массы тела ($p < 0,0005$) в сравнении с контролем. По данным ЭхоКГ, у лиц с диссекциями реже встречались расширение левого ($p = 0,014$) и правого (p = 0,018) предсердий и аортальный стеноз ($p = 0,017$). При наличии диссекций достоверно реже наблюдали атеросклеротические бляшки в общей сонной артерии (ОСА) ($p < 0,002$) и деформации БЦА ($p < 0,05$). По данным ДС БЦА, у лиц с диссекциями достоверно реже ($p < 0,0001$) наблюдали нарушение дифференцировки комплекса интима-медиа в ОСА и достоверно чаще отмечали наличие признаков тромбоза внутренней сонной артерии ($p = 0,021$ и $p = 0,004$), а по данным МРТ, у них были менее выражены изменения перивентрикулярного и глубокого белого вещества головного мозга ($p < 0,0005$ и $p = 0,001$) и не встречались стратегические инфаркты, затрагивающие область таламуса ($p < 0,0005$). Сравнение результатов обследования перенесших ИИ пациентов с диссекциями и без них выявило различия, вероятно, связанные с более молодым возрастом лиц с диссекциями.

Ключевые слова: диссекция, дуплексное сканирование, брахиоцефальные артерии, КТ-ангиография, ишемический инсульт

Финансирование: работа выполнена в рамках Государственного задания №388-00083-22-00 от 30.12.2021, регистрационный номер НИР 122022100113-7 от 21 февраля 2022 г.

Вклад авторов: Е. В. Орлова — планирование исследования, написание обзора статьи, анализ результатов; А. Б. Бердалин — создание базы данных, сбор информации, статистическая обработка, анализ и участие в написании обсуждения результатов; И. Д. Решетаров — написание обзора статьи, анализ и интерпретация результатов статистической обработки; В. Г. Лелюк — планирование исследования, редактирование статьи, поиск источников финансирования.

Соблюдение этических стандартов: исследование одобрено этическим комитетом ФГБУ «ФЦМН» ФМБА России (протокол № 09/03-07-23 от 03 июля 2023 г.). Все пациенты, включенные в исследование, подписывали добровольное информированное согласие.

✉ **Для корреспонденции:** Екатерина Владимировна Орлова
ул. Островитянова, д. 1, стр. 10, г. Москва, 117513, Россия; ekaterina.shlyk@gmail.com

Статья получена: 04.08.2023 **Статья принята к печати:** 30.09.2023 **Опубликована онлайн:** 20.10.2023

DOI: 10.24075/vrgmu.2023.037

Effectiveness of secondary prevention of ischemic stroke (IS) largely depends on verification of the causes of its development, and their multifactorial nature and heterogeneity complicate the process and require application of a combination of various diagnostic techniques [1, 2].

The role of brachiocephalic artery dissections in IS pathogenesis has been established, but there are some issues that need to be clarified. Thus, there is no clear understanding of the exact mechanism of development of cerebral infarction with dissections in the background; the true prevalence of dissections remains unknown because in a significant number of cases the course is asymptomatic; there is no unequivocal consensus as to the optimal diagnostic and therapeutic strategies for dissections of various localization and genesis. Dissection of neck arteries leads to rupture of the intima or rupture of the vasa vasorum with bleeding into the media [3], which causes dissection of the vessel wall and yields a false lumen. Hematoma may increase towards adventitia, which translates into subadventitial dissection with pseudoaneurysm of the artery, and if it moves towards intima, the lumen grows narrower [4].

Digital subtraction angiography is the golden standard of diagnostics of craniocervical dissections [5], however, these disorders are mainly looked for with the help of MRI (magnetic resonance imaging) and msCTA (multispiral computed tomography angiography), which are practiced as routine studies [6]. These methods are effective in determining the extent of stenosis and intramural hematoma, and, with sensitivity up to 99%, they allow assessing condition of a vessel over a considerable length, but their ultimate utility is very dependent on the scanning protocols used and equipment enabling the process [7–9].

Ultrasound duplex scanning grows increasingly popular as the method of diagnosing extracranial dissections of brachiocephalic arteries, because resolution of the scanners is improving constantly and they are more and more readily available on the whole [10–12].

This study analyzed a significant array of relatively homogeneous clinical data acquired under similar conditions using various ultrasound diagnostic modes (methods) that complement and/or refine the results obtained, with some of those modes relatively rare.

The purpose of the study was to analyze and compare the results of comprehensive examinations of people who suffered an ischemic stroke with and without brachiocephalic artery dissections.

METHODS

This study includes data on 1451 individuals who had IS not later than 12 months ago. Neuroimaging methods allowed registering or confirming dissections of extracranial BCA (brachiocephalic arteries) in 53 of them (3.65%).

The inclusion criteria were: ischemic stroke verified by CT (computed tomography) or MRI; score 3 or below on the modified Rankin scale.

The exclusion criteria were: contraindications to MRI; history of serious diseases of the central nervous system.

We factored in demographic, anthropometric and anamnestic data: age, gender, height, weight, smoking status, alcohol consumption status, history of hypertension, atrial fibrillation, myocardial infarction, diabetes mellitus, characteristics of the IS (multiplicity, lesion side, basin, pathogenetic variant); body mass index (BMI) was calculated for each patient.

For electrocardiography (ECG), a Neurosoft electrocardiograph with Poly-spectrum software (Neurosoft, Russia) was used. The studies involved registration of the heart rate, direction of the heart's electrical axis, rhythm and conduction disorders, ischemic changes in the ST segment.

A Philips Epiq 7G scanner (Philips; USA) enabled duplex scanning of brachiocephalic arteries (DS BCA) and transcranial duplex scanning (TCDS), as well as duplex scanning of the lower extremity veins. A broadband multifrequency linear sensor operating at 3–12 MHz allowed assessing condition of extracranial stretches of the BCA and lower extremity veins, and another sensor working at 1–5 MHz was used for TCDS and transthoracic echocardiography (TTE).

Examination of extracranial sections of the BCA (B-mode) involved assessment of thickness of the intima-media complex; search for and assessment of severity of formations stenosing the lumens, their localization, degree of stenosis (applying the ECST methodology for the internal carotid artery), diameter of the artery, acoustic structure of the formations, its surface, complications.

Lower extremity veins were examined in a horizontal position. To detect thrombosis or post-thrombotic changes, the veins (all accessible segments of superficial and deep veins of both lower extremities) were subjected to compression tests every 1–2 cm.

Embologicity was established with the help of transcranial Doppler monitoring (TCDM) of blood flow at the base of brain through transtemporal access, in microembolodetection (MED) mode. The minimum duration of an examination was 60 minutes; it was enabled by an Angiodin Universal scanner (JSC NPF BIOS; Russia) operating dual frequency multi-depth sensors. Whenever signs of embolism were detected, its intensity was assessed.

Echocardiography (standard positions) was used to assess size and volume of the chambers of the heart, its contractility, left ventricle systolic and diastolic functions, presence of zones of hypo/akinesis, dyskinesis, pathological formations in the heart's chambers, condition of the valves (valvular stenosis and regurgitation, prosthetic heart valves), presence/absence of signs of blood shunting between the chambers, condition of the ascending aorta and the aortic arch.

MR studies of the brain were preformed with a Discovery MR750w system (General Electric, USA), magnetic field induction of 3 T. Results of each MR examination were assessed and described by by three doctors with sufficient experience, randomly selected from six doctors participating in the study.

Regional atrophy of the gray matter was evaluated using the GCA (Global Cortical Atrophy) qualitative scale. Lesions of hyperintensivity (deep and periventricular white matter) were scored on the qualitative Fazekas scale using the T2 weighted images with free fluid signal suppressed. Additionally, the researchers measured width of the third ventricle, looked for obstructive or normotensive hydrocephalus, micro-hemorrhages in the brain substance, hemosiderosis, gliosis/encephalomalacia sites and strategic infarcts (in the thalamus, angular gyrus artery basin, areas of adjacent blood supply in the frontal or parietal lobes, medial part of temporal lobes, in the basins of the anterior cerebral artery bilaterally).

Fifty-three patients from the dissection group and 453 patients from the control group had msCTA done with a 128 slice Optima CT scanner (GE; USA), voltage of 120 kV, current of 350 mAs. In all cases, 60 ml of preheated Ultravist nonionic contrast agent (iodine concentration of 370 mg/ml) were administered at the rate of 5 ml/second, followed by 40 ml of saline, also preheated. Aortic arch and all sections

Table 1. Main characteristics of patients with signs of dissection

Characteristic	Number of patients	Share (%)
Smoking status	20	37.7
Arterial hypertension	38	71.7
History of myocardial infarction	2	3.8
Atrial fibrillation	1	1.9
Diabetes mellitus	4	7.5
Signs of connective tissue insufficiency	3	5.7
History of injuries shortly before development of dissection	4	7.5
ARVI shortly before development of dissection (including Covid-19)	6	11.3
The alleged genesis of dissection: – cryptogenic – traumatic or iatrogenic	 49 4	 92.5 7.5
Dissection localization – right CCA – left CCA – right ICA – left ICA – right ECA – right VA – left VA – right ICA and right VA – left CCA, ICA and VA	 2 4 11 16 1 9 8 1 1	 3.8 7.5 20.8 30.2 1.9 17 15.1 1.9 1.9
Ischemic stroke side – right – left – cannot be determined (both sides simultaneously or in the stem structures, medially)	 24 23 6	 45.3 43.4 11.3
Ischemic stroke basin – vertebro-basilar – carotid	 7 46	 13.2 86.8
Multiple foci detected by MRI	16	30.2
Initial ischemic stroke	39	73.6
Coincidence of side of dissection and stroke	35	66.0

Note: CCA — common carotid artery; ICA — internal carotid artery; ECA — external carotid artery; VA — vertebral artery.

of the extra- and intracranial arteries were scanned. The images were analyzed using AW server (GE; USA); the process included 3D reconstruction of brachiocephalic arteries, quantitative assessment of arterial stenoses that relied on the NASCET criteria (North American Symptomatic Carotid Endarterectomy Trial) for extracranial artery stretches and WASID criteria (Warfarin-Aspirin Symptomatic Intracranial Disease) for intracranial sections.

Indicators detectable by msCTA, MRI and MRA that ensured admission to the dissections group were demilune symptom, which corresponds to an intramural hematoma [13], eccentric lumen stenosis with increased outer diameter of the artery [14–16], pseudoaneurysm, and "candle flame" symptom [17].

The data obtained were processed (statistical processing) with the help of SPSS Statistics 26.0 (IBM; USA) and R software 4.0.2 (R Core Team; Austria). The null hypothesis was rejected at the level of significance of $p \leq 0.05$. For quantitative variables, we used arithmetic mean and standard deviation or median and quartiles (in case of abnormal distribution), for qualitative variables — frequency and fraction (as a percentage). Normality of distribution of quantitative variables was checked with the help of Kolmogorov–Smirnov test. Pearson's χ^2 test or Fisher's exact test enabled comparison of the frequencies of qualitative dependent variables between categories of independent (grouping) variables. The relationship between quantitative and ordinal variables was assessed with the Pearson correlation. For quantitative dependent variables, the comparison relied on the Mann–Whitney test. Bonferroni correction was used for multiple comparisons.

RESULTS

Twelve (22.6%) of 53 patients with brachiocephalic artery dissections were female, 41 (77.4%) male. The mean age of the patients was 51.9 ± 14.8 (21-83) years. Body mass index in the dissections group was 25.2 ± 3.55 (19.0–33.9 kg/m^2), that is, those with dissections were more likely to have normal body weight (Table 1).

Most often, cerebral infarction developed in the basin of right (19 patients (35.8%)) and left middle cerebral artery (MCA) (15 patients (28.3%)). There was no relationship between the patient's age and the frequency of coincidence of infarct focus and dissection localizations: among patients below 50 years of age, such were found in 64% of cases. There was no connection between multiplicity of MRI-registered foci and coincidence of localization of the infarct focus and dissection ($p = 1.0$; Fig. 1). Consequently, the pattern of brain damage with multiple ischemic foci and dissections was as frequent as that without dissections.

There was no association registered between localization of dissection and gender/age. Patients with cryptogenic dissections were somewhat younger than those with traumatic ones (as a trend, $p = 0.101$).

Microembolic signals, according to TCDM with MED, were registered only in 1 (1.9%) out of 39 (73.5%) tests taken from individuals with dissections.

Patients with brachiocephalic artery dissections did not differ from other participants by gender ($p = 0.358$), but were significantly younger (age of IS patients without dissections was

Fig. 1. The ratio between coincidence of localization of the infarct focus and dissection, depending on the multiplicity status of the infarction foci

60.73 ± 11.95; $p < 0.0005$; Fig. 2) and had a lower body mass index (in patients without dissections, it was 27.70 ± 4.87; $p < 0.0005$; Fig. 3).

The characteristics of ischemic strokes (pathogenetic variant, side of infarction focus, lesion pool, stroke-affected artery) did not differ between patients with and without dissections. People with dissections were smokers more often (39.2% vs. 21.3%, $p = 0.005$), and less often suffered from atrial fibrillation (1.9% vs. 13.2%, $p = 0.01$), hypertension (71.7% vs. 84.2%, $p = 0.022$), diabetes mellitus (7.5% vs. 21.7%, $p = 0.01$).

As a trend (p = 0.066), there was registered the relationship between dissection and history of thromboextraction. As for the relationship between dissection and history of carotid stenting, the link between them was significant ($p = 0.015$).

ECG revealed no specific features in patients with dissections compared to patients without them ($p > 0.05$).

According to echocadiography, patients with dissections were less likely to have dilation of the left ($p = 0.014$) and right ($p = 0.018$) atria, and atherosclerotic changes in the thoracic aorta (as a trend, $p = 0.073$) (Table 2).

According to echocadiography, patients with dissections were significantly less likely to have signs of aortic stenosis (4.0% vs. 16.7%, $p = 0.017$).

In the dissections group (patients with dissections), according to msCTA, atherosclerotic plaques (ASP) in the CCA were significantly less common (30-40% vs. 60%, depending on the side, $p < 0.002$).

Computed tomography and DS of BCA revealed that brachiocephalic arteries, including ICA, were less frequently deformed in patients with dissections ($p < 0.05$) (Table 3).

According to DS of BCA, patients with dissections were significantly less likely to have intraluminal formations in the right subclavian artery (24.0% vs. 39.3%, $p = 0.037$). No such pattern was revealed for the left subclavian artery, nor for CCA and ICA ($p > 0.05$). The intima-media complex differentiation disruptions in the right and left CCA were significantly less common in dissection cases ($p < 0.0001$).

In the dissection group, signs of thrombosis of right and left ICA were detected with DS of BCA significantly more often (13% vs. 4.6%, $p = 0.021$ and 15.2% vs. 4.2%, $p = 0.004$, respectively) than in the control group. In dissection cases, DS of BCA has also revealed more frequent decrease in the peak systolic blood flow rate in intracranial sections of the right and left ICA ($p = 0.005$ and $p = 0.003$, respectively), signs of anastomosis on the left ($p = 0.058$), and collateralization within the circle of Willis — flow along the anterior ($p = 0.026$) and posterior communicating artery ($p = 0.006$).

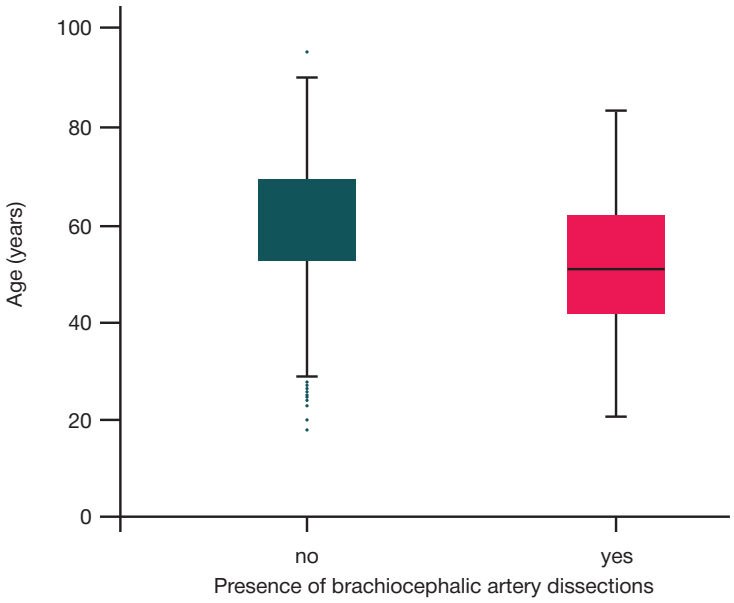

Fig. 2. Stroke patients with and without dissections: comparison of age

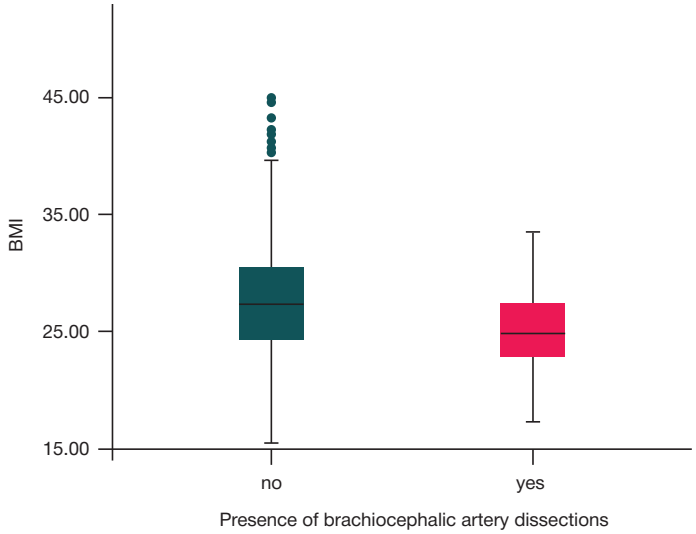

Fig. 3. Stroke patients with and without dissections: comparison of BMI

Lower extremities DS has shown that patients with dissections had signs of superficial vein thrombosis significantly more often ($p = 0.037$).

According to the msCTA, there was no relationship between dissections and structure of ASP (calcified, soft, mixed), as well as signs of their ulceration and localization features relative to the walls of the arteries ($p > 0.05$).

In the dissection group, according to MRI, changes in the periventricular and deep white matter of the brain were less pronounced ($p < 0.0005$ and $p = 0.001$). A noteworthy fact revealed by this examination is lack of strategic infarcts affecting the thalamus area in dissection cases (0% vs. 40.2%; $p < 0.0005$).

DISCUSSION

Considering that the sample analyzed in our study consists of IS patients, the data demonstrate lack of serious differences in the characteristics of strokes in cases with and without dissections. It is possible that, regardless of the intravascular thrombosis triggering factor (ASP or dissection), further events (arterio-arterial embolism) develop stereotypically. This opinion is the prevailing one in the published papers [18].

Patients with dissections tend to be younger than IS patients without dissections, which is a fact deserving attention. That noted, the mean age of participants of our study was similar to that reported by other authors [19–25]. It is possible that the pattern reflects the role of hereditary background predisposing to the development of BCA dissections.

The relationship between presence of dissections and thromboextraction in the acute IS period, as well as carotid artery stenting, may show the significance of the role of some interventions in certain cases with BCA dissections.

Various diagnostic methods revealed differences that depend on the dissections status, i.e., presence or lack thereof. In particular, patients with dissections were less likely to have intraluminal formations in individual arteries, and disrupted differentiation of the intima-media complex into layers signaling of the atherosclerotic process. At the same time, these patients exhibited signs of ICA thrombosis significantly more often. It cannot be excluded that the reason behind this is adhesion of platelets in the area of damage (or secondary involvement) of intima against the background of dissection of artery walls.

Echocadiography demonstrated that patients with dissections are less likely to have left and right atrial dilation, as well as atherosclerotic changes in the thoracic aorta and aortic stenosis. Previously published papers contain no such findings. In addition, msCTA revealed ASP in CCA less frequently in such cases. There was also no relationship between the presence of dissection and structure and localization of ASP. Obviously, the prevalence of these phenomena increases with age, so it is quite natural that in younger patients with dissections, atherosclerotic lesions of the aorta and main arteries, as well as manifestations of cardiac pathology, were less common. In addition, a DNA analysis seeking to determine polymorphism of apolipoprotein E has shown that the epsilon4 allele appears to be involved in the development of premature atherosclerosis of carotid arteries, and, at the same time, can protect against dissections [26]. Therefore, it cannot be completely excluded that hereditary characteristics could have played a part in our study in addition to the age-related intergroup differences.

The fact that dissection cases more frequently present decreased linear blood flow rates in the intracranial ICA, functioning of the ocular anastomosis on the dissection side, collateralization towards the affected artery basin along the anterior and posterior communicating arteries, may indicate the

Table 2. Echocadiography data, patients with and without dissections

Indicator	No dissection detected	Dissections
Left atrium dilation, persons (share, %) – yes – no	716 (54.2%) 606 (45.8%)	18 (36%) 32 (64%)
Right atrium dilation, persons (share, %) – yes – no	537 (40.8%) 778 (59.2%)	12 (24%) 38 (76%)
Thoracic aortic lesion, persons (share, %) – yes – no	272 (20.7%) 1045 (79.3%)	5 (10%) 45 (90%)

Table 3. Deformations of ICA as registered with DS of BCA, depending on dissections status

Characteristic	No dissections	Dissections
Deformation of right ICA – yes – no	 91 (7.0%) 1211 (93%)	 1 (2.1%) 46 (97.9%)
Deformation of left ICA – yes – no	 96 (7.5%) 1185 (92.5%)	 1 (2.1%) 46 (97.9%)

hemodynamic significance of a number of identified dissections, but it is still difficult to make conclusions about their role in the genesis of cerebral stroke if localization of the infarct focus and the dissection coincide. The frequency and nature of stroke do not depend on the degree of stenosis associated with artery dissection, however, in cases with occlusive dissections, infarctions turned out more extensive in comparison to non-occlusive cases [27].

On the context of this study, msCTA returned various BCA deformations in dissection cases less often, which may have links to the younger age or be a manifestation of greater stiffness of the vessel walls (perhaps, this is one of the important factors predisposing to dissections). There are opposite conclusions in the earlier studies, which state association of connective tissue weakness, tortuosity of the carotid arteries and their dissections against the background of fibromuscular dysplasia [28], which, apparently, should be attributed to the excessive "softness" (insufficient stiffness) of artery walls in cases of connective tissue insufficiency. There were few such cases in our sample, which is also confirmed by lack of association between dissections and signs of lower limb varicose veins. Nevertheless, in individuals with dissections, signs of superficial vein thrombosis were detected significantly more often, which, in addition to the state of the hemostasis system, may be a consequence of the structural features of vessel walls.

In dissection cases, MRI-detected manifestations of microangiopathy, i.e., changes in the periventricular and deep white matter of the brain, were less pronounced, which, apparently, was also associated with a younger age. At that, there were no significant differences in the severity of local atrophy of the cerebral cortex.

It is difficult to explain the lack of lesions in the thalamus zone in IS cases with dissections. This fact needs to be verified on more numerous samples.

It is known that, according to MRI data, the nature of infarction in carotid artery dissection is predominantly cortical (80%), subcortical (60%), in the MCA basin (99%), in the areas of adjacent blood supply (5%), anterior (4%) and posterior cerebral artery (3%) [29, 30]. According to the results of our study, 94% of patients with carotid artery dissections had infarction in the MCA basin, which is consistent with these data.

CONCLUSIONS

According to the results of this study, IS patients with BCA dissections were younger than those without dissections, they were less likely to have dilated left and right atria, signs of atherosclerotic changes in the thoracic aorta and common carotid arteries, and deformities of various BCA. In this dissection group, changes in the periventricular and deep white matter of the brain were also less pronounced (MRI-registered manifestations of microangiopathy or small vessel disease).

Comparison of the results of comprehensive examinations of IS patients with and without extracranial BCA dissections revealed that the differences identified are most likely related to age (younger age of patients with dissections), as well as other factors, including hereditary characteristics.

References

1. Tian C, Cao X, Wang J. Recanalisation therapy in patients with acute ischaemic stroke caused by large artery occlusion: choice of therapeutic strategy according to underlying aetiological mechanism? Stroke Vasc Neurol. 2017; 2 (4): 244–50. DOI: 10.1136/svn-2017-000090.
2. Patil S, Rossi R, Jabrah D, Doyle K. Detection, diagnosis and treatment of acute ischemic stroke: current and future perspectives. Front Med Technol. 2022; 4. DOI:10.3389/fmedt.2022.748949.
3. Willey JZ, Dittrich R, Kuhlenbaeumer G, Ringelstein EB. The outer arterial wall layers are primarily affected in spontaneous cervical artery dissection. Neurology. 2011; 77 (20): 1859. DOI:10.1212/WNL.0b013e318239bdcc.
4. Lee VH, Brown RD, Mandrekar JN, Mokri B. Incidence and outcome of cervical artery dissection: A population-based study. Neurology. 2006; 67 (10): 1809–12. doi:10.1212/01.wnl.0000244486.30455.71.
5. Grossberg JA, Haussen DC, Cardoso FB, et al. Cervical carotid pseudo-occlusions and false dissections. Stroke. 2017; 48 (3): 774–7. DOI:10.1161/STROKEAHA.116.015427.
6. Provenzale JM, Sarikaya B. Comparison of test performance characteristics of MRI, MR angiography, and CT angiography in the diagnosis of carotid and vertebral artery dissection: a review of the medical literature. American Journal of Roentgenology. 2009; 193 (4): 1167–74. DOI:10.2214/AJR.08.1688.
7. Vertinsky AT, Schwartz NE, Fischbein NJ, Rosenberg J, Albers GW, Zaharchuk G. Comparison of Multidetector CT Angiography and MR Imaging of cervical artery dissection. American Journal of Neuroradiology. 2008; 29 (9):1753–60. DOI:10.3174/ajnr.A1189.
8. Chen CJ, Tseng YC, Lee TH, Hsu HL, See LC. Multisection CT angiography compared with catheter angiography in diagnosing vertebral artery dissection. AJNR Am J Neuroradiol. 2004; 25 (5): 769–74.
9. Rodallec MH, Marteau V, Gerber S, Desmottes L, Zins M. Craniocervical arterial dissection: spectrum of imaging findings and differential diagnosis. RadioGraphics. 2008; 28 (6): 1711–28. DOI:10.1148/rg.286085512.
10. Yang L, Ran H. Extracranial vertebral artery dissection. Medicine. 2018; 97 (9): e0067. DOI:10.1097/MD.0000000000010067.
11. Gardner DJ, Gosink BB, Kallman CE. Internal carotid artery dissections: duplex ultrasound imaging. Journal of Ultrasound in Medicine. 1991; 10 (11): 607–14. DOI:10.7863/jum.1991.10.11.607.
12. Nebelsieck J, Sengelhoff C, Nassenstein I, et al. Sensitivity of neurovascular ultrasound for the detection of spontaneous cervical artery dissection. Journal of Clinical Neuroscience. 2009; 16 (1): 79–82. DOI:10.1016/j.jocn.2008.04.005.
13. Ben Hassen W, Machet A, Edjlali-Goujon M, et al. Imaging of cervical artery dissection. Diagn Interv Imaging. 2014; 95 (12):

1151–61. DOI:10.1016/j.diii.2014.10.003.
14. Petro G, Witwer G, Cacayorin E, et al. Spontaneous dissection of the cervical internal carotid artery: correlation of arteriography, CT, and pathology. American Journal of Roentgenology. 1987; 148 (2): 393–8. DOI:10.2214/ajr.148.2.393.
15. Zuber M, Meary E, Meder JF, Mas JL. Magnetic resonance imaging and dynamic CT scan in cervical artery dissections. Stroke. 1994; 25 (3): 576–81. DOI:10.1161/01.STR.25.3.576.
16. Leclerc X, Godefroy O, Salhi A, Lucas C, Leys D, Pruvo JP. Helical CT for the diagnosis of extracranial internal carotid artery dissection. Stroke. 1996; 27 (3): 461–6. DOI:10.1161/01.STR.27.3.461.
17. Rodallec MH, Marteau V, Gerber S, Desmottes L, Zins M. Craniocervical arterial dissection: spectrum of imaging findings and differential diagnosis. RadioGraphics. 2008; 28 (6): 1711–28. DOI:10.1148/rg.286085512.
18. Morel A, Naggara O, Touzé E, et al. Mechanism of ischemic infarct in spontaneous cervical artery dissection. Stroke. 2012; 43 (5): 1354–61. DOI:10.1161/STROKEAHA.111.643338.
19. Nedeltchev K. Ischaemic stroke in young adults: predictors of outcome and recurrence. J Neurol Neurosurg Psychiatry. 2005; 76 (2): 191–5. DOI:10.1136/jnnp.2004.040543.
20. Leys D, Bandu L, Henon H, et al. Clinical outcome in 287 consecutive young adults (15 to 45 years) with ischemic stroke. Neurology. 2002; 59 (1): 26–33. DOI:10.1212/WNL.59.1.26.
21. Redekop GJ. Extracranial carotid and vertebral artery dissection: a review. Canadian Journal of Neurological Sciences / Journal Canadien des Sciences Neurologiques. 2008; 35 (2): 146–52. DOI:10.1017/S0317167100008556.
22. Tepper SJ, Bigal M, Taylor FR. Abstracts and citations. Headache: the journal of head and face pain. 2007; 47 (3): 454–60. DOI:10.1111/j.1526-4610.2007.00744.x.
23. Raser JM, Mullen MT, Kasner SE, Cucchiara BL, Messe SR. Cervical carotid artery dissection is associated with styloid process length. Neurology. 2011; 77 (23): 2061–6. DOI:10.1212/WNL.0b013e31823b4729.
24. Schievink WI, Roiter V. Epidemiology of cervical artery dissection. In: handbook on cerebral artery dissection. KARGER; 2005: 12–5. DOI:10.1159/000088125.
25. Fusco MR, Harrigan MR. Cerebrovascular dissections — a review part I: spontaneous dissections. Neurosurgery. 2011; 68 (1): 242–57. DOI:10.1227/NEU.0b013e3182012323.
26. Orlandi G, Fanucchi S, Mancuso M, et al. Dissection and atherosclerosis of carotid arteries in the young: role of the apolipoprotein E polymorphism. Eur J Neurol. 2002; 9 (1): 19–21. DOI:10.1046/j.1468-1331.2002.00340.x.
27. Naggara O, Morel A, Touzé E, et al. Stroke occurrence and patterns are not influenced by the degree of stenosis in cervical artery dissection. Stroke. 2012; 43 (4): 1150–2. DOI:10.1161/STROKEAHA.111.639021.
28. Bilman V, Apruzzi L, Baccellieri D, Sanvito F, Bertoglio L, Chiesa R. Symptomatic internal carotid artery dissection and kinking in a patient with fibromuscular dysplasia. J Vasc Bras. 2021; 20. DOI:10.1590/1677-5449.200243.
29. Lucas C, Moulin T, Deplanque D, et al. Stroke patterns of internal carotid artery dissection in 40 patients. Stroke. 1998; 29 (12): 2646–8. DOI:10.1161/01.STR.29.12.2646.
30. Baumgartner RW, Arnold M, Baumgartner I, et al. Carotid dissection with and without ischemic events: Local symptoms and cerebral artery findings. Neurology. 2001; 57 (5): 827–32.

Литература

1. Tian C, Cao X, Wang J. Recanalisation therapy in patients with acute ischaemic stroke caused by large artery occlusion: choice of therapeutic strategy according to underlying aetiological mechanism? Stroke Vasc Neurol. 2017; 2 (4): 244–50. DOI: 10.1136/svn-2017-000090.
2. Patil S, Rossi R, Jabrah D, Doyle K. Detection, diagnosis and treatment of acute ischemic stroke: current and future perspectives. Front Med Technol. 2022; 4. DOI:10.3389/fmedt.2022.748949.
3. Willey JZ, Dittrich R, Kuhlenbaeumer G, Ringelstein EB. The outer arterial wall layers are primarily affected in spontaneous cervical artery dissection. Neurology. 2011; 77 (20): 1859. DOI:10.1212/WNL.0b013e318239bdcc.
4. Lee VH, Brown RD, Mandrekar JN, Mokri B. Incidence and outcome of cervical artery dissection: A population-based study. Neurology. 2006; 67 (10): 1809–12. doi:10.1212/01.wnl.0000244486.30455.71.
5. Grossberg JA, Haussen DC, Cardoso FB, et al. Cervical carotid pseudo-occlusions and false dissections. Stroke. 2017; 48 (3): 774–7. DOI:10.1161/STROKEAHA.116.015427.
6. Provenzale JM, Sarikaya B. Comparison of test performance characteristics of MRI, MR angiography, and CT angiography in the diagnosis of carotid and vertebral artery dissection: a review of the medical literature. American Journal of Roentgenology. 2009; 193 (4): 1167–74. DOI:10.2214/AJR.08.1688.
7. Vertinsky AT, Schwartz NE, Fischbein NJ, Rosenberg J, Albers GW, Zaharchuk G. Comparison of Multidetector CT Angiography and MR Imaging of cervical artery dissection. American Journal of Neuroradiology. 2008; 29 (9):1753–60. DOI:10.3174/ajnr.A1189.
8. Chen CJ, Tseng YC, Lee TH, Hsu HL, See LC. Multisection CT angiography compared with catheter angiography in diagnosing vertebral artery dissection. AJNR Am J Neuroradiol. 2004; 25 (5): 769–74.
9. Rodallec MH, Marteau V, Gerber S, Desmottes L, Zins M. Craniocervical arterial dissection: spectrum of imaging findings and differential diagnosis. RadioGraphics. 2008; 28 (6): 1711–28. DOI:10.1148/rg.286085512.
10. Yang L, Ran H. Extracranial vertebral artery dissection. Medicine. 2018; 97 (9): e0067. DOI:10.1097/MD.0000000000010067.
11. Gardner DJ, Gosink BB, Kallman CE. Internal carotid artery dissections: duplex ultrasound imaging. Journal of Ultrasound in Medicine. 1991; 10 (11): 607–14. DOI:10.7863/jum.1991.10.11.607.
12. Nebelsieck J, Sengelhoff C, Nassenstein I, et al. Sensitivity of neurovascular ultrasound for the detection of spontaneous cervical artery dissection. Journal of Clinical Neuroscience. 2009; 16 (1): 79–82. DOI:10.1016/j.jocn.2008.04.005.
13. Ben Hassen W, Machet A, Edjlali-Goujon M, et al. Imaging of cervical artery dissection. Diagn Interv Imaging. 2014; 95 (12): 1151–61. DOI:10.1016/j.diii.2014.10.003.
14. Petro G, Witwer G, Cacayorin E, et al. Spontaneous dissection of the cervical internal carotid artery: correlation of arteriography, CT, and pathology. American Journal of Roentgenology. 1987; 148 (2): 393–8. DOI:10.2214/ajr.148.2.393.
15. Zuber M, Meary E, Meder JF, Mas JL. Magnetic resonance imaging and dynamic CT scan in cervical artery dissections. Stroke. 1994; 25 (3): 576–81. DOI:10.1161/01.STR.25.3.576.
16. Leclerc X, Godefroy O, Salhi A, Lucas C, Leys D, Pruvo JP. Helical CT for the diagnosis of extracranial internal carotid artery dissection. Stroke. 1996; 27 (3): 461–6. DOI:10.1161/01.STR.27.3.461.
17. Rodallec MH, Marteau V, Gerber S, Desmottes L, Zins M. Craniocervical arterial dissection: spectrum of imaging findings and differential diagnosis. RadioGraphics. 2008; 28 (6): 1711–28. DOI:10.1148/rg.286085512.
18. Morel A, Naggara O, Touzé E, et al. Mechanism of ischemic infarct in spontaneous cervical artery dissection. Stroke. 2012; 43 (5): 1354–61. DOI:10.1161/STROKEAHA.111.643338.
19. Nedeltchev K. Ischaemic stroke in young adults: predictors of outcome and recurrence. J Neurol Neurosurg Psychiatry. 2005; 76 (2): 191–5. DOI:10.1136/jnnp.2004.040543.
20. Leys D, Bandu L, Henon H, et al. Clinical outcome in 287 consecutive young adults (15 to 45 years) with ischemic stroke. Neurology. 2002; 59 (1): 26–33. DOI:10.1212/WNL.59.1.26.
21. Redekop GJ. Extracranial carotid and vertebral artery dissection: a review. Canadian Journal of Neurological Sciences / Journal Canadien des Sciences Neurologiques. 2008; 35 (2): 146–52.

DOI:10.1017/S0317167100008556.
22. Tepper SJ, Bigal M, Taylor FR. Abstracts and citations. Headache: the journal of head and face pain. 2007; 47 (3): 454–60. DOI:10.1111/j.1526-4610.2007.00744.x.
23. Raser JM, Mullen MT, Kasner SE, Cucchiara BL, Messe SR. Cervical carotid artery dissection is associated with styloid process length. Neurology. 2011; 77 (23): 2061–6. DOI:10.1212/WNL.0b013e31823b4729.
24. Schievink WI, Roiter V. Epidemiology of cervical artery dissection. In: handbook on cerebral artery dissection. KARGER; 2005: 12–5. DOI:10.1159/000088125.
25. Fusco MR, Harrigan MR. Cerebrovascular dissections — a review part I: spontaneous dissections. Neurosurgery. 2011; 68 (1): 242–57. DOI:10.1227/NEU.0b013e3182012323.
26. Orlandi G, Fanucchi S, Mancuso M, et al. Dissection and atherosclerosis of carotid arteries in the young: role of the apolipoprotein E polymorphism. Eur J Neurol. 2002; 9 (1): 19–21. DOI:10.1046/j.1468-1331.2002.00340.x.
27. Naggara O, Morel A, Touzé E, et al. Stroke occurrence and patterns are not influenced by the degree of stenosis in cervical artery dissection. Stroke. 2012; 43 (4): 1150–2. DOI:10.1161/STROKEAHA.111.639021.
28. Bilman V, Apruzzi L, Baccellieri D, Sanvito F, Bertoglio L, Chiesa R. Symptomatic internal carotid artery dissection and kinking in a patient with fibromuscular dysplasia. J Vasc Bras. 2021; 20. DOI:10.1590/1677-5449.200243.
29. Lucas C, Moulin T, Deplanque D, et al. Stroke patterns of internal carotid artery dissection in 40 patients. Stroke. 1998; 29 (12): 2646–8. DOI:10.1161/01.STR.29.12.2646.
30. Baumgartner RW, Arnold M, Baumgartner I, et al. Carotid dissection with and without ischemic events: Local symptoms and cerebral artery findings. Neurology. 2001; 57 (5): 827–32.

CEREBRAL NEURAL NETWORKS IN CASES OF CONCOMITANT CHRONIC CEREBRAL ISCHEMIA AND TYPE 2 DIABETES MELLITUS

Fokin VF✉, Ponomareva NV, Konovalov RN, Shabalina AA, Medvedev RB, Lagoda OV, Boravova AI, Krotenkova MV, Tanashyan MM

Research Center of Neurology, Moscow, Russia

With type 2 diabetes mellitus (DM2) as a concomitant disease, chronic cerebral ischemia (CCI) has a more severe course because of chronic hyperglycemia. Using resting state functional MRI (fMRI) data, this study aimed to investigate connectivity of cerebral neural networks in patients that have CCI with DM2 and without DM2. The study involved 257 CCI patients (81 male and 176 female, aged 50-85 years) some of whom had DM2. We assessed metabolic parameters, state of cerebral circulation, and cognitive functions. Resting fMRI was used for the analysis of structure of connectivity of cerebral neural networks. With false discovery rate (FDR) factored in, CCI patients with DM2 had values of some indicators of connectivity of cerebral neural networks at a level significantly lower than CCI patients without DM2 ($p_{(FDR)} < 0.05$). Namely, the indicators in question were those of connectivity of right hemisphere's speech neural network, left hemisphere's parahippocampal region, and angular gyrus of the right hemisphere, which is an integral part of the brain's passive mode network. Also, CCI patients with DM2 had significantly poorer connectivity of anterior cingulate gyrus, part of the salient neural network, and superior temporal gyrus. There are significant changes in the cerebellar networks, too. Overall, the size and intensity of most of the neural networks studied in resting state are lower in CCI patients with DM2.

Keywords: chronic cerebral ischemia, type 2 diabetes mellitus, resting state functional MRI, connectivity, size and intensity of neural networks

Funding: the study was supported through the grant by RSF 22-15-00448.

Author contribution: Fokin VF — article authoring; Ponomareva NV — design of physiological and neuropsychological tests, general design of the study; Konovalov RN — design of neuroimaging evaluation; Shabalina AA — biochemical tests; Medvedev RB — dopplerogaphy; Lagoda OV — clinical tests; Boravova AI — psychophysiological tests; Krotenkova MV — management of neuroimaging evaluation; Tanashyan MM — management of clinical tests, general design of the study.

Compliance with ethical standards: the study was approved by the local Ethical Committee of the Research Center of Neurology (Minutes #5-6/22 of June 1, 2022). All participants submitted signed informed consent forms.

✉ **Correspondence should be addressed:** Vitaly F. Fokin
Volokolamskoye shosse, 80, Moscow, 125367, Russia; fvf@mail.ru

Received: 14.09.2023 **Accepted:** 22.09.2023 **Published online:** 31.10.2023

DOI: 10.24075/brsmu.2023.042

НЕЙРОСЕТИ ГОЛОВНОГО МОЗГА ПРИ СОЧЕТАНИИ ХРОНИЧЕСКОЙ ЦЕРЕБРАЛЬНОЙ ИШЕМИИ И САХАРНОГО ДИАБЕТА 2-ГО ТИПА

В. Ф. Фокин✉, Н. В. Пономарева, Р. Н. Коновалов, А. А. Шабалина, Р. Б. Медведев, О. В. Лагода, А. И. Боравова, М. В. Кротенкова, М. М. Танашян

Научный центр неврологии, Москва, Россия

Хроническая ишемия головного мозга (ХИМ), осложненная сахарным диабетом 2-го типа (СД2), характеризуется более тяжелым течением, связанным с хронической гипергликемией. Цель работы — исследовать организацию коннективности нейросетей мозга по данным функциональной магнитно-резонансной томографии (фМРТ) покоя у пациентов с ХИМ, страдающих диабетом 2-го типа, по сравнению с больными ХИМ без диабета. В исследовании приняли участие 257 пациентов: 81 мужчина и 176 женщин в возрасте 50–85 лет с ХИМ, часть из которых болели СД2. Оценивали метаболические показатели, состояние мозгового кровообращения, а также когнитивные функции. С помощью фМРТ покоя анализировали коннективную организацию нейросетей мозга. У больных ХИМ с СД2 показатели коннективности ряда нейросетей мозга с учетом поправки на множественность сравнений FDR (False discovery rate) статистически достоверно снижены ($p_{(FDR)} < 0,05$) по сравнению с больными ХИМ без СД2. Это коннективности речевой нейросети правого полушария с парагиппокампальной областью левого полушария и с угловой извилиной правого полушария, которая является составной частью сети пассивного режима работы мозга. Коннективность передней поясной извилины, входящей в салиентную нейросеть, с верхней височной извилиной была значимо ниже у больных ХИМ с СД2. Достоверные изменения затрагивают и мозжечковые сети. В целом, размер и нормированная интенсивность большинства исследованных нейросетей покоя ниже у больных ХИМ с диабетом.

Ключевые слова: хроническая ишемия мозга, сахарный диабет 2-го типа, функциональная МРТ покоя, коннективность, размер и интенсивность нейросетей

Финансирование: работа поддержана грантом РНФ 22-15-00448.

Вклад авторов: В. Ф. Фокин — написание статьи; Н. В. Пономарева — дизайн физиологических и нейропсихологических исследований, общий дизайн работы; Р. Н. Коновалов — дизайн нейровизуалиционных исследований; А. А. Шабалина — биохимические исследования; Р. Б. Медведев — допплерографические исследования; О. В. Лагода — клинические исследования; А. И. Боравова — психофизиологические исследования; М. В. Кротенкова — руководство нейровизуализационными исследованиями; М. М. Танашян — руководство клиническими исследованиями, общий дизайн работы.

Соблюдение этических стандартов: исследование одобрено локальным этическим комитетом Научного центра неврологии (протокол № 5-6/22 от 1 июня 2022 г.). Получено информированное согласие всех участников обследований.

✉ **Для корреспонденции:** Виталий Федорович Фокин
Волоколамское шоссе, д. 80, г. Москва, 125367, Россия; fvf@mail.ru

Статья получена: 14.09.2023 **Статья принята к печати:** 22.09.2023 **Опубликована онлайн:** 31.10.2023

DOI: 10.24075/vrgmu.2023.042

Chronic cerebral ischemia (CCI) is a disease that degrades the flow of blood to the brain through main and small arteries, which leads to various cerebral disorders. As a rule, CCI develops in old and senile age. The typical concomitant conditions are narrowed cerebral arteries that are also growing less elastic due to atherosclerosis, hypertension, diabetic angiopathy, and other pathological processes. Comorbidity of CCI and type 2 diabetes mellitus (DM2) is common. DM2 aggravates ischemic

brain damage, but the effect of this comorbidity on cerebral connectivity has not been studied sufficiently [1].

Excess glucose in patients with DM2 can cause neuron degeneration and the related neurological diseases and cognitive impairments. High blood glucose levels affect cells that can regulate its intake only in a limited fashion. These are, first of all, endothelial cells, as well as neurons of the peripheral and central nervous system [2]. Spikes in glucose levels modify microglial activity, which contributes to the development of inflammatory processes [3]. Chronic hyperglycemia causes a number of pathophysiological changes that aggravate its toxic effects on cells, tissues and organ systems. Some neurons begin to oversecrete neurotransmitters, including glutamate, one of the most common excitatory neurotransmitters that can have an excitotoxic effect [4]. Excess glucose dampens the ability of neurons to process information and disrupts interneuronal contacts. In part, this may be due to lower levels of glucose in the intercellular space, which conditions interaction between neurons [5–7]. There is evidence that brain plays an active role in glucose homeostasis, but the relative importance of this factor in comparison with others is still unclear [8].

Glucose is delivered to brains cells by transporter proteins, including Glut1 and Glut2, which facilitate glucose transfer across cell membranes. Insulin resistance associated with DM2 can handicap glucose's ability to enter brain cells, which hampers cerebral energy metabolism. Studies that employed positron emission tomography have shown that this compromises glucose metabolism in certain areas of the brain, such as prefrontal cortex and hippocampus, which are important for cognitive functions, memory, and decision-making. For example, it has been shown that, compared to healthy individuals, DM2 patients have less glucose metabolized in the prefrontal cortex, which translates into lower scores in cognitive tests. There is also evidence that this disease can disrupt mitochondrial dysfunction in the brain, which, again, translates into lower cognitive test scores as compared to those shown by people that do not have DM2 [9–12].

Disrupted glucose metabolism is associated with restructuring of interneuronal connections, which should be investigated in order to understand how the brain of CCI patients with DM2 works. Some studies designed for this purpose employ functional magnetic resonance imaging (fMRI), which allows examining connectivity, i.e., functional connections between different areas of the brain; such neuroimaging enables progress in neurology today [13]. Many published papers describe features of the structural and functional organization of the brain of CCI patients with DM2, but few address connectivity changes therein as registered with resting fMRI. BOLD signal is the ratio between oxidized and reduced forms of hemoglobin. It is assumed that synchronization of BOLD signals in different areas of the brain reflects synchronization of neural activity therein. This assumption has proven effective in practice, thus, the respective approach allows investigating communications between different areas of the brain. Assessment of synchronization of the BOLD signals yields quantification of the strength of interneuronal connections, and shows if the interaction is positive or negative.

Against the background of CCI, disruption of cerebral circulation can have significant consequences for functioning of the central nervous system, including deterioration of cognitive abilities and an increased risk of stroke. With DM2 as a concomitant disease, patients run a higher risk of microvascular and macrovascular complications, including ischemic stroke and small vessel disease, which significantly aggravates the overall pathogenic effect of the vascular dysfunction, and reduces the effectiveness of interactions between different regions of the brain [14].

Using the resting fMRI data, this study aimed to investigate connectivity of cerebral neural networks in patients that have CCI with DM2 and without DM2. We sought to understand the potential impact of DM2 on the organization of connectivity in a brain of a CCI patient, and assess the role comorbidity of these diseases plays in the development of cognitive and other disorders associated with CCI, such understanding and assessment potentially enabling development of the new methods of treatment and prevention of these diseases.

METHODS

The study involved 257 patients, 81 male and 176 female, aged 50–85 years, all diagnosed with CCI (Table 1). Part of them, 80 people (31%), also had DM2. Table 1 presents demographic characteristics of the participants. The average duration of CCI was 10.1 ± 0.7 years. The patients were divided into two groups: without DM2 (group 1) and with DM2 (group 2). The key causes of CCI were atherosclerosis, arterial hypertension, venous insufficiency, diabetic angiopathy, vasculitis of various etiologies, etc. The duration of DM2 was 15.8 ± 1.1 years; no patient had severe macrovascular complications nor ran the risk of severe hypoglycemia. The inclusion criteria were: initial manifestations and subcompensation of CCI, no need for constant care from others [15–17]. The exclusion criteria were: score 1 up dementia as per the Clinical Dementia Rating Scale [18], a history of acute cerebral circulatory disorders, traumatic brain injuries, severe cardiac, renal insufficiency, uncompensated thyroid dysfunction. All the patients were right-handed.

Body mass index (BMI) was higher in both male and female patients with DM2 (p = 0.006 and p = 0.009, respectively). There were significantly more men that graduated from an higher education establishment than women (both groups; $p < 0.01$).

There were no differences in statistical BMI, age indicators for men and women in both groups; the number of male participants in the groups was similar (difference insignificant). Thus, it is possible to investigate the organization of neural networks in combined groups.

Table 1. Demographic characteristics of CCI patients with DM2 and without DM2

	Number of men	Number of women	BMI, men	BMI, women	Age, men	Age, women	Education higher / secondary, men	Education higher/secondary, women
CCI patients w/o DM2 (group 1)	59	120	27.1 ± 0.5	27.6 ± 0.5	64.7 ± 1.4	67.2 ± 0.7	*35/23	57/52
patients with DM2 (group 2)	23	57	*30.2 ± 1.3	*30.2 ± 0.9	67.2 ± 2.1	68.9 ± 1.1	*14/8	24/25

Note: the table shows mean values ± standard errors.

Table 2. Biochemical, psychometric, and hemodynamic indicators significantly different in the two groups of CCI patients (with and without DM2), as revealed by ANOVA, as well as means and standard errors of the indicators

	Analysis of Variance (ANOVA)			Mean ± standard error	
	n	F	*p*	Group 1	Group 2
Glucose, mmol/l	257	154.9	0	5.2 ± 0.03	7.1 ± 0.22
Triglycerides, mmol/l	247	24.4	0.000001	1.4 ± 0.005	1.9 ± 0.12
IL6, pg/ml	112	4.1	0.045333	157.03 ± 8.2	188.95 ± 14.2
ESR, mm/hour	248	16.2	0.000075	14.4 ± 0.7	19.5 ± 1.1
Fibrinogen g/l	236	10.9	0.001088	3.6 ± 0.06	3.9 ± 0.08
Left MCA resistance index	92	7.8	0.006389	0.52 ± 0.009	0.57 ± 0.016
LP proofreading test (K = F/A)	242	9.4	0.002424	0.86 ± 0.0106	0.78 ± 0.0229

Note: *n* — number of subjects, F — Fisher's test, *p* — level of significance, MCA — middle cerebral artery, LP — letter patterns, K — proof-reading test success rate.

Resting fMRI

The participants (83 CCI patients, 27 of them with DM2) underwent brain fMRI aimed at registering the BOLD signal. The tomograph was Magnetom Verio (Siemens; Germany), with magnetic field strength of 3.0 Tl. T2 weighted EPI sequence was used to obtain the resting functional scans: TR = 1500 ms, TE = 30 ms, flip angle = 70°, section thickness — 2 mm, FOV = 190 mm, FoV phase — 100.0%. The participants were instructed to fully relax, lie calmly with eyes closed (to exclude stimulation of the visual analyzer) and not think about anything specific. The MRI data were processed in the MATLAB SPM12 software. With the help of CONN-18b application on the SPM-12 platform, we analyzed connectivity in various neural networks of the brain; CONN-18b is an open source toolkit based on MATLAB [19].

Using CONN-18b, we compared connectivity in two groups of CCI patients, with and without DM2. The reliability of differences was assessed by a standardized regression coefficient adjusted for false discovery rate (FDR).

Analysis of the neural networks relied on their two main features, size and intensity. These indicators are convenient and natural tools for describing connectivity graphs [20–22]. Size of a neural network is the number of connections it has to other formations. Its intensity is the sum of T-test values (absolute) describing connectivities of the given neural network. We used normalized connectivity, i.e., the network's intensity-to-size ratio.

Cognitive tests

The patients did a proof-reading test: for 3 minutes, they searched for two adjacent similar letters (letter patterns) in a text without spaces. This test is based on Kirchner's n-back test; in our case, n equaled 1, since at n > 1 the test was difficult for most participants. Evaluating the participants' performance, we factored in the number of letter patterns found as it related to the total number of such combinations and to the number of lines viewed, the total volume of text viewed, and the difference between all letter patterns and the number of patterns found. In addition, patients undertook verbal fluency test, Luria's memory words test and the MoCA test. These cognitive tests were described before [23].

Duplex scanning

At this stage, we evaluated the linear velocity of systolic and diastolic blood flow in the right and left internal carotid, middle cerebral (MCA) and brachial arteries. The system used for the purpose was Toshiba Viamo. To assess systolic linear blood flow velocity and index of peripheral resistance in the arteries, we relied on the generally accepted method and used a linear sensor with a frequency of 5.0–12.0 MHz.

Biochemical studies

The patients donated blood for a blood panel, which assessed levels of glucose, triglycerides, fibrinogen, ESR (erythrocyte sedimentation rate) and other indicators. To learn the level of interleukins, we used saliva samples, same as for cytokines, which were established using a sandwich solid-phase enzyme immunoassay (ELISA). The content of IL6 was determined with the help of Vector-Best kits (Vector-Best; Russia). The measuring range was 1–2000 pg/ml. In all studies, we used calibrators provided by manufacturers of the reagents, and additional calibrators purchased for the purpose.

The study was done in duplicates, on a VICTOR 2 microplate reader (Perken Elmer; USA), using control samples with low and high content of the studied parameters. Saliva samples were collected from the patients; they refrained from alcohol for a week before sampling, did not drink neither tea nor coffee 1 hour before that, and rinsed their mouth with water before spitting at least 1.5 ml of saliva into a test tube. Saliva samples contaminated with blood were excluded from the study, with contamination tested for using an enzyme immunoassay kit [23]. In addition, we registered blood pressure and heart rate.

Statistical data processing

Statistica 12 software package (Dell; USA) was used to statistically process the data acquired. Kolmogorov-Smirnov test was used to establish whether the distribution is normal or abnormal. We calculated arithmetic means, standard errors, and did one-factor variance and correlation analyses. The analysis of neural networks involved determination of Student's *t*-test and adjustment for FDR. The size and normalized intensity of neural networks were evaluated.

RESULTS

The registered difference between patients with DM2 and without it was evident in a number of biochemical, hemodynamic and cognitive indicators, and in the characteristics of inflammatory processes, which point to serious metabolic and other differences in the activity of the brain and the body (Table 2).

The resulting data indicate serious differences between the groups that concern carbohydrate and lipid metabolism (glucose, triglycerides), inflammatory processes (IL6, ESR), hemodynamic parameters and cognitive functions. All the participating patients exhibited high values of inflammation

indicators, but those with DM2 had the respective symptoms more pronounced. The results of proof-reading test in group 2 (with DM2) were inferior to those in group 1.

The revealed differences may have a connection with the organization of neural networks. Figure 1 and Table 3 show data on the cerebral neural networks that had values of all the significantly different connectivities significantly higher in group 1 compared to group 2.

Thus, between the two groups, we identified neural networks that have different connectivity parameters, the difference being significant with p(FDR) < 0.05 factored in. The resulting data indicate that altered connectivities are associated with large neural networks (default network, salient, cerebellar, speech networks). This suggests that potential changes in the organization of neural networks may affect their performance and significant regions of the brain.

Therefore, it can be assumed that with DM2 in the background, rearrangement of connections in the brain extends beyond the four mentioned connectivities; moreover, this disease probably triggers other changes in each network, less significant yet characteristic of most neural networks, which are often disregarded. There are two parameters used to describe a network: its size and its intensity [24]. The latter depends on the former: the larger the size, the higher the intensity. Therefore, it is feasible to consider a normalized neural network intensity indicator, i.e., intensity divided by size. Table 4 presents values of these parameters peculiar to the two groups of this study.

The resulting data suggest that patients with DM2, as a rule, have less significant connectivity indicators than patients not suffering DM2. Moreover, the normalized intensity of most neural networks in them is lower. Based on both parametric and non-parametric criteria, these data are reliable; the latter includes the sign test, which confirms reliability (p < 0.01) of the observation showing that CCI patients without DM2 have greater size and normalized intensity of neural networks than CCI patients with DM2.

Figure 2 presents distribution of connectivities coming out of the dorsal attention network in the right hemisphere.

The right hemisphere's dorsal attention network in group 1 is almost twice as large as that in group 2 (86 and 44, respectively). As for the left hemisphere, the difference in size is only 1.7, but CCI patients without DM2, which comprise group 1, have normalized intensity 2.2 greater than registered in CCI patients with DM2, group 2; this is more than recorded for the right hemisphere (Table 4). The differences in connectivity of this neural network are most noticeable in the frontal medial gyrus of left hemisphere, in the dorsal attention network of right and left hemispheres, in the right half of the cerebellum, in the right parietal region and other regions. However, some of the high-intensity connectivities remain stably high in CCI patients with DM2. This applies, first of all, to the left hemisphere's dorsal attention network, postcentral gyrus, additional motor area of both hemispheres and some other formations.

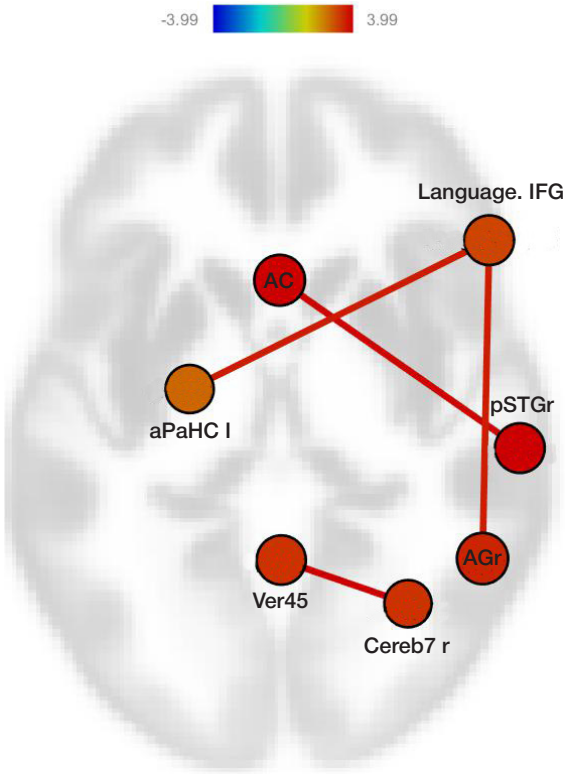

Fig. 1. Statistically significant prevalence of positive connectivities in group 1 (CCI patients without DM2) compared to group 2 (CCI patients with DM2). Distribution of connectivities by brain regions. At the top — T-test color scale. Legend: Cereb — Cerebellum; Ver — Vermis; Language — speech neural network; IFG — Inferior Frontal Gyrus; AC — Cingulate Gyrus, anterior division; pSTG r — Superior Temporal Gyrus, posterior division, right hemisphere; aPAHC l — Parahippocampal Gyrus, anterior division, left hemisphere; AG r — Angular Gyrus, right hemisphere. The numbers after Cereb and Ver are regions of the cerebellum and the vermis.

Comparison of the data from Table 2 shows what changes neural networks' reorganization triggers in carbohydrate, lipid metabolism, inflammation, hemodynamics and cognitive functions. Further studies will help to understand reliability of network reorganization in patients with DM2 as a marker of these changes.

DISCUSSION

DM2 is a common concomitant disease in patients with chronic cerebral ischemia. According to our own research data and published reports, up to a third of CCI patients have DM2 [25]. This disease damages vascular endothelium, which is vitally important with its part in paracrine, endocrine and autocrine functions that maintain normal vascular balance of the body. Endothelium regulates integrity of blood vessels, their permeability, angiogenesis, hemostasis and immune responses. It controls vascular tone, vasodilation and vasoconstriction, migration and proliferation of smooth muscle cells, fibrinolysis

Table 3. Neural networks' connectivity differences prevailing in group 1 compared to group 2

Neural network connectivities	T-test (71)	p(unadjusted)	p(FDR)
Cereb7 r — Ver45	3.99	0.0002	0.0259
AC — pSTG r	3.89	0.0002	0.0364
Language, IFG r — aPaHC	3.62	0.0006	0.0472
Language, IFG r — AG r	3.6	0.0006	0.0472

Note: legend for Figure 1 applies; T-test is a two-tailed sided Student's T-test, numbers in parentheses — number of degrees of freedom; p(unadjusted) — level of significance unadjusted for FDR; p(FDR) — level of significance adjusted for false discovery rate.

Table 4. Quantity of cerebral neural networks' connectivities (size) and their normalized intensity, based on fMRI data, group 1 (CCI without DM2) and group 2 (CCI with DM2)

	Size			Normalized intensity		
Groups	1	2	1–2	1	2	1–2
Default Mode Network, Lateral Prefrontal (L)	105	69	36	5.2	4.8	0.4
Default Mode Network, Lateral Prefrontal (R)	93	60	33	6	5.5	0.5
Sensory Motor Lateral (L)	115	90	25	7.3	6	1.3
Sensory Motor Lateral (R)	114	94	20	7.5	6.1	1.4
Visual Lateral (L)	91	72	19	5.9	5.8	0.1
Visual Lateral (R)	94	67	27	6.1	6.3	–0.2
Salience anterior Insula (L)	95	66	29	6.9	6.7	0.2
Salience anterior Insula (R)	108	83	25	7.1	6.7	0.4
Dorsal Attention, Frontal Eye (L)	55	32	23	5.3	3.1	2.2
Dorsal Attention, Frontal Eye (R)	86	44	42	5	4.9	0.1
Fronto Parietal, Posterior Parietal Cortex (L)	95	103	–8	6.2	4.8	1.4
Fronto Parietal, Posterior Parietal Cortex (R)	70	69	1	6.5	5.8	0.7
Language posterior, Superior Temporal Gyrus (L)	87	57	30	6.1	5.4	0.7
Language posterior, Superior Temporal Gyrus (R)	86	59	27	6.3	5.3	1
Cerebellar Anterior	97	76	21	6.5	5.1	1.4
Cerebellar Superior	112	93	19	6.5	5.5	1
Average sizes of neural networks	93.4 ± 3.8	69.3 ± 4.5	23.7 ± 3.1	6.3 ± 0.18	5.5 ± 0.22	0.78 ± 0.16

Note: (L) — left hemisphere, (R) — right hemisphere; 1 and 2 — group 1 (without DM2) and group 2 (with DM2); 1–2 — difference between the parameters' values registered in the groups.

and thrombogenesis. Disruption of endothelial regulation can lead to endothelial dysfunction, which is often observed in DM2 cases [26]. With complications of microvascular nature, this dysfunction primarily causes lower secretion of NO, higher oxidative stress, increased production of inflammatory factors, expression of proinflammatory cytokines and impaired angiogenesis [27]. According to our data, compared to CCI patients without DM2, patients suffering both of these diseases have more proinflammatory interleukin 6 in saliva, significantly higher ESR, disrupted lipid metabolism, as well as increased MCA resistance index and impairments of some of the cognitive functions [28]. Our research has shown that DM2 affects organization of neural networks and handicaps their functioning.

This study has shown that, compared to people that have CCI only, the significantly lower connectivity values registered in CCI patients with DM2 is associated with a number of large neural networks: right hemisphere's speech neural network and its connections with the left hemisphere's parahippocampal region and right hemisphere's angular gyrus, which is part of the brain's passive mode network. Also, CCI patients without DM2 had significantly better connectivity of anterior cingulate gyrus, part of the salient neural network, and superior temporal gyrus. There are significant changes in the cerebellar networks, too. Thus, a relatively small number of altered connectivities is associated with large neural networks: the default network, speech, and salient networks. There are also numerous changes in other neural networks, evident in the dropping normalized intensity of connective links in CCI patients with DM2 (compared to those without DM2). Also, in such cases, reorganization of neural networks results in them shrinking by a fourth. It is clear that if the correlation of individual nodes of a neural network deteriorates, the accuracy of information transmission is compromised. Other researchers have

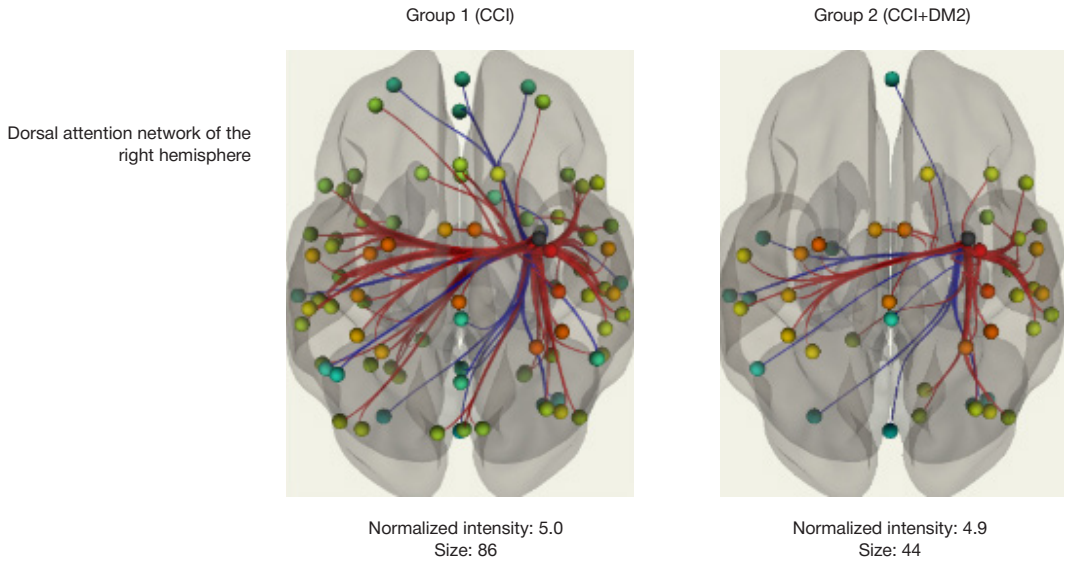

Fig. 2. presents distribution of connectivities coming out of the dorsal attention network in the right hemisphere.

also shown that DM2 can affect neural networks of the brain [29, 30]. They used various methods, including resting fMRI. These studies suggest that DM2 can alter neural networks, increasing the risk of significant cognitive decline and dementia, which seems likely due to the reduction of a large number of connectivity indicators significantly different from zero.

CONCLUSIONS

DM2 is a common concomitant disease in CCI cases; it exacerbates chronic inflammation and endothelial dysfunction. We registered significant differences in carbohydrate, lipid metabolism, inflammation, hemodynamics, and cognitive functions between CCI patients without DM2 and CCI patients without DM2. All the participating patients exhibited high values of inflammation indicators, but those with DM2 had the respective symptoms more pronounced. As expected, we detected significant changes in neural networks in patients with DM2, especially in the parahippocampal region, angular, anterior cingulate and superior temporal gyri, cerebellar networks. These changes entail decrease of the size and intensity of neural networks, deterioration of their synchronization, which is obviously associated with compromised accuracy of information transmission between different brain structures. Further studies may aim at finding markers of initial changes in the organization of neural networks shaped by DM2 in CCI patients, and developing means of their prevention.

References

1. Tanashyan MM. Tserebrovaskulyarnaya patologiya i metabolicheskiy sindrom. M.: «AST 345», 2019; p. 376. Russian.
2. Bakker W, Eringa EC, Sipkema P, van Hinsbergh VW. Endothelial dysfunction and diabetes: roles of hyperglycemia, impaired insulin signaling and obesity. Cell Tissue Res. 2009 Jan; 335 (1): 165–89. DOI: 10.1007/s00441-008-0685-6. PMID: 18941783.
3. Hsieh CF, Liu CK, Lee CT, Yu LE, Wang JY. Acute glucose fluctuation impacts microglial activity, leading to inflammatory activation or self-degradation. Sci Rep. 2019 Jan 29; 9 (1): 840. DOI: 10.1038/s41598-018-37215-0. PMID: 30696869; PMCID: PMC6351546.
4. Huang XT, Li C, Peng XP, Guo J, Yue SJ, Liu W, et al. An excessive increase in glutamate contributes to glucose-toxicity in β-cells via activation of pancreatic NMDA receptors in rodent diabetes. Sci Rep. 2017 Mar 17; 7: 44120. DOI: 10.1038/srep44120. PMID: 28303894. PMCID: PMC5356012.
5. Khalid M, Alkaabi J, Khan MAB, Adem A. Insulin signal transduction perturbations in insulin resistance. Int J Mol Sci. 2021 Aug 10; 22 (16): 8590. DOI: 10.3390/ijms22168590. PMID: 34445300. PMCID: PMC8395322.
6. Sasaki-Hamada S, Sanai E, Kanemaru M, Kamanaka G, Oka JI. Long-term exposure to high glucose induces changes in the expression of AMPA receptor subunits and glutamate transmission in primary cultured cortical neurons. Biochem Biophys Res Commun. 2022 Jan 22; 589: 48–54. DOI: 10.1016/j.bbrc.2021.11.108. PMID: 34891041.
7. Giri B, Dey S, Das T, Sarkar M, Banerjee J, Dash SK. Chronic hyperglycemia mediated physiological alteration and metabolic distortion leads to organ dysfunction, infection, cancer progression and other pathophysiological consequences: An update on glucose toxicity. Biomed Pharmacother. 2018 Nov; 107: 306–28. DOI: 10.1016/j.biopha.2018.07.157. PMID: 30098549.
8. Roh E, Song DK, Kim MS. Emerging role of the brain in the homeostatic regulation of energy and glucose metabolism. Exp Mol Med. 2016 Mar 11; 48 (3): e216. DOI: 10.1038/emm.2016.4. PMID: 26964832. PMCID: PMC4892882.
9. Musen MA, Noy NF, Shah NH, Whetzel PL, Chute CG, Story MA, et al. The National Center for Biomedical Ontology: advancing biomedicine through structured organization of scientific knowledge. Journal of the American Medical Informatics Association. 2012; 19 (2): 190–5. DOI: 10.1136/amiajnl-2011-000523.
10. Convit A, Wolf OT, Tarshish CY, de Leon MJ, Golomb J. Reduced glucose tolerance is associated with poor memory performance and hippocampal atrophy among normal elderly. Proceedings of the National Academy of Sciences. 2003; 100 (4): 2019–22. DOI: /10.1073/pnas.0336073100.
11. Lowell BB, Shulman GI. Mitochondrial dysfunction and type 2 diabetes. Science. 2005; 307 (5708): 384–7. DOI: 10.1126/science.1104343.
12. Stiernman LJ, Grill F, Hahn A, Rischka L, Lanzenberger R, Panes Lundmark V, et al. Dissociations between glucose metabolism and blood oxygenation in the human default mode network revealed by simultaneous PET-fMRI. Proc Natl Acad Sci U S A. 2021 Jul 6; 118 (27): e2021913118. DOI: 10.1073/pnas.2021913118. PMID: 34193521. PMCID: PMC8271663.
13. Hu B, Yan LF, Sun Q, Yu Y, Zhang J, Dai YJ, et al. Disturbed neurovascular coupling in type 2 diabetes mellitus patients: Evidence from a comprehensive fMRI analysis. Neuroimage Clin. 2019; 22: 101802. DOI: 10.1016/j.nicl.2019.101802. PMID: 30991623. PMCID: PMC6447740.
14. Chen R, Ovbiagele B, Feng W. Diabetes and stroke: epidemiology, pathophysiology, pharmaceuticals and outcomes. Am J Med Sci. 2016 Apr; 351 (4): 380–6. DOI: 10.1016/j.amjms.2016.01.011. PMID: 27079344. PMCID: PMC5298897.
15. Tanashyan MM, Maksimova MYu, Domashenko MA. Distsirkulyatornaya entsefalopatiya. Putevoditel' vrachebnykh naznacheniy. 2015; 2: 1–25. Russian.
16. Batysheva TT, Artemova IYu, Vdovichenko TV. Khronicheskaya ishemiya mozga: mekhanizmy razvitiya i sovremennoe kompleksnoe lechenie. Consilium medicum. 2004; 3 (4). Russian.
17. Zakharov VV, Lokshina AB. Kognitivnye narusheniya pri distsirkulyatornoy entsefalopatii. RMZh. 2009; (20): 1325–31. Russian.
18. Morris JC. Clinical dementia rating: a reliable and valid diagnostic and staging measure for dementia of the Alzheimer type. Int. Psychogeriatric. 1997; (9 Suppl 1): 173–6.
19. Whitfield-Gabrieli S, Nieto-Castanon A. Conn: a functional connectivity toolbox for correlated and anticorrelated brain networks. Brain Connect. 2012; 2 (3): 125–41. DOI: 10.1089/brain.2012.0073. PMID: 22642651.
20. Farahani FV, Karwowski W, Lighthall NR. Application of Graph Theory for Identifying Connectivity Patterns in Human Brain Networks: A Systematic Review. Front Neurosci. 2019 Jun 6; 13: 585. DOI: 10.3389/fnins.2019.00585. PMID: 31249501. PMCID: PMC6582769.
21. Pedersini CA, Guàrdia-Olmos J, Montalà-Flaquer M, Cardobi N, Sanchez-Lopez J, Parisi G, et al. Functional interactions in patients with hemianopia: A graph theory-based connectivity study of resting fMRI signal. PLoS One. 2020 Jan 6; 15 (1): e0226816. DOI: 10.1371/journal.pone.0226816. PMID: 31905211. PMCID: PMC6944357.
22. Xiong Y, Ye C, Chen Y, Zhong X, Chen H, Sun R, et al. Altered Functional Connectivity of Basal Ganglia in Mild Cognitive Impairment and Alzheimer's Disease. Brain Sci. 2022 Nov 15; 12 (11): 1555. DOI: 10.3390/brainsci12111555. PMID: 36421879. PMCID: PMC9688931.
23. Fokin VF, Shabalina AA, Ponomareva NV, Medvedev RB, Lagoda OV, Tanashyan MM. Interleukin dynamics during cognitive stress in patients with chronic cerebral ischemia. Bulletin of RSMU. 2020; 6: 142–8. DOI: 10.24075/vrgmu.2020.085. Russian.
24. CONN Tutorial. Available from: https://web.conn-toolbox.org/tutorials.
25. Lau LH, Lew J, Borschmann K, Thijs V, Ekinci EI. Prevalence of diabetes and its effects on stroke outcomes: A meta-analysis and literature review. J Diabetes Investig. 2019 May; 10 (3): 780–92. DOI: 10.1111/jdi.12932. PMID: 30220102. PMCID: PMC6497593.
26. Kaur R, Kaur M, Singh J. Endothelial dysfunction and platelet hyperactivity in type 2 diabetes mellitus: molecular insights and therapeutic strategies. Cardiovasc Diabetol. 2018 Aug 31; 17 (1): 121. DOI: 10.1186/s12933-018-0763-3. PMID: 30170601.

PMCID: PMC6117983.
27. Shi Y, Vanhoutte PM. Macro- and microvascular endothelial dysfunction in diabetes. J Diabetes. 2017 May; 9 (5): 434–49. DOI: 10.1111/1753-0407.12521. PMID: 28044409.
28. Fokin VF, Ponomareva NV, Medvedev RB, Konovalov RN, Krotenkova MV, Lagoda OV, et al. Resistive index of internal carotid artery and brain networks in patients with chronic cerebral ischemia. Bulletin of RSMU. 2021; 6: 34–40. DOI: 10.24075/vrgmu.2021.055. Russian.
29. Xu J, Chen F, Liu T, Wang T, Zhang J, Yuan H, et al. Brain Functional Networks in Type 2 Diabetes Mellitus Patients: A Resting-State Functional MRI Study. Front Neurosci. 2019 Mar 19; 13: 239. DOI: 10.3389/fnins.2019.00239. PMID: 30941007. PMCID: PMC6433793.
30. Zhang Y, Wang J, Wei P, Zhang J, Zhang G, Pan C, et al. Interhemispheric resting-state functional connectivity abnormalities in type 2 diabetes patients. Ann Palliat Med. 2021 Jul; 10 (7): 8123–33. DOI: 10.21037/apm-21-1655. PMID: 34353097.

Литература

1. Танашян М. М. Цереброваскулярная патология и метаболический синдром. М.: «АСТ 345», 2019; 376 с.
2. Bakker W, Eringa EC, Sipkema P, van Hinsbergh VW. Endothelial dysfunction and diabetes: roles of hyperglycemia, impaired insulin signaling and obesity. Cell Tissue Res. 2009 Jan; 335 (1): 165–89. DOI: 10.1007/s00441-008-0685-6. PMID: 18941783.
3. Hsieh CF, Liu CK, Lee CT, Yu LE, Wang JY. Acute glucose fluctuation impacts microglial activity, leading to inflammatory activation or self-degradation. Sci Rep. 2019 Jan 29; 9 (1): 840. DOI: 10.1038/s41598-018-37215-0. PMID: 30696869; PMCID: PMC6351546.
4. Huang XT, Li C, Peng XP, Guo J, Yue SJ, Liu W, et al. An excessive increase in glutamate contributes to glucose-toxicity in β-cells via activation of pancreatic NMDA receptors in rodent diabetes. Sci Rep. 2017 Mar 17; 7: 44120. DOI: 10.1038/srep44120. PMID: 28303894. PMCID: PMC5356012.
5. Khalid M, Alkaabi J, Khan MAB, Adem A. Insulin signal transduction perturbations in insulin resistance. Int J Mol Sci. 2021 Aug 10; 22 (16): 8590. DOI: 10.3390/ijms22168590. PMID: 34445300. PMCID: PMC8395322.
6. Sasaki-Hamada S, Sanai E, Kanemaru M, Kamanaka G, Oka JI. Long-term exposure to high glucose induces changes in the expression of AMPA receptor subunits and glutamate transmission in primary cultured cortical neurons. Biochem Biophys Res Commun. 2022 Jan 22; 589: 48–54. DOI: 10.1016/j.bbrc.2021.11.108. PMID: 34891041.
7. Giri B, Dey S, Das T, Sarkar M, Banerjee J, Dash SK. Chronic hyperglycemia mediated physiological alteration and metabolic distortion leads to organ dysfunction, infection, cancer progression and other pathophysiological consequences: An update on glucose toxicity. Biomed Pharmacother. 2018 Nov; 107: 306–28. DOI: 10.1016/j.biopha.2018.07.157. PMID: 30098549.
8. Roh E, Song DK, Kim MS. Emerging role of the brain in the homeostatic regulation of energy and glucose metabolism. Exp Mol Med. 2016 Mar 11; 48 (3): e216. DOI: 10.1038/emm.2016.4. PMID: 26964832. PMCID: PMC4892882.
9. Musen MA, Noy NF, Shah NH, Whetzel PL, Chute CG, Story MA, et al. The National Center for Biomedical Ontology: advancing biomedicine through structured organization of scientific knowledge. Journal of the American Medical Informatics Association. 2012; 19 (2): 190–5. DOI: 10.1136/amiajnl-2011-000523.
10. Convit A, Wolf OT, Tarshish CY, de Leon MJ, Golomb J. Reduced glucose tolerance is associated with poor memory performance and hippocampal atrophy among normal elderly. Proceedings of the National Academy of Sciences. 2003; 100 (4): 2019–22. DOI: /10.1073/pnas.0336073100.
11. Lowell BB, Shulman GI. Mitochondrial dysfunction and type 2 diabetes. Science. 2005; 307 (5708): 384–7. DOI: 10.1126/science.1104343.
12. Stiernman LJ, Grill F, Hahn A, Rischka L, Lanzenberger R, Panes Lundmark V, et al. Dissociations between glucose metabolism and blood oxygenation in the human default mode network revealed by simultaneous PET-fMRI. Proc Natl Acad Sci U S A. 2021 Jul 6; 118 (27): e2021913118. DOI: 10.1073/pnas.2021913118. PMID: 34193521. PMCID: PMC8271663.
13. Hu B, Yan LF, Sun Q, Yu Y, Zhang J, Dai YJ, et al. Disturbed neurovascular coupling in type 2 diabetes mellitus patients: Evidence from a comprehensive fMRI analysis. Neuroimage Clin. 2019; 22: 101802. DOI: 10.1016/j.nicl.2019.101802. PMID: 30991623. PMCID: PMC6447740.
14. Chen R, Ovbiagele B, Feng W. Diabetes and stroke: epidemiology, pathophysiology, pharmaceuticals and outcomes. Am J Med Sci. 2016 Apr; 351 (4): 380–6. DOI: 10.1016/j.amjms.2016.01.011. PMID: 27079344. PMCID: PMC5298897.
15. Танашян М. М., Максимова М. Ю., Домашенко М. А. Дисциркуляторная энцефалопатия. Путеводитель врачебных назначений. 2015; 2: 1–25.
16. Батышева Т. Т., Артемова И. Ю., Вдовиченко Т. В. Хроническая ишемия мозга: механизмы развития и современное комплексное лечение. Consilium medicum. 2004; 3 (4).
17. Захаров В. В., Локшина А. Б. Когнитивные нарушения при дисциркуляторной энцефалопатии. РМЖ. 2009; (20): 1325–31.
18. Morris JC. Clinical dementia rating: a reliable and valid diagnostic and staging measure for dementia of the Alzheimer type. Int. Psychogeriatric. 1997; (9 Suppl 1): 173–6.
19. Whitfield-Gabrieli S, Nieto-Castanon A. Conn: a functional connectivity toolbox for correlated and anticorrelated brain networks. Brain Connect. 2012; 2 (3): 125–41. DOI: 10.1089/brain.2012.0073. PMID: 22642651.
20. Farahani FV, Karwowski W, Lighthall NR. Application of Graph Theory for Identifying Connectivity Patterns in Human Brain Networks: A Systematic Review. Front Neurosci. 2019 Jun 6; 13: 585. DOI: 10.3389/fnins.2019.00585. PMID: 31249501. PMCID: PMC6582769.
21. Pedersini CA, Guàrdia-Olmos J, Montalà-Flaquer M, Cardobi N, Sanchez-Lopez J, Parisi G, et al. Functional interactions in patients with hemianopia: A graph theory-based connectivity study of resting fMRI signal. PLoS One. 2020 Jan 6; 15 (1): e0226816. DOI: 10.1371/journal.pone.0226816. PMID: 31905211. PMCID: PMC6944357.
22. Xiong Y, Ye C, Chen Y, Zhong X, Chen H, Sun R, et al. Altered Functional Connectivity of Basal Ganglia in Mild Cognitive Impairment and Alzheimer's Disease. Brain Sci. 2022 Nov 15; 12 (11): 1555. DOI: 10.3390/brainsci12111555. PMID: 36421879. PMCID: PMC9688931.
23. Фокин В. Ф., Шабалина А. А., Пономарева Н. В., Медведев Р. Б., Лагода О. В., Танашян М. М. Изменчивость интерлейкинов при когнитивной нагрузке у больных с хронической ишемией мозга. Вестник РГМУ. 2020; 6: 142–8. DOI: 10.24075/vrgmu.2020.085.
24. CONN Tutorial. Available from: https://web.conn-toolbox.org/tutorials.
25. Lau LH, Lew J, Borschmann K, Thijs V, Ekinci EI. Prevalence of diabetes and its effects on stroke outcomes: A meta-analysis and literature review. J Diabetes Investig. 2019 May; 10 (3): 780–92. DOI: 10.1111/jdi.12932. PMID: 30220102. PMCID: PMC6497593.
26. Kaur R, Kaur M, Singh J. Endothelial dysfunction and platelet hyperactivity in type 2 diabetes mellitus: molecular insights and therapeutic strategies. Cardiovasc Diabetol. 2018 Aug 31; 17 (1): 121. DOI: 10.1186/s12933-018-0763-3. PMID: 30170601. PMCID: PMC6117983.
27. Shi Y, Vanhoutte PM. Macro- and microvascular endothelial dysfunction in diabetes. J Diabetes. 2017 May; 9 (5): 434–49. DOI: 10.1111/1753-0407.12521. PMID: 28044409.
28. Фокин В. Ф., Пономарева Н. В., Медведев Р. Б., Коновалов Р. Н., Кротенкова М. В., Лагода О. В. и др. Индекс резистентности внутренних сонных артерий и нейросети мозга при хронической церебральной ишемии. Вестник РГМУ. 2021; 6: 34–40. DOI: 10.24075/vrgmu.2021.055.
29. Xu J, Chen F, Liu T, Wang T, Zhang J, Yuan H, et al. Brain Functional Networks in Type 2 Diabetes Mellitus Patients: A Resting-State Functional MRI Study. Front Neurosci. 2019 Mar 19; 13: 239. DOI: 10.3389/fnins.2019.00239. PMID: 30941007. PMCID: PMC6433793.
30. Zhang Y, Wang J, Wei P, Zhang J, Zhang G, Pan C, et al. Interhemispheric resting-state functional connectivity abnormalities in type 2 diabetes patients. Ann Palliat Med. 2021 Jul; 10 (7): 8123–33. DOI: 10.21037/apm-21-1655. PMID: 34353097.

STATISTICAL ANALYSIS OF DATA ON EMERGENCY MAXILLOFACIAL SURGERY

Markarov AE[1], Eremin DA[2], Martirosov AV[1,2] ✉, Khandzratsyan AS[1], Orazvaliev AI[1], Bugayan SA[2], Khalifaev OI[3]

[1] Inozemtsev Municipal Clinical Hospital, Moscow, Russia

[2] Pirogov National State Medical University, Moscow, Russia

[3] Evdokimov Moscow State University of Medicine and Dentistry, Moscow, Russia

There are no actual statistical data on maxillofacial trauma, nor is there a published analysis addressing morbidity patterns, including cases requiring admission to maxillofacial surgery departments. Such data and the respective analysis could help to assess effectiveness of the maxillofacial trauma and diseases prevention and treatment measures, improve the emergency care approaches, identify problems in the medical aid system's maxillofacial surgery domain. This study aimed to analyze the aspects of emergency admission to hospitals for reasons requiring maxillofacial surgery. We processed hospital records of 15,227 patients admitted from 2018 through 2022. The analysis revealed the number of emergency maxillofacial cases to be at a fairly high level and show no downward trend. The majority of the patients are young, able-bodied men. Of all the admitted persons, 28.6% came to the hospital on their own; 22.9% were nonresidents and foreigners. The average hospital stay was 3.85 days, it did not change significantly during the studied period. The prevailing types of trauma were maxillofacial injuries and mandibular fractures. For 29.9% of patients with the latter type, the treatment method of choice was osteosynthesis. Up to 70% of all the patients needed to be followed-up by a maxillofacial surgeon after discharge. The mortality rate in maxillofacial surgery departments is extremely low; all such cases involved concomitant pathologies.

Keywords: trauma, wounds, face, maxillofacial surgery, statistics

Author contribution: Markarov AE, Eremin DA — manuscript editing, preparation of the final version of the article; Martirosov AV, Khandzratsyan AS, Orazvaliev AI — study planning, data interpretation, manuscript drafting; Bugayan SA, Khalifaev OI — data collection, analysis. Authors claim to have contributed to the study equally.

✉ **Correspondence should be addressed:** Aram V. Martirosov
Fortunatovskaya, 1, Moscow, 105187, Russia; dr.martirosov@mail.ru

Received: 09.08.2023 **Accepted:** 06.09.2023 **Published online:** 23.10.2023

DOI: 10.24075/brsmu.2023.038

СТАТИСТИЧЕСКИЙ АНАЛИЗ ДАННЫХ ПО НЕОТЛОЖНОЙ ЧЕЛЮСТНО-ЛИЦЕВОЙ ХИРУРГИИ

А. Э. Маркаров[1], Д. А. Еремин[2], А. В. Мартиросов[1,2] ✉, А. С. Хандзрацян[1], А. И. Оразвалиев[1], С. А. Бугаян[2], О. И. Халифаев[3]

[1] Городская клиническая больница имени Ф. И. Иноземцева, Москва, Россия

[2] Российский национальный исследовательский медицинский университет имени Н. И. Пирогова, Москва, Россия

[3] Московский государственный медико-стоматологический университет имени А. И. Евдокимова, Москва, Россия

Актуальные статистические данные по травме ЧЛО (челюстно-лицевой области) с анализом структуры заболеваемости и по госпитализируемой заболеваемости в отделении челюстно-лицевой хирургии (ЧЛХ) отсутствуют. Анализ этих данных необходим для оценки результативности мер по профилактике и лечению заболеваний и травм ЧЛО, повышения эффективности оказания неотложной помощи пациентам, выявления проблем в системе оказания медицинской помощи по профилю «Челюстно-лицевая хирургия». Целью исследования было провести статистический анализ структуры госпитализации по профилю экстренной челюстно-лицевой хирургии. Проанализирована медицинская документация 15 227 пациентов, госпитализированных с 2018 по 2022 г. Было выявлено, что число пациентов с экстренной патологией челюстно-лицевой области сохраняется на достаточно высоком уровне без тенденции к снижению. Основная часть госпитализированных — мужчины молодого, трудоспособного возраста. Из числа всех госпитализированных 28,6% составили пациенты, обратившиеся в стационар самостоятельно, а 22,9% — иногородние и иностранцы. Средняя продолжительность госпитализации составила 3,85 суток и существенно не менялась за исследуемый период. В структуре травматизма преобладали раны ЧЛО и переломы нижней челюсти. Остеосинтез применяли при переломах нижней челюсти в 29,9% случаев. До 70% всех пациентов после выписки нуждались в динамическом наблюдении челюстно-лицевого хирурга. Летальность в отделении ЧЛХ крайне низкая и обусловлена наличием у пациентов тяжелой сопутствующей патологии.

Ключевые слова: травма, раны, лицо, челюстно-лицевая хирургия, статистика

Вклад авторов: А. Э. Маркаров, Д. А. Еремин — внесение правок, подготовка финального варианта статьи; А. В. Мартиросов, А. С. Хандзрацян, А. И. Оразвалиев — планирование исследования, интерпретация данных, подготовка черновика рукописи; С. А. Бугаян, О. И. Халифаев — сбор, анализ данных. Авторы заявляют о равнозначности вклада каждого.

✉ **Для корреспонденции:** Арам Вачаганович Мартиросов
ул. Фортунатовская, д. 1, г. Москва, 105187, Россия; dr.martirosov@mail.ru

Статья получена: 09.08.2023 **Статья принята к печати:** 06.09.2023 **Опубликована онлайн:** 23.10.2023

DOI: 10.24075/vrgmu.2023.038

Maxillofacial trauma is a problem both medical and socio-economical. Domestic and criminal violence, development of personal mobility devices and their growing availability, and road accidents condition the significant share of maxillofacial injuries in the overall number of trauma cases [1–4]. At the same time, despite the continued improvement of prevention programs as well as introduction of the new methods of diagnosis and treatment of maxillofacial diseases, the quantity of patients with purulent-inflammatory forms thereof does not grow down, and the percentage of those in whom the said diseases have progressed to severe stages grows up every year [5]. Both the injured and the ill with these types of trauma/disorders and concomitant pathologies (coagulopathy, allergy to local anesthetics, central nervous system diseases, cardiovascular diseases, etc.), as well as pregnant women and limited mobility individuals, are admitted to maxillofacial surgery departments, since there are neither dental offices in multidisciplinary hospitals of Moscow that provide specialized care to such patients, nor a complex of therapeutic and preventive measures designed to render qualified dental care to the latter category of citizens [6].

Inozemtsev Moscow City Clinical Hospital has a maxillofacial surgery department (№ 1) and a purulent maxillofacial surgery

department (№ 2). As per the SanPiN regulations, there are two separate patient examination rooms in the emergency section (ER). Both departments are under the trauma unit of the hospital.

Since 2018, short-term stay section of Inozemtsev Moscow City Clinical Hospital has been performing planned maxillofacial surgery procedures. Maxillofacial surgeons of the department № 1 formed a visiting team, the only of its kind in Moscow, that gives round-the-clock consultations to patients with acute maxillofacial pathologies treated in Moscow hospitals. Large number of maxillofacial injury cases involving purulence and inflammation substantiated establishing department № 2 as a separate unit. Currently, it is the only such department in Russia.

There are up-to-date statistical data on purulent and inflammatory maxillofacial pathologies [5], but no reports covering maxillofacial trauma morbidity patterns nor study of reasons for admission to maxillofacial surgery departments. Such reports/studies could help to assess effectiveness of the maxillofacial trauma and diseases prevention and treatment measures, improve the emergency care approaches, identify problems in the medical aid system's maxillofacial surgery domain.

This study aimed to statistically analyze referrals and admissions to the maxillofacial surgery department № 1, one of the leading units rendering emergency medical assistance to patients with maxillofacial trauma and pathology in Moscow, operating 39 beds.

METHODS

The study was conducted at the premises of maxillofacial surgery department № 1 of F.I. Inozemtsev Moscow City Clinical Hospital. We analyzed medical records (discharge reports, form № 066/u-02, and universal discharge/postmortem summaries, form № 027/u) of 15,227 patients admitted from 2018 through 2022. These are all the patients that stayed in the maxillofacial surgery department № 1 during the said period. People admitted at a different time or to another department were excluded. Statistical data processing relied on the mean and the extensive indicator calculation methods.

RESULTS

General statistics

According to the admission department of Inozemtsev Moscow City Clinical Hospital, during the mentioned period of time, 27,571 cases were referred to the maxillofacial surgery department. The months when the number of patients peaks are May through August, and October; this pattern applies every year. The peaks are mainly due to the increasing incidence of maxillofacial trauma. From 2018 through 2022, 15,227 people were admitted to the maxillofacial surgery department (Table 1).

The reason behind the almost twofold decrease in the number of referrals in 2020 is the COVID-19 pandemic and the associated self-isolation rules, admission plan revision, etc. With this fact factored in, the continuous year-over-year growth of the number of maxillofacial trauma cases is obvious. However, the rate of admissions remains stable, which indicates there are increasingly more outpatient cases (wounds, bruises, abrasions, hematomas).

During the studied period, 4,359 (28.6%) inpatients were self-referrals. There were 3,494 nonresidents and foreigners, which accounted for 22.9% of all those admitted. The prevailing types of injuries were maxillofacial, including mandibular fractures (33.7%), midface fractures (16.5%), wounds (12.4%). The majority of inpatients, 10,354, were male (68%), and 7,665 (74%) of them had maxillofacial trauma. The pattern persists through the years, only the ratio changes (1 : 2, 1 : 3) (Fig. 1).

Maxillary sinusitis, periodontitis, bleeding after tooth extraction, teething pathologies are more common in women (Fig. 2).

Analysis of age of the patients has shown that most of them are young and able-bodied, 18 through 44 years old. All in all, during the studied period, there were admitted 9,759 (64.1%) young, 2,497 (16.4%) middle-aged, 1,822 (12%) senior, 995 (6.5%) elderly and 154 (1.0%) senile people (Table 2).

An average hospital stay lasted 3.85 days. During the studied period, this value was changing unevenly: 4.22 b/d (bed-days) in 2018, 3.33 — in 2019, 3.67 — in 2020, 3.86 — in 2021 and 4.38 — in 2022.

The longest hospital stays were associated with combined mandibular and midface fractures (7.3 b/d), multiple mandibular fractures (6.7 b/d), and zygomatic complex fractures (5.87 b/d), the shortest stays — with post-extraction bleeding (1.9 b/d) and periodontitis (1.6 c/d) (Table 3).

There are interesting specifics about average bed-days in maxillary fracture cases: the figure is rather small for severe Le Fort II and III fractures because the patients therewith are admitted with a combined TBI (traumatic brain injury), and, after examination by an interdisciplinary team, forwarded to the neurosurgical resuscitation department for comprehensive treatment, and only once their condition is stabilized, they are transferred to the maxillofacial surgery department [7–9]. During the studied period, seven people died in the department (five in 2019, two in 2020). In all cases, the cause of death was decompensation of a severe concomitant pathology.

Inozemtsev Moscow City Clinical Hospital has an outreach team of maxillofacial surgeons that provide medical assistance to patients with acute maxillofacial pathology treated in other hospitals of Moscow without a maxillofacial surgery department. During the studied period, the team attended to 4,729 cases, including 566 trips to infectious diseases departments to patients with COVID-19 (707 in 2018, 994 in 2019, 722 in 2020, 1,135 in 2021 and 1,171 in 2022).

The department has a rehabilitation room for patients with maxillofacial pathology, where they are followed-up after discharge with the aim to adjust treatment plan as necessary or continue as outpatients (removal and/or adjustment of splints, rubber rods, removal of sutures, bandages, etc.). Through the

Table 1. ER referrals admitted with maxillofacial pathology

	2018	2019	2020	2021	2022
Maxillofacial surgery department referrals	5757	5886	3057	6286	6485
Admitted to the maxillofacial surgery department	2757	3509	2791	3416	2754
Brought by an ambulance	1144	1522	1757	1726	1348
Self-referrals	873	1255	672	770	789
Admitted nonresidents/foreigners	632	806	696	696	664

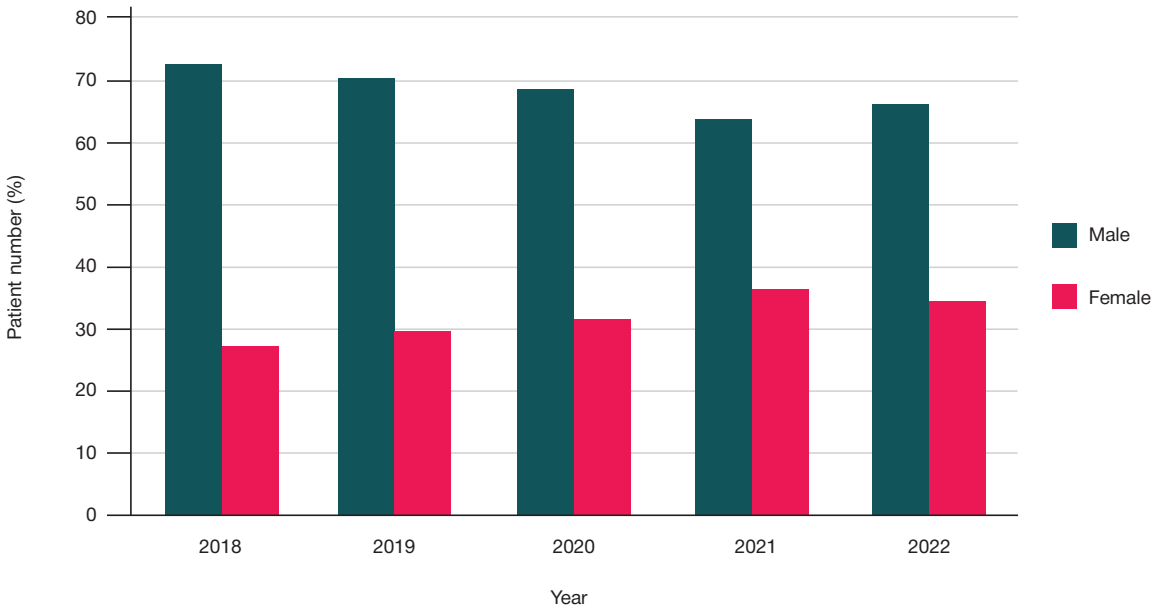

Fig. 1. Distribution of patients by gender

studied period, 10,275 patients applied to the rehabilitation room for reexamination (2,401 in 2018, 2,262 in 2019, 1,853 in 2020, 2,233 in 2021 and 1,526 in 2022), which accounted for 67.5% of all the admitted persons.

Private statistics

Patients with chronic and aggravated periodontitis accounted for 12.6% of the admitted, and 67.5% of them were women. Indications for hospitalization with this pathology were:

1) Pregnancy.

2) Polyvalent allergy to local anesthetics.

3) Coagulopathy, primarily associated with the use of anticoagulants.

4) Severe general somatic pathology (primarily cardiovascular by nature).

5) Limited mobility of patients.

During the studied period, 962 people were admitted with post-extraction bleeding, the majority of such patients over 60 years old (63%). Among other conditions necessitating admission were incomplete tooth extraction (87 cases), maxillary sinus perforation, including with a foreign body, such as tooth root and implant (161), dislocation of tooth root into soft tissues during extraction (12).

Neoplasm in the maxillofacial area caused hospitalization of 202 (1.3%) patients, 58.9% of them male and 41.1% — female, predominantly young (40.1% — young, 27.7% — middle-aged, 26.2% — senior, 7.4% — elderly and 0.5% — senile). These patients were admitted under the plan (not emergency cases).

Gunshot wounds were extremely rare: 8 cases (three of them with damaged facial bones, five with damage only to the jaw's soft tissues); traumatic tooth luxation — 23 cases; painful TMJ (temporomandibular joint) dysfunction — 11 cases; fractures of the anterior wall of maxillary sinus and zygomaticomaxillary complex — 8 and 17 cases, respectively.

The majority of the admitted patients had maxillofacial trauma; most of them were male, aged 18 through 44.

In 10.85% of cases, maxillofacial injury was combined with CTBI (closed traumatic brain injury) and BC (brain concussion), the latter most often diagnosed concomitant with maxillary fractures and combined mandibular and midface fractures (88.8% and 36.15%, respectively). Only 5% of mandibular fractures were associated with BC.

Patients with injuries of soft tissues in the maxillofacial area accounted for 12.4% (1,889) of the total number of the admitted. Among such injuries, most were wounds (80.6%), hematomas (9.9%) and bruises (9.5%). All patients with bite wounds underwent rabies and tetanus vaccination. Some patients admitted with soft tissue damage also exhibited moderate to severe alcohol intoxication, extensive damage areas, traumatic brain injury, general somatic pathology.

Midface fractures

Patients with zygomatic bone and arch fractures accounted for 20.2% of the total number of those admitted with facial bone fractures. In 72% of such cases, bone fragments were displaced; in 92.3% of cases, they were reduced under general anesthesia using the Limberg technique, and in the remaining 8.7% of cases, the method of choice was osteosynthesis, mainly enabled by metallic pins (Makienko technique).

Orbital fractures and zygomaticomaxillary complex fractures accounted for 6.4% and 18.0% of all midface fractures, the former treated surgically in 23.1% of cases, the latter — in 67.9% of cases.

Four percent of all the admitted had maxillary fractures. Patients with Le Fort I fractures and alveolar bone fractures accounted for 2.5%, Le Fort II fractures — 1.37%, Le Fort III fractures — 0.1%.

Isolated nose fractures are treated by otorhinolaryngologists, however, if there is damage to soft tissues, patients are referred to maxillofacial surgeons. During the studied period, there were 90 such cases.

Paranasal sinus wall fractures were extremely rare and did not require surgical intervention.

Mandibular fractures

Mandibular fractures were the most common among facial bone fractures (65.2%), their unilateral variety registered somewhat more often (54.7% of the total number of mandibular fractures), predominantly — jaw angle fractures (50.7%). Bilateral mandibular fractures were less common (43.1%) (Table 4).

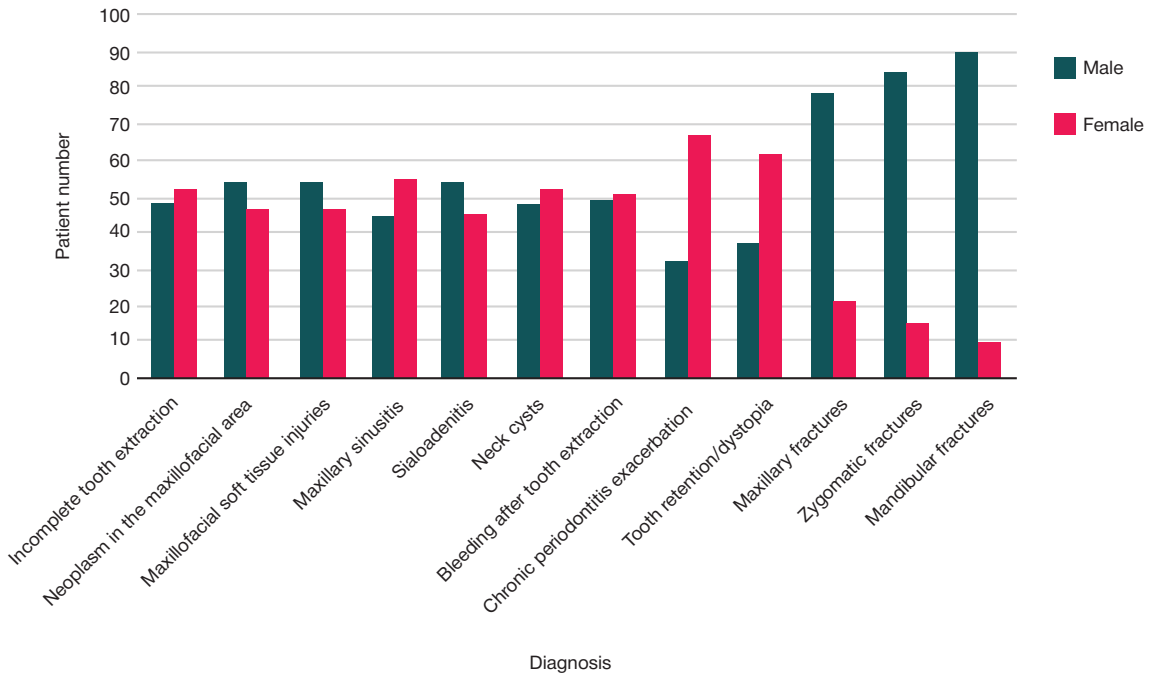

Fig. 2. Distribution of patients by nosology and gender

Teeth affected by the fracture were extracted in 5% of cases when the body of the lower jaw was damaged, and in 16.5% of cases when the fractured part was the jaw's angle.

Multiple mandibular fractures accounted for 1.75%. Most often, the combination included angle, body and articular process (73%).

Combined trauma — mandibular and midface fractures — was rare: only 2.73% of the total number of facial bones fractures.

For 29.9% of patients with mandibular fractures, the treatment method of choice was osteosynthesis. Other patients had the mandible immobilized with a two-jaw splint.

DISCUSSION

Many Russian and foreign authors describe the problem of general spread of individual mobility devices [1–3]. The injury rate associated with them is high, with the key reasons therefor being neglect of their operation instructions and traffic laws. Other authors highlight the problem of extremely low availability of outpatient dental care to people with limited mobility, which translates into greater load on the maxillofacial surgery departments. [6]. The number of patients with maxillofacial trauma has been steadily growing since 1970s [10], the situation acknowledged such in all regions by all the authors exploring the subject [10–15]. Also, all authors underscore domination of men in the sample, and decreasing average bed-day value [10–15].

Clinical experience described by the colleagues has mandibular fractures prevailing overall, but the reported percentage varies: 92% [12], 70–85% [13], 67–87% [14], 73.5–80.5% [15]. The data we have processed suggests that the share of mandibular fractures is slightly lower: 65.2%. The reasons for such a significant difference may be sample size, timing and region of the respective research.

Our study confirms that unilateral fractures around mandibular's angle are more common than other varieties. Shares of unilateral and bilateral fractures in different studies: 54.7% and 43.1% — our study, 60% and 40% [14], 49% and 49% [12], 61.1 and 38.9% [13].

Previous studies also present statistical assessment of the causes of fractures: road accidents (43.9%) and assaults (26.7%). Another source puts household trauma on the first place (82.7%), and road accidents on the second (11.8%) [14]. In countries with aging population, household injuries, including falls, prevail, while in those with younger population the predominant reasons for such injuries are road-related [16]. The conclusion is indirectly confirmed by other foreign authors [4]. In our study, we did not consider this criterion, because patients frequently refuse to disclose the true causes of their injuries.

Mandibular fractures are combined with midface fractures in 2.4% of cases, and midface fractures account for 13.9% through 20% of the total number of fractures of facial bones, and this figure tends to grow annually [14, 15]. The amount of midface fractures has been growing rapidly from 2000 through 2007, and afterwards the growth turned uniform [10]. Our data confirm conclusions of the authors of that study. The share of combined injuries has increased to 2.73%, and that of midface fractures — to 25.85%.

As for the combinations of facial trauma and TBI, different authors present different data: from 21.3% to 46% [7], and 13.92% [8]. Mandibular fractures are much less often

Table 2. Dynamics of distribution of patients by age

Age	2018	2019	2020	2021	2022
18–44	67.6	63.5	71.4	63.5	61.7
45–59	14.6	18	15.4	17.6	15.3
60–74	10.3	12.1	8.4	12.1	14.9
75–89	6.65	6.3	4.3	6.5	7.5
90+	0.66	0.4	0.3	0.3	0.6

Table 3. Average hospital stay at maxillofacial surgery department by nosology (bed-days)

Diagnosis	Average bed-days				
	2018	2019	2020	2021	2022
Incomplete tooth extraction	1.6	1.5	2.5	2	2.4
Neoplasm in the maxillofacial area	2.6	1.9	2.6	2.3	3.3
Maxillofacial soft tissue injuries	2.87	2.1	2.3	1.75	2.4
Maxillary sinusitis	4.9	4.2	5.0	4.8	4.7
Sialoadenitis	4.8	3.5	5.4	4.9	4.56
Neck cysts	4.5	4.75	3.6	3.6	2.5
Bleeding after tooth extraction	1.92	1.98	1.6	1.9	1.8
Periodontitis	1.8	1.5	1.6	1.7	1.6
Tooth retention/dystopia	1.8	2.1	2.1	2.7	2.1
Zygomatic fractures	5.4	5.3	4.87	4.95	4.6
Unilateral mandibular fractures	4.7	3.9	4.6	4.6	5.2
Bilateral mandibular fractures	5.75	4.9	5.2	5.5	6.1
Multiple mandibular fractures	6.5	5.45	5.0	6.9	5.1
Cheekbone complex fractures	10.7	9.5	9.5	7	6
Combined fractures (mandibular and midface)	10.8	11.0	9.2	6.1	8.7
Le Fort I fracture	3.9	2.7	3.1	3.0	3.2
Le Fort II fracture	5.3	4.7	5.4	5	5.8
Le Fort III fracture	0	9	5.7	5	4

combined with TBI (3.2 – 3.83%) [7] than midface fractures, which is confirmed by our data. On average, the hospital stay of patients with TBI and BC is 59.7% longer [8].

According to some authors, a rehabilitation (follow-up care) room in the maxillofacial surgery department improves the results of treatment by 31.6 — 50%, under various criteria, and the efficiency of work — by 16.7 — 21.9% [17]. The data we processed in the context of this study confirm the need for further treatment in the vast majority of cases. One of the solutions for the rehabilitation availability and effectiveness problem, according to our colleagues, is telemedicine [6].

None of the research reports mention mortality from maxillofacial injuries, which indirectly confirms our conclusion that there are no such cases.

CONCLUSIONS

The number of emergency calls related to maxillofacial trauma and pathology increases every year, but the amount of cases requiring hospitalization remains stable, which means a large number of patients are treated in the emergency room. Up to 70% of all patients need follow-up monitoring by a maxillofacial surgeon after discharge. Maxillofacial surgery departments receive emergency patients with concomitant general somatic pathologies, pregnant women and low-mobility patients when the hospital does not have an inpatient dental department, A maxillofacial surgeon in the outpatient unit could reduce the load on hospitals' emergency rooms as well as make post-discharge rehabilitation more easily accessible, and setting up emergency dental care departments could lessen the burden of maxillofacial surgery departments and improve the quality of dental care provided. It is also necessary to reinforce dental diseases prevention measures designed for the limited mobility patients. Patients with maxillofacial trauma dominate among those needing hospital stay for treatment. Every year, the number of injuries peaks summertime. This fact should be taken into account when planning preventive measures to reduce household, street and road traffic injuries. Every year, up to 71.4% of those admitted to the hospitals are young, able-bodied men, 18-44 years old. The most common injuries are mandibular fractures, more often unilateral (54.7%), in the area of the jaw's angle (50.7%). For 29.9% of patients with mandibular fractures, the treatment method of choice was osteosynthesis. Patients with injuries of soft tissues in the maxillofacial area accounted for 12.4% of the total number of the admitted. Among such injuries, most were wounds

Table 4. Mandibular fractures statistics

Fracture in the area of	%	Displacement (%)	TBI (%)
Unilateral			
Angle	50.7	58.1	3.3
Body	17.75	49.4	4
Articular process	28.7	66.0	4.4
Branch	2.7	61.2	7.5
Bilateral			
Body and angle	48.7	72.4	5
Body and articular process	38.3	74.3	7.9
Angle and articular process	9.0	75.5	6.2
Body and branch	4.0	74.4	6.4

(80.6%), hematomas (9.9%) and bruises (9.5%). Patients with maxillofacial trauma combined with TBI stay in the hospitals longer. Midface fractures are much more common mandibular fractures; they are combined with TBI of varying severity. The mortality rate in maxillofacial surgery departments is extremely low; all such cases involve concomitant pathologies.

References

1. Aksenova EI, Podchernina AM. The main trends in the increase in the share of injuries of muscovites based on medical statistics. Current problems of health care and medical statistics. 2021; 2: 403–16. Russian.
2. Grechuhin IV. The condition of traumatism problem according to data of official statistics and scientific foundation for its control. Manager of health care. 2017; 7: 41–9. Russian.
3. Baranchikova MV. Individuals driving personal mobility aids as subjects and victims in criminal road accidents. Victimology. 2022; 9 (4): 408–16. Russian.
4. Mohammadi H, Roochi MM, Heidar H, Garajei A, Dallband M, Sadeghi M, et al. A meta-analysis to evaluate the prevalence of maxillofacial trauma caused by various etiologies among children and adolescents. Dent Traumatol. 2023; 39 (5): 403–17. DOI: 10.1111/edt.12845. PMID: 37073864.
5. Markarov AE, Eremin DA, Martirosov AV, Orazvaliev AI, Krasnov NM, Shen PA, et al. The statistical analysis of purulent-inflammatory diseases of the maxillo-facial region. Medical alphabet. 2022; 7: 40–6. Russian.
6. Lebedev MV, Kerimova KI, Zakharova IYu, Bakhturin NA. System of rendering medical assistance to population in the profile "oral and maxillofacial surgery" in the territory of the Russian Federation. Current problems of health care and medical statistics. 2020; 1: 383–402. Russian.
7. McCarty JC, Kiwanuka E, Gadkaree SK, Siu JM, Caterson EJ. Traumatic brain injury in trauma patients with isolated facial fractures. Journal of Craniofacial Surgery. 2020; 31 (5): 1182–5.
8. Yuchen Y, Romero J, Diaz G, Evans R. Concurrent traumatic brain injury with craniofacial trauma: a 10-year analysis of a Single Institution's Trauma Registry. Trauma Care. 2023; 3: 108–13.
9. Lucke-Wold B, Pierre K, Aghili-Mehrizi S, Murad GJA. Facial fractures: independent prediction of neurosurgical intervention. Asian Journal of Neurosurgery. 2022; 17: 17–22.
10. Kopetski IS, Pritiko AG, Polunina NV, Nasibullin AM. Traumatism of maxillofacial region (during 50 years). Bulletin of RSMU. 2010; 2: 31–4. Russian.
11. Dregalkina AA, Kostina IN. The structure of diseases of the maxillofacial region among residents of Sverdlovsk Region. Actual problems in dentistry. 2018; 14 (2): 68–73. Russian.
12. Bakhteeva GR, Kuzmin AS. Statistical research of maxillofacial injuries. Bulletin of Medical Internet Conferences. 2012; 2 (11): 930. Russian.
13. Shashkov VA, Gaivoronsky IV, Gaivoronskaya MG, Iordanishvili AK, Rodionov AA, Nichiporuk GI. Prevalence of different types of lower jaw fractures in adults. Medical Newsletter of Vyatka. 2021; 1 (69): 41–7. Russian.
14. Chzhan Sh, Petruk PS, Medvedev YuA. Fractures of the mandible at the body and angle region: patterns, epidemiology, diagnostic principles. Part I. Russian Journal of Dentistry. 2017; 21 (2): 100–3. Russian.
15. Romeo I, Sobrero F, Roccia F, Dolan S, Laverick S, Carlaw K, et al. A multicentric, prospective study on oral and maxillofacial trauma in the female population around the world. Dent Traumatol. 2022; 38 (3): 196–205. DOI: 10.1111/edt.12750. PMID: 35390219.
16. Romeo I, Sobrero F, Roccia F, Dolan S, Laverick S, Carlaw K, et al. A multicentric, prospective study on oral and maxillofacial trauma in the female population around the world. Dent Traumatol. 2022; 38 (3): 196–205. DOI: 10.1111/edt.12750. PMID: 35390219.
17. Goncharova AV. Use of stationary substituting technologies in rehabilitation of patients with inflammatory diseases of the maxillofacial region. Bulletin of RSMU. 2011; 5: 76–9. Russian.

Литература

1. Аксенова Е. И., Подчернина А. М. Основные тенденции в увеличении доли травматизма москвичей на основе данных медицинской статистики. Современные проблемы здравоохранения и медицинской статистики. 2021; 2: 403–16.
2. Гречухин И. В. Состояние проблемы травматизма по данным официальной статистики и научное обоснование совершенствования его учета. Менеджер здравоохранения. 2017; 7: 41–9.
3. Баранчикова М. В. Лица, управляющие средствами индивидуальной мобильности как субъекты и потерпевшие в криминальных дорожно-транспортных происшествиях. Виктимология. 2022; 9 (4): 408–16.
4. Mohammadi H, Roochi MM, Heidar H, Garajei A, Dallband M, Sadeghi M, et al. A meta-analysis to evaluate the prevalence of maxillofacial trauma caused by various etiologies among children and adolescents. Dent Traumatol. 2023; 39 (5): 403–17. DOI: 10.1111/edt.12845. PMID: 37073864.
5. Маркаров А. Э., Еремин Д. А., Оразвалиев А. И., Мартиросов А. В., Краснов Н. М., Шень П. А. и др. Статистический анализ гнойно-воспалительных заболеваний челюстно-лицевой области. Медицинский алфавит. 2022; 7: 40–6.
6. Лебедев М. В., Керимова К. И., Захарова И. Ю., Бахтурин Н. А. Система оказания медицинской помощи населению по профилю «челюстно-лицевая хирургия» на территории Российской Федерации. Современные проблемы здравоохранения и медицинской статистики. 2020; 1: 383–402.
7. McCarty JC, Kiwanuka E, Gadkaree SK, Siu JM, Caterson EJ. Traumatic brain injury in trauma patients with isolated facial fractures. Journal of Craniofacial Surgery. 2020; 31 (5): 1182–5.
8. Yuchen Y, Romero J, Diaz G, Evans R. Concurrent traumatic brain injury with craniofacial trauma: a 10-year analysis of a Single Institution's Trauma Registry. Trauma Care. 2023; 3: 108–13.
9. Lucke-Wold B, Pierre K, Aghili-Mehrizi S, Murad GJA. Facial fractures: independent prediction of neurosurgical intervention. Asian Journal of Neurosurgery. 2022; 17: 17–22.
10. Копецкий И. С., Притыко А. Г., Полунина Н. В., Насибуллин А. М. Травматизм челюстно-лицевой области (опыт 50-летнего наблюдения). Вестник РГМУ. 2010; 2: 31–4.
11. Дрегалкина А. А., Костина А. Н. Структура заболеваний челюстно-лицевой области среди жителей Свердловской области. Проблемы стоматологии. 2018; 14 (2): 68–73.
12. Бахтеева Г. Р., Кузьмин А. С. Статистическое исследование травм челюстно-лицевой области. Bulletin of Medical Internet Conferences. 2012; 2 (11): 930.
13. Шашков В. А., Гайворонский И. В., Гайворонская М. Г., Иорданишвили А. К., Родионов А. А., Ничипорук Г. И. Распространенность различных видов переломов нижней челюсти у взрослых. Вятский медицинский вестник. 2021; 1 (69): 41–7.
14. Чжан Ш., Петрук П. С., Медведев Ю. А. Переломы нижней челюсти в области тела и угла: структура, эпидемиология, принципы диагностики. Часть I. Российский стоматологический журнал. 2017; 21 (2): 100–3.
15. Фокас Н. Н., Левенец А. А., Горбач Н. А. Характеристика повреждений челюстно-лицевой области у взрослого населения и анализ деятельности отделения челюстно-лицевой хирургии по материалам КГБУЗ ККБ (г. Красноярск).

Сибирское медицинское обозрение. 2014; 3: 44–8.
16. Romeo I, Sobrero F, Roccia F, Dolan S, Laverick S, Carlaw K, et al. A multicentric, prospective study on oral and maxillofacial trauma in the female population around the world. Dent Traumatol. 2022; 38 (3): 196–205. DOI: 10.1111/edt.12750. PMID: 35390219.
17. Гончарова А. В. Роль стационарзамещающих технологий в реабилитации больных с воспалительными заболеваниями челюстно-лицевой области. Вестник РГМУ, 2011; 5: 76–9.

EFFECT OF DIFFERENT MOBILE DEVICE SCREEN TIME DURATIONS ON NEUROPSYCHIATRIC HEALTH OF SCHOOLCHILDREN

Solovyova YuV ✉, Paunova SS, Semicheva VR, Skoblina NA, Milushkina OYu

Pirogov Russian National Research Medical University, Moscow, Russia

Uncontrolled screen time is a worldwide menace to health of the population. Today, the state of neuropsychiatric health of schoolchildren depends on various factors, including screen time, i.e., the time they spend using mobile electronic devices. This study aimed to investigate how different screen time durations affect the said neuropsychiatric health of this population group. In the 2022–2023 academic year, we surveyed 109 Moscow schoolchildren (35 boys and 74 girls) using questionnaires compiled by A.M. Vane (identification of signs of vegetative symptoms) and S.K. Kulakov (identification of internet addiction). The mean age of the participants was 14.9 ± 0.12 years. The children were divided into two groups: those staying within the regulated limit of mobile screen time (group 1, n = 11), and those exceeding that limit (group 2, n = 98). In group 1, the average mobile screen time, as measured for one month, was 110.50 ± 10.00 minutes per day, in group 2 — 345.00 ± 15.00. The average Vane questionnaire scores differed significantly between the groups ($p \leq 0.01$): 12.30 ± 1.89 points in group 1 and 22.54 ± 1.16 points in group 2. Signs of vegetative symptoms were registered in 45.9% of group 1 participants and 63.6% of group 2 participants ($p \leq 0.01$). The average Kulakov questionnaire scores differed significantly between the groups ($p \leq 0.05$): 28.7 ± 1.88 points in group 1 and 37.1 ± 1.09 points in group 2. Schoolchildren who exceed the regulated mobile screen time limit are at risk of developing vegetative disorders and internet addiction.

Keywords: neuropsychiatric health, schoolchildren, mobile electronic devices

Author contribution: all authors contributed to the publication equally.

Compliance with ethical standards: the study was approved by the local Ethics Committee of the N.I. Pirogov Russian National Research Medical University (Minutes № 655 of April 23, 2019); signed voluntary informed consent forms were obtained for each participant

✉ **Correspondence should be addressed:** Yulia V. Solovyova
Ostrovityanova, 1, Moscow, 117997, Russia; yula_24@mail.ru

Received: 02.10.2023 **Accepted:** 20.10.2023 **Published online:** 29.10.2023

DOI: 10.24075/brsmu.2023.040

СОСТОЯНИЕ НЕРВНО-ПСИХИЧЕСКОГО ЗДОРОВЬЯ ШКОЛЬНИКОВ ПРИ РАЗЛИЧНОМ ВРЕМЕНИ ИСПОЛЬЗОВАНИЯ МОБИЛЬНЫХ ЭЛЕКТРОННЫХ УСТРОЙСТВ

Ю. В. Соловьева ✉, С. С. Паунова, В. Р. Семичева, Н. А. Скоблина, О. Ю. Милушкина

Российский национальный исследовательский медицинский университет имени Н. И. Пирогова Минздрава России, Москва

Мировая проблема для здоровья населения — неконтролируемое время использования электронных устройств. Состояние нервно-психического здоровья современных школьников связано с различными факторами, в том числе со временем использования мобильных электронных устройств. Цель исследования — анализ состояния нервно-психического здоровья школьников при различном времени использования мобильных электронных устройств. В 2022—2023 учебном году с помощью опросников А. М. Вейна для выявления признаков вегетативных изменений и С. К. Кулакова для выявления интернет-зависимости было опрошено 109 школьников (35 мальчиков и 74 девочек), обучающихся в образовательных организациях г. Москвы. Средний возраст составил 14,9 ± 0,12 лет. Школьники были разделены на две группы: соблюдающие регламент использования мобильных электронных устройств (первая группа, n = 11) и превышающих регламент (вторая группа, n = 98). Средний показатель экранного времени использования мобильных электронных устройств за месяц составил в первой группе 110,50 ± 10,00 мин/день, во второй — 345,00 ± 15,00. Средние значения баллов по опроснику А. М. Вейна в первой и второй группах имели достоверные различия ($p \leq 0,01$) и составили 12,30 ± 1,89 и 22,54 ± 1,16 баллов. Наличие признаков вегетативных изменений в первой и второй группах составило 45,9% и 63,6% ($p \leq 0,01$). Средние значения баллов по опроснику С. К. Кулакова в первой и второй группах имели достоверные различия ($p \leq 0,05$) и составили 28,7 ± 1,88 и 37,1 ± 1,09 баллов. Школьники, превышающие регламент использования мобильных электронных устройств, находятся в группе риска по формированию вегетативных нарушений и интернет-зависимости.

Ключевые слова: нервно-психическое здоровье, школьники, мобильные электронные устройства

Вклад авторов: все авторы внесли равносильный вклад в подготовку публикации.

Соблюдение этических стандартов: исследование одобрено этическим комитетом РНИМУ имени Н. И. Пирогова (протокол № 655 от 23 апреля 2019 г.), для каждого участника было получено добровольное информированное согласие.

✉ **Для корреспонденции:** Юлия Валерьевна Соловьева
ул. Островитянова, д. 1, г. Москва, 117997, Россия; yula_24@mail.ru

Статья получена: 02.10.2023 **Статья принята к печати:** 20.10.2023 **Опубликована онлайн:** 29.10.2023

DOI: 10.24075/vrgmu.2023.040

Digitalization of all aspects of life and daily use of various electronic devices by schoolchildren, both at school and at home, up the risk of various diseases, including neuropsychiatric disorders; this problem is universal throughout the world nowadays [1–3].

Today, the range of use cases for mobile electronic devices (MED) extends beyond the learning process and includes the search for and analysis of various information, and communication. In this connection, schoolchildren tend to spend more time with mobile devices, computers, tablets not only in the context of studying, but also during their leisure time [4–6].

This entails the increasing prevalence of health disorders among schoolchildren whose mobile screen time exceeds the limit set by the hygienic standards. The disorders include deterioration of visual acuity and impaired posture, as well as disrupted functioning of other organs and systems, nervous system in particular [7, 8].

This study aimed to investigate how different screen time durations affect the neuropsychiatric health of schoolchildren.

METHODS

In the 2022–2023 academic year, we monitored the neuropsychiatric health of Moscow schoolchildren (n = 109, 35 boys and 74 girls) with the help of questionnaires. Their mean age was 14.9 ± 0.12 years. At the time of this study, all participants were equally healthy (no significant differences in health status), and had no diagnosed neuropsychiatric diseases.

We determined the vegetative status of schoolchildren with the help of a questionnaire by A.M. Vane (1998), which is designed to identify individuals with signs of vegetative symptoms. The questionnaire was adapted and recommended by A.G. Sukharev, Academician of the Russian Academy of Sciences; authors of the study tested its applicability to the studied population group [9]. The signs of internet addiction in schoolchildren were identified with a standard S.K. Kulakov questionnaire (2004) [9].

Monitoring began only after parents/legal guardians of children filled and signed the voluntary informed consent form, and if the child was 14 years old, he/she signed the form, too. The study did not endanger the participants; it met the biomedical ethics requirements and conformed to the provisions of the Declaration of Helsinki 1983.

The average time of use of an MED in the course of a month was registered from the Screen Time application.

The inclusion criteria were: status of a schoolchild in a Moscow comprehensive school, voluntary informed consent form filled by parents/legal guardians, including the child himself/herself, questionnaire filled by the child, data on the average screen time covering a month.

The exclusion criteria were: a different age group, lack of a voluntary informed consent filled by parents/legal guardians, including the child himself/herself, lack of the questionnaire filled by the child, lack of data on the average screen time covering a month.

The results were compiled into a database "Influence of mobile electronic devices and screen time with them on the development of autonomic disorders and internet addiction in schoolchildren," registered under the certificate 2023620126 of 11.01.2023. Application #022623302 of 24.11.2022.

Statistica 10.0 (StatSoft; USA) was used for statistical processing of the data. Kolmogorov–Smirnov test was run preliminarily to find out whether distribution of the values was normal or not. The collected quantitative data distributed normally, which allowed application of the methods of parametric statistics with calculation of sample mean (M), mean error (m) and sample standard deviation (σ). Significance of differences in the mean values were assessed with the Student's t-test; the differences were considered significant at $p < 0.05$. Vegetative symptoms were registered when the respective questionnaire returned 25 points and above, internet addiction — at 50 points and more.

RESULTS

Screen time was analyzed against provisions of SanPiN (sanitary rules and standards) 1.2.3685-21 "Hygienic standards and requirements for safety and/or harmlessness of an individual's environment", which limit the maximum total time of use of an MED in an educational establishment and at home at 120 minutes a day. Therefore, the children were divided into two groups: those staying within the regulated limit of mobile screen time (group 1, n = 11), and those exceeding that limit (group 2, n = 98). In group 1, the average mobile screen time, as measured in one month, was 110.50 ± 10.00 minutes per day, in group 2 — 345.00 ± 15.00 ($p < 0.05$).

The mean Vane questionnaire score for all the schoolchildren was 21.69 ± 1.02 points. The means between the groups differed significantly ($p \leq 0.01$): 12.30 ± 1.89 points in group 1 and 22.54 ± 1.16 points in group 2.

Overall, 55.0% of the participating schoolchildren exhibited signs of vegetative symptoms, 45.9% of the first group and 63.6% of all those constituting the second group ($p < 0.01$).

For signs of vegetative symptoms and mobile screen time, the Person correlation coefficient was 0.55 ($p = 0.04$).

In group 2, where the schoolchildren exceeded the regulated MED screen time limit, vegetative symptoms were registered 15 — 40 times more often than in group 1, and the most common of them were numbness and cold fingers (50.0%), sleep disturbance (45.0%), decreased performance and fatigue (42.0%), paroxysmal headaches (40.0%). Almost a third of the group 2 participants (29.0%) complained of rapid breathing and a dyspnea (Fig. 1).

The mean Kulakov questionnaire scores was 33.0 ± 1.02 points. The means between the groups differed significantly ($p \leq 0.05$): 12.30 ± 1.89 points in group 1 and 22.54 ± 1.16 points in group 2. Although this study did not reveal any the participants to have internet addiction, 74.0% of the respondents regularly used social media (up to 20 times a day), viewed various videos, positioned themselves as bloggers and preferred online communication to live interactions (Fig. 2).

In group 2, where schoolchildren exceeded the regulated MED screen time limit, symptoms of internet addiction were registered 10 - 40 times more often than in group 1. As a rule, if a participant had one such symptom, he/she was likely to also exhibited other symptoms, making up a combination thereof. In group 1, internet addiction symptoms were detected at the level of statistical error, 1.0%.

DISCUSSION

Today, children and adolescents cannot imagine a full life without internet, a state of affairs that has been especially evident in the last 10 years. Schoolchildren are not alone: their parents and teachers spend more and more time online, both for work and leisure purposes, and also using the internet to find information, answers to questions and solutions to the tasks set [10, 11].

The study involved 15-year-old schoolchildren, active internet users with well-developed respective skills and sufficient experience.

A positive point about internet in the life of contemporary schoolchildren: it is a readily available, modern knowledge acquisition medium that also offers skill practicing capacities. Schoolchildren, their parents, and teachers also perceive internet as a source of leisure activities, which allows watching movies, sightseeing online and much more. Most of all, children and teenagers use it as means of communication with both friends and relatives, and their parents and teachers also connect with their colleagues online [12, 13].

Our study confirmed the above statements: 74.0% of the respondents regularly used social media (up to 20 times a day), viewed various videos, positioned themselves as bloggers and preferred online communication to live interactions.

However, spending much time online may entail internet addiction, which is characterized by mental disorders and possible behavioral problems; this risk is relevant both for

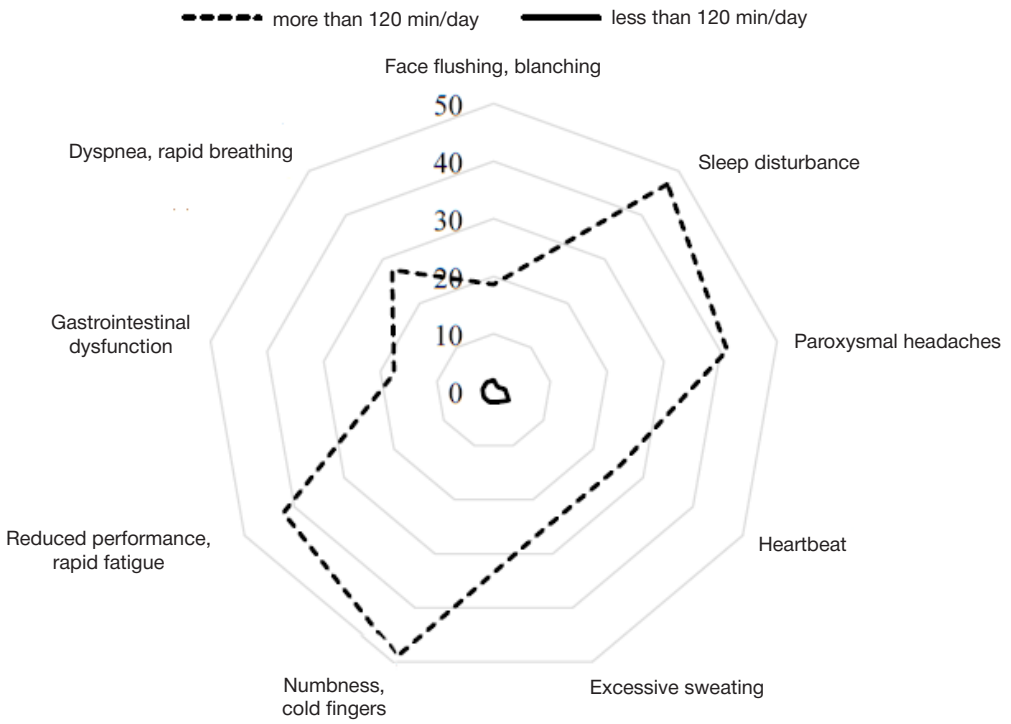

Fig. 1. Vegetative symptoms manifestations relative to mobile screen time, %

children/adolescents and adults. According to pediatricians, psychiatrists, psychologists, general practitioners, internet addiction is similar to alcohol and drug addictions. I. Goldberg, a psychiatrist, suggested this term, internet addiction, back in 1996, describing a behavioral disorder associated with use of internet or a computer [14].

Today, researchers investigate physiological processes associated with internet addiction. There are studies indicating that long a frequent online sessions cause cognitive impairment not only in schoolchildren, but also in adults [15]. Moreover, such behavior adversely affects communication skills, and, consequently, links with the society in general. The need for a personal meeting disappears if there is an opportunity to communicate online and using a mobile phone [15].

It was established that every eighth student who exceeds the regulated mobile screen time limit prefers communicating online rather than in real life. In such cases, parents and friends of the person in question feel that he/she is constantly online.

Prolonged use of internet disturbs sleep, removes outdoor time/physical activity from the daily routine or reduces its duration [15, 16].

The data collected in the context of this study indicate that every second schoolchild that exceeds the regulated mobile screen time limit has sleep problems.

Addiction to internet as a source of information, in turn, promotes endless and unrestrained online journeys. The so-called web surfing is an aimless search for information, playing.

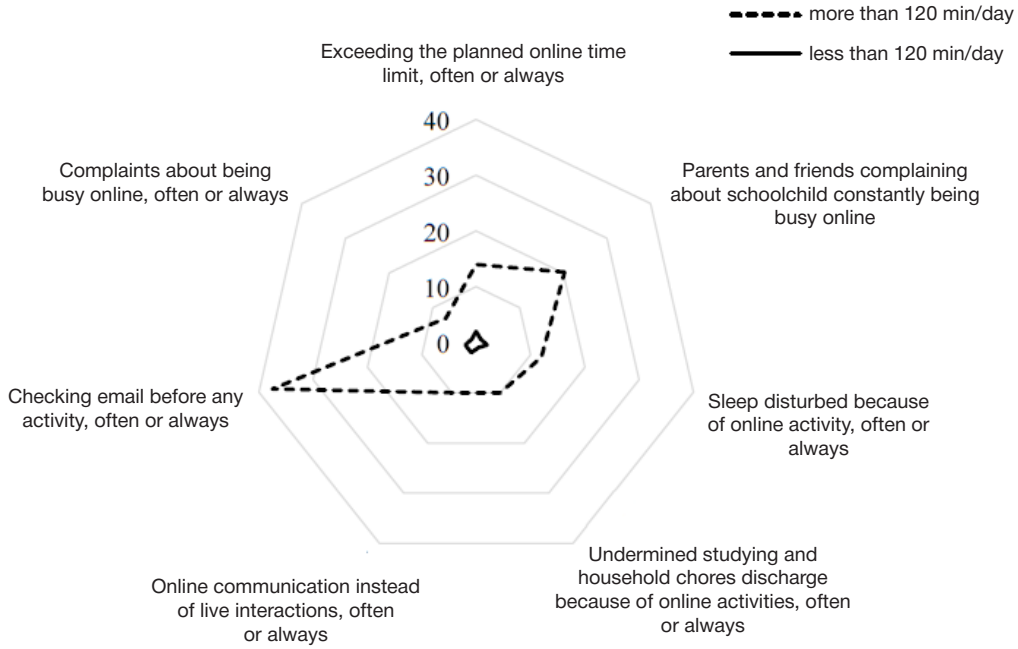

Fig. 2. Internet addiction symptoms manifestations relative to mobile screen time, %

Long online sessions and quests for information may degrade performance and translate into wasted time [15, 16].

It should be emphasized that every eighth schoolchild who exceeds the regulated mobile screen time limit stays online longer than planned, and unsuccessfully tries to reduce the said screen time, which may indicate onset of internet addiction. In this study, it was found that such schoolchildren have more complaints related to their vegetative status, with a third of them reporting three or more respective problems.

For the purposes of prevention, it is necessary to raise awareness of schoolchildren, teachers and parents about the possible health risks associated with daily prolonged use of electronic devices. The respective activities can be staged directly in the educational establishments [17–20].

CONCLUSIONS

In conclusion, it should be noted that the age of digitalization of all aspects of life, and daily use of various electronic devices inevitably create conditions upping the risk of various diseases, including neuropsychiatric disorders. Schoolchildren are especially vulnerable: their physiological and neuropsychiatric development is in the active phase, they face increasing loads at school, have to search for information online, and some of the educational materials are available in electronic form exclusively. Schoolchildren who exceed the regulated mobile screen time limit are at risk of developing vegetative disorders and internet addiction, which may entail chronic somatic and neuropsychiatric diseases. It should be remembered that supported development of healthy habits and compliance with the screen time rules can help mitigate the risk of vegetative and neuropsychiatric conditions in schoolchildren, and therefore, preserve their health in the future. The results of this study are a contribution to the global knowledge about the problem of uncontrolled mobile screen time associated with studying and leisure in the context of the effects on health and functional state of the neuropsychic sphere of children and adolescents.

References

1. Obrubov SA, Markelova SV. Impact of life activity in conditions of digital environment on the students' organ of sight. Russian Bulletin of Hygiene. 2021; 2: 4–9. DOI: 10.24075/rbh.2021.014. Russian.
2. Tereshchenko SYu, Shubina MV, Semenova NB, Evert LS, Gorbacheva NN. The relationship between internet addiction and sleep disorders in adolescents of Central Siberia in different types of consumed content. The Korsakov's Journal of Neurology and Psychiatry. Special issues. 2022; 122 (5–2): 58–64. DOI: 10.17116/jnevro202212205258. Russian.
3. Grigoryev SL. Psychophysical effects of active use of technical means of on-screen communication. Izvestiya of the Samara Science Centre of the Russian Academy of Sciences. Social, Humanitarian, Biomedical Sciences,. 2022; 24 (86): 42–50. DOI 10.37313/2413-9645-2022-24-86-42-50. Russian.
4. Milushkina OYu., Popov VI, Skoblina NA, Markelova SV, Sokolova NV. The use of electronic devices by students, parents and teachers before and after the transition to distance learning. Bulletin of RSMU. 2020; 3: 85–91. Russian.
5. Skoblina NA, Milushkina OYu, Tatarinchik AA, Fedotov DM. The place of gadgets in the life of modern schoolchildren and students. Public health and life environment. 2017; 7 (292): 41–3. DOI: 10.35627/2219-5237/2017-292-7-41-43. Russian.
6. Milushkina OYu, Skoblina NA, Markelova SV, Tatarinchik AA, Bokareva NA, Fedotov DM. Assessing health risks for schoolchildren and students caused by exposure to educational and entertaining information technologies. Health Risk Analysis. 2019; 3: 135–43. DOI: 10.21668/health.risk/2019.3.16. Russian.
7. Goncharova GA. Mental health of the children who are active users of digital media. Russian Bulletin of Hygiene. 2021; 3: 33–5. DOI: 10.24075/rbh.2021.017. Russian.
8. Kovalenko SV, Makovetskaya AD, Tyustina GG. Analysis of Internet addiction of teenagers in the educational environment as a factor of psychological safety of the personality. World of Science. Pedagogy and psychology. 2022; 10 (5): 43. Russian.
9. Kuchma VR, Sukhareva LM, Rapoport IK. Rukovodstvo po shkol'noy meditsine: Meditsinskoe obespechenie detey v doshkol'nykh, obshcheobrazovatel'nykh uchrezhdeniyakh i uchrezhdeniyakh nachal'nogo i srednego professional'nogo obrazovaniya. M.: NTsZD RAMN, 2012; p. 215. ISBN 5-94302-067-5. Russian.
10. Kojima R, Sato M, Akiyama Y, Shinohara R, Mizorogi S, Suzuki K, et al. Problematic Internet use and its associations with health-related symptoms and lifestyle habits among rural Japanese adolescents. Psychiatry Clin Neurosci. 2019 Jan; 73 (1): 20–6. DOI: 10.1111/pcn.12791.
11. Bogomolova MA, Buzina TS. Internet addiction: forming aspects and psychological correction opportunities. Med. psihol. Ross. 2018; 10 (2): 8. DOI: 10.24411/2219-8245-2018-12080. Russian.
12. Avdeeva EA, Kornilova OA. Influence of digital environment on the cognitive function of schoolchildren and students. Cardiovascular therapy and prevention. 2022; 21 (S3): 3331. DOI 10.15829/1728-8800-2022-3331. Russian.
13. Cimino S, Cerniglia L. A longitudinal study for the empirical validation of an etiopathogenetic model of internet addiction in adolescence based on early emotion regulation. Biomed Res Int. 2018 Mar 7; 2018: 4038541. DOI: 10.1155/2018/4038541.
14. Torres-Rodríguez A, Griffiths MD, Carbonell X. The treatment of Internet gaming disorder: A brief overview of the PIPATIC program. International Journal of Mental Health and Addiction. 2018; 16 (4): 1000–15. DOI: 10.1007/s11469-017-9825.
15. Kraynov AL. Internet addiction as a global problem of our time. Philosophy and Humanities in Information Society. 2020; 4: 38–45. Russian.
16. Kardashyan RA. Komp'yuternaya igrovaya zavisimost' u uchashchikhsya obshcheobrazovatel'nykh uchrezhdeniy: rasprostranennost', sposobstvuyushchie i predraspolagayushchie faktory, diagnostika, klinika, terapiya, profilaktika. M.: Izdatel'stvo RUDN, 2018; p. 286. ISBN 978-5-209-08625-3. Russian.
17. Kuchma VR, Milushkina OYu, Bokareva NA, Skoblina NA. Modern trends of preventive work in educational institutions. Hygiene and Sanitation. 2014; 93 (6): 107–11. Russian.
18. Smirnova AA, Zakharova TYu, Sinogina ES. Cyberthreats to security of teenagers. Pedagogical Review. 2017; 3 (17): 99–107. DOI 10.23951/2307-6127-2017-3-99-107. Russian.
19. Yarygina II. Training as prevention form of teenagers' internet dependence. Psychological-Pedagogical Journal "Gaudeamus". 2019; 18 (39): 89–93. Russian.
20. Makarova IA, Reznikov SA. Organizatsiya profilaktiki internet-zavisimosti podrostkov v sovremennoy shkole. Voprosy pedagogiki. 2020; 6–2: 143–6. Russian.

Литература

1. Обрубов С. А., Маркелова С. В. Влияние жизнедеятельности в условиях цифровой среды на состояние органа зрения обучающихся. Российский вестник гигиены. 2021; 2: 4–9. DOI: 10.24075/rbh.2021.014.
2. Терещенко С. Ю., Шубина М. В., Семенова Н. Б., Эверт Л. С., Горбачева Н. Н. Взаимосвязь интернет-зависимости и нарушений сна у подростков Центральной Сибири при разных видах потребляемого контента. Журнал неврологии и психиатрии им. С. С. Корсакова. Спецвыпуски. 2022; 122 (5–2): 58–64. DOI: 10.17116/jnevro202212205258.
3. Григорьев С. Л. Психофизические эффекты активного использования технических средств экранной коммуникации. Известия Самарского научного центра Российской академии наук. Социальные, гуманитарные, медико-биологические науки. 2022; 24 (86): 42–50. DOI 10.37313/2413-9645-2022-24-86-42-50.
4. Милушкина О. Ю., Попов В. И., Скоблина Н. А., Маркелова С. В., Соколова Н. В. Использование электронных устройств участниками образовательного процесса при традиционной и дистанционной формах обучения. Вестник РГМУ. 2020; 3: 85–91.
5. Скоблина Н. А., Милушкина О. Ю., Татаринчик А. А., Федотов Д. М. Место гаджетов в образе жизни современных школьников и студентов. ЗНиСО. 2017; 7 (292): 41–3. DOI: 10.35627/2219-5237/2017-292-7-41-43.
6. Милушкина О. Ю., Скоблина Н. А., Маркелова С. В., Татаринчик А. А., Бокарева Н. А., Федотов Д. М. Оценка рисков здоровью школьников и студентов при воздействии обучающих и досуговых информационно-коммуникационных технологий. Анализ риска здоровью. 2019; 3: 135–43. DOI: 10.21668/health.risk/2019.3.16.
7. Гончарова Г. А. Нервно-психическое здоровье детей — активных пользователей цифровых средств. Российский вестник гигиены. 2021; 3: 33–5. DOI: 10.24075/rbh.2021.017.
8. Коваленко С. В., Маковецкая А. Д., Тюстина Г. Г. Исследование интернет-зависимости подростков в условиях образовательной среды как фактора психологической безопасности личности. Мир науки. Педагогика и психология. 2022; 10 (5): 43.
9. Кучма В. Р., Сухарева Л. М., Рапопорт И. К. Руководство по школьной медицине: Медицинское обеспечение детей в дошкольных, общеобразовательных учреждениях и учреждениях начального и среднего профессионального образования. М.: НЦЗД РАМН, 2012; 215 с. ISBN 5-94302-067-5.
10. Kojima R, Sato M, Akiyama Y, Shinohara R, Mizorogi S, Suzuki K, et al. Problematic Internet use and its associations with health-related symptoms and lifestyle habits among rural Japanese adolescents. Psychiatry Clin Neurosci. 2019 Jan; 73 (1): 20–6. DOI: 10.1111/pcn.12791.
11. Богомолова М. А., Бузина Т. С. Интернет-зависимость: аспекты формирования и возможности психологической коррекции. Медицинская психология в России. 2018; 10 (2): 8. DOI: 10.24411/2219-8245-2018-12080.
12. Авдеева Е. А., Корнилова О. А. Влияние цифровой электронной среды на когнитивные функции школьников и студентов. Кардиоваскулярная терапия и профилактика. 2022; 21 (S3): 3331. DOI 10.15829/1728-8800-2022-3331.
13. Cimino S, Cerniglia L. A longitudinal study for the empirical validation of an etiopathogenetic model of internet addiction in adolescence based on early emotion regulation. Biomed Res Int. 2018 Mar 7; 2018: 4038541. DOI: 10.1155/2018/4038541.
14. Torres-Rodríguez A, Griffiths MD, Carbonell X. The treatment of Internet gaming disorder: A brief overview of the PIPATIC program. International Journal of Mental Health and Addiction. 2018; 16 (4): 1000–15. DOI: 10.1007/s11469-017-9825.
15. Крайнов А. Л. Интернет-зависимость как глобальная проблема современности. Философия и гуманитарные науки в информационном обществе. 2020; 4: 38–45.
16. Кардашян Р. А. Компьютерная игровая зависимость у учащихся общеобразовательных учреждений: распространенность, способствующие и предрасполагающие факторы, диагностика, клиника, терапия, профилактика. М.: Издательство РУДН, 2018; 286 с. ISBN 978-5-209-08625-3.
17. Кучма В. Р., Милушкина О. Ю., Бокарева Н. А., Скоблина Н. А. Современные направления профилактической работы в образовательных организациях. Гигиена и санитария. 2014; 93 (6): 107–11.
18. Смирнова А. А., Захарова Т. Ю., Синогина Е. С. Киберугрозы безопасности подростков. Научно-педагогическое обозрение. 2017; 3 (17): 99–107. DOI 10.23951/2307-6127-2017-3-99-107.
19. Ярыгина И. И. Тренинг как форма профилактики Интернет-зависимости подростков. Психолого-педагогический журнал Гаудеамус. 2019; 18 (39): 89–93.
20. Макарова И. А., Резников С. А. Организация профилактики интернет-зависимости подростков в современной школе. Вопросы педагогики. 2020; 6–2: 143–6.